LA-12562-MS

Measured Solubilities and Speciations of Neptunium, Plutonium, and Americium in a Typical Groundwater (J-13) from the Yucca Mountain Region

Milestone Report 3010-WBS 1.2.3.4.1.3.1

Los Alamos
NATIONAL LABORATORY

Los Alamos National Laboratory is operated by the University of California for the United States Department of Energy under contract W-7405-ENG-36.

This work was supported by the Yucca Mountain Site Characterization Project Office as part of the Civilian Radioactive Waste Management Program. This project is managed by the US Department of Energy, Yucca Mountain Site Characterization Project.

This work was performed at the Lawrence Berkeley Laboratory for the Los Alamos National Laboratory. The Lawrence Berkeley Laboratory is operated by the University of California for the US Department of Energy under Contract DE-AC-03-76SF00098.

An Affirmative Action/Equal Opportunity Employer

LA-12562-MS

UC-802
Issued: July 1993

Measured Solubilities and Speciations of Neptunium, Plutonium, and Americium in a Typical Groundwater (J-13) from the Yucca Mountain Region Milestone Report 3010-WBS 1.2.3.4.1.3.1

*H. Nitsche**
*R. C. Gatti**
*E. M. Standifer**
*S. C. Lee**
*A. Müller**
*T. Prussin**
*R. S. Deinhammer**
*H. Maurer**
*K. Becraft**
*S. Leung**
*S. A. Carpenter**

**Lawrence Berkeley Laboratory, University of California, Earth Sciences Division, 1 Cyclotron Road, Mail Stop 70-A-1150, Berkeley, CA 94720.*

Los Alamos
NATIONAL LABORATORY
Los Alamos, New Mexico 87545

TABLE OF CONTENTS

TABLE OF CONTENTS (continued)

LIST OF FIGURES

LIST OF FIGURES (continued)

LIST OF FIGURES (continued)

LIST OF FIGURES (continued)

Section **Page**

LIST OF TABLES

LIST OF TABLES (continued)

LIST OF TABLES (continued)

MEASURED SOLUBILITIES AND SPECIATIONS OF NEPTUNIUM, PLUTONIUM, AND AMERICIUM IN A TYPICAL GROUNDWATER (J-13) FROM THE YUCCA MOUNTAIN REGION MILESTONE REPORT 3010-WBS 1.2.3.4.1.3.1

by

H. Nitsche, R. C. Gatti, E. M. Standifer, S. C. Lee,
A. Müller, T. Prussin, R. S. Deinhammer, H. Maurer,
K. Becraft, S. Leung, and S. A. Carpenter

ABSTRACT

Solubility and speciation data are important in understanding aqueous radionuclide transport through the geosphere. They define the source term for transport retardation processes such as sorption and colloid formation. Solubility and speciation data are useful in verifying the validity of geochemical codes that are part of predictive transport models. Results are presented from solubility and speciation experiments of $^{237}NpO_2^+$, $^{239}Pu^{4+}$, $^{241}Am^{3+}/Nd^{3+}$, and $^{243}Am^{3+}$ in J-13 groundwater (from the Yucca Mountain region, Nevada, which is being investigated as a potential high-level nuclear waste disposal site) at three different temperatures (25°, 60°, and 90°C) and pH values (5.9, 7.0, and 8.5). The solubility-controlling steady-state solids were identified and the speciation and/or oxidation states present in the supernatant solutions were determined. The neptunium solubility decreased with increasing temperature and pH. Plutonium concentrations decreased with increasing temperature and showed no trend with pH. The americium solutions showed no clear solubility trend with increasing temperature and increasing pH.

1. EXECUTIVE SUMMARY

We studied the solubilities of neptunium, plutonium, and americium in J-13 groundwater from the Yucca Mountain region (Nevada) at three temperatures and three hydrogen ion concentrations. They are 25°, 60, and 90°C and pH 5.9, 7.0, and 8.5. Tables I, II, and III summarize the results for neptunium, plutonium, and americium, respectively. The solubilities were studied from oversaturation. The nuclides were added at the beginning of each experiment as NpO_2^+, Pu^{4+}, and Am^{3+}.

The neptunium solubility decreased with increasing temperature and with increasing pH. The soluble neptunium did not change oxidation state at steady state. The pentavalent neptunium was increasingly complexed by carbonate with increasing pH. The steady-state solids were crystalline sodium neptunium carbonate hydrates with different water content, except the solid formed at 90°C and pH 5.9. We identified this solid as crystalline Np_2O_5. The 90°C, pH 7 solid was a mixture of sodium neptunium carbonate hydrate and neptunium pentoxide.

Plutonium concentrations decreased with increasing temperature and showed no trend with pH. Pu(V) and Pu(VI) were the dominant oxidation states in the supernatant solution; as the amount of Pu(V) increased with pH, Pu(VI) decreased. The solubility-controlling steady-state solids were mostly amorphous, although some contained a crystalline component. They contained mainly Pu(IV) polymer and smaller portions of plutonium carbonates.

For the americium solutions, no clear solubility trend was found with increasing temperature and increasing pH. Much higher solubilities were found for 60°C compared with 25°C and 90°C. All solids were $AmOHCO_3$, with orthorhombic structure for all temperatures at pH 7 and 8.5 and for 60°C at pH 6 and with hexagonal structure for 25°C and 90° at pH 6. Orthorhombic $AmOHCO_3$ appears to have a much higher solubility at pH 6 and 60°C than the hexagonal form at the same pH and 25°C or 90°C.

Table I. Summary of results for solubility experiments on neptunium in J-13 groundwater at pH 5.9, 7.0, and 8.5 and at 25°, 60°, and 90°C.

	Steady-state concentration (M)			Oxidation state in supernatant solution		
	25°C	60°C	90°C	25°C	60°C	90°C
pH 5.9	$(5.3 \pm 0.3) \times 10^{-3}$	$(6.4 \pm 0.4) \times 10^{-3}$	$(1.2 \pm 0.1) \times 10^{-3}$	V: 100% 9% carbonate complexed	V: 100%, 8% carbonate complexed	V: 100%, uncomplexed
pH 7.0	$(1.3 \pm 0.2) \times 10^{-4}$	$(9.8 \pm 1.0) \times 10^{-4}$	$(1.5 \pm 0.4) \times 10^{-4}$	V: 100%, 54% carbonate complexed	V: 100%, 15% carbonate complexed	V: 100%, uncomplexed
pH 8.5	$(4.4 \pm 0.7) \times 10^{-5}$	$(1.0 \pm 0.1) \times 10^{-4}$	$(8.9 \pm 0.4) \times 10^{-5}$	V: 100%, 62% carbonate complexed	V: 100%, 84% carbonate complexed	V: 100%, 100% carbonate complexed

	Eh(mV) vs. NHE			Solid phase		
	25°C	60°C	90°C	25°C	60°C	90°C
pH 5.9	588 ± 10	440 ± 10	392 ± 10	$Na_{0.6}NpO_2(CO_3)_{0.8} \cdot 2.5H_2O$	$Na_{0.6}NpO_2(CO_3)_{0.8} \cdot 2.5H_2O$	Np_2O_5
pH 7.0	482 ± 10	325 ± 10	299 ± 10	$NaNpO_2(CO_3) \cdot 2H_2O$	$Na_{0.6}NpO_2(CO_3)_{0.8} \cdot 2.5H_2O$	Np_2O_5 and a carbonate-containing solid
pH 8.5	497 ± 10	215 ± 10	159 ± 10	$Na_{0.6}NpO_2(CO_3)_{0.8} \cdot 2.5H_2O$	$Na_{0.6}NpO_2(CO_3)_{0.8} \cdot 2.5H_2O$	crystalline, contains carbonate, unidentified

Table II. Summary of results for solubility experiments on plutonium in J-13 groundwater at pH 5.9, 7.0, and 8.5 and at 25°, 60°, and 90°C.

	Steady-state concentration (M)			Oxidation state in supernatant solution		
	25°C	60°C	90°C	25°C	60°C	90°C
pH 5.9	$(1.1 \pm 0.4) \times 10^{-6}$	$(2.7 \pm 1.1) \times 10^{-8}$	$(6.2 \pm 1.9) \times 10^{-9}$	III + poly: (3 ± 1)% IV: (5 ± 1)% V: (68 ± 7)% VI: (29 ± 3)%	III + poly: (10 ± 2)% IV: (2 ± 1)% V: (17 ± 5)% VI: (72 ± 5)%	III + poly: (9 ± 5)% IV: (6 ± 5)% V: (79 ± 7)% VI: (6 ± 5)%
pH 7.0	$(2.3 \pm 1.4) \times 10^{-7}$	$(3.7 \pm 0.9) \times 10^{-8}$	$(8.8 \pm 0.8) \times 10^{-9}$	III + poly: (5 ± 1)% IV: (6 ± 1)% V: (73 ± 7)% VI: (18 ± 2)%	III + poly: (3 ± 1)% IV: (2 ± 1)% V: (44 ± 9)% VI: (52 ± 4)%	III + poly: (45 ± 2)% IV: (13 ± 1)% V: (48 ± 3)% VI: (3 ± 3)%
pH 8.5	$(2.9 \pm 0.8) \times 10^{-7}$	$(1.2 \pm 0.1) \times 10^{-7}$	$(7.3 \pm 0.4) \times 10^{-9}$	III + poly: (3 ± 1)% IV: (6 ± 1)% V: (63 ± 6)% VI: (27 ± 3)%	III + poly: (5 ± 4)% IV: (13 ± 1)% V: (58 ± 2)% VI: (24 ± 1)%	III + poly: (11 ± 2)% IV: (10 ± 2)% V: (85 ± 4)% VI: (3 ± 3)%

	Eh(mV) vs. NHE			Solid phase		
	25°C	60°C	90°C	25°C	60°C	90°C
pH 5.9	342 ± 10	451 ± 10	360 ± 10	mostly amorphous with some crystallinity, contain carbonate and Pu(IV) polymer.		
pH 7.0	126 ± 10	386 ± 10	376 ± 10			
pH 8.5	259 ± 10	241 ± 10	133 ± 10			

Table III. Summary of results for solubility experiments on americium in J-13 groundwater at pH 5.9, 7.0, and 8.4 and at 25°, 60°, and 90°C.

	Steady-state concentration (M)			Oxidation state in supernatant solution		
	25°C	60°C	90°C	25°C	60°C	90°C
pH 6.0	$(1.8 \pm 0.6) \times 10^{-9}$	$(2.5 \pm 0.7) \times 10^{-6}$	$(1.7 \pm 1.9) \times 10^{-9}$	III: 100%	III: 100%	NA
pH 7.0	$(1.2 \pm 0.3) \times 10^{-9}$	$(9.9 \pm 9.2) \times 10^{-9}$	$(3.1 \pm 1.7) \times 10^{-10}$	III: 100%	III: 100%	NA
pH 8.4	$(2.4 \pm 1.9) \times 10^{-9}$	$(1.2 \pm 1.3) \times 10^{-8}$	$(3.4 \pm 2.1) \times 10^{-10}$	III: 100%	III: 100%	NA

	Eh(mV) vs. NHE			Solid phase		
	25°C	60°C	90°C	25°C	60°C	90°C
pH 5.9	331 ± 10	393 ± 10	NA	$AmOHCO_3$ hexagonal	$AmOHCO_3$ orthorhombic	$AmOHCO_3$ hexagonal
pH 7.0	361 ± 10	385 ± 10	NA	$AmOHCO_3$ orthorhombic	$AmOHCO_3$ orthorhombic	$AmOHCO_3$ orthorhombic
pH 8.4	182 ± 10	343 ± 10	NA	$AmOHCO_3$ orthorhombic	$AmOHCO_3$ orthorhombic	$AmOHCO_3$ orthorhombic

2. PURPOSE AND OBJECTIVE

Yucca Mountain, Nevada, was identified for site characterization as a potential site for a repository of high-level nuclear waste As a worst case scenario, intrusion of water into the repository must be considered for risk assessment. Water moving through the emplacement area towards the accessible environment can transport radionuclides in two ways: either as dissolved species in the water or as particulate material by the water. The Yucca Mountain Site Characterization Plan (SCP) requires "Studies to Provide the Information Required on Radionuclide Retardation by Precipitation Processes along Flow Paths to the Accessible Environment" before licensing and construction of the repository.[1] The purpose of this study is to supply data for calculating radionuclide transport along potential transport pathways from the repository to the accessible environment. Data derived from solubility studies are important for validating geochemical codes that are part of predictive radionuclide transport models. Such codes should be capable of predicting the results of solubility experiments. Furthermore, agreement between geochemical calculations and experimental results can validate the thermodynamic data base used with the modeling calculation.

To predict behavior at higher temperatures, data bases used for modeling calculations must contain data on thermodynamic functions at elevated temperatures. To date, many of these data are unavailable and are therefore estimated by extrapolation from lower temperature data. Agreement between modeling calculations and experimental results would also validate such estimates, whereas significant discrepancies would identify the need for data base improvement. Improvements can be made by filling the gaps with generic experimental data.

In addition, experimental solubility data also provide the source terms or the starting concentrations for experimental sorption studies. To be valid, sorption studies should be conducted at or below the solubility limit because only soluble species can be transported and participate in the sorption process.

In selecting these experiments, we have considered the generic U.S. Nuclear Regulatory Commission (NRC) technical position titled "Determination of Radionuclide Solubility in Groundwater for Assessment of High-Level Waste Isolation."[2] This technical position served as guidance for our experiments to determine radionuclide solubility. It requires that if radionuclide solubility is used as a factor in limiting radionuclide release, experiments must be designed to determine solubility under site-specific conditions.

Radionuclide concentrations in water passing through the emplacement area can be limited by two mechanisms: low dissolution rates of the solid waste form or solubilities of individual radionuclides. If solid waste dissolution rates are low enough, it may not be necessary to depend on solubilities to limit radionuclide concentrations. However, the solid waste forms have not yet been determined, and therefore the dissolution rates of the solid waste are unknown. Determination of radionuclide solubility limits provides an upper bound on radionuclide concentrations in solution and provides a basis for extrapolation to long-term behavior. The rate of groundwater flow through the waste is expected to be sufficiently slow to permit saturation of water with radionuclides. Dissolution limited by saturation will provide maximum concentration limits. Therefore, an assessment of radionuclide release rates using a saturation-limited dissolution model represents the most conservative approach possible.

As radionuclides are transported along flow paths to the accessible environment, changing conditions of the water (pH, Eh, oxidation state, and concentrations of complexing species) can alter solubilities. Decreases in solubility can decrease radionuclide concentrations. A knowledge of radionuclide solubilities under the conditions along possible flow paths is necessary to assess this scenario. Solubility studies are very time-consuming because long times are often needed to reach steady-state conditions. Because we cannot investigate every possible solubility scenario, we selected pH and temperature values to bracket the expected range of conditions by choosing parameters that represent lower and upper limits.

Neptunium, plutonium, and americium are expected to be sparingly soluble with solubility-limited dissolution rates. Water samples with compositions that bracket the range of waters expected in the vicinity of Yucca Mountain were chosen for solubility measurements.[3] These samples come from two sources. Water from Well J-13 is a reference water for the unsaturated zone near the proposed emplacement area. Well UE25p#1 taps the carbonate aquifer that underlies the emplacement horizon. This water has an ionic strength and total carbonate content higher by approximately an order of magnitude than Well J-13 water. Well J-13 water represents natural water with the highest concentrations of dissolved species expected in the vicinity of Yucca Mountain. The water from both wells is oxidizing. Generally, radionuclide solubility studies under oxidizing conditions lead to higher solubilities for a number of radionuclides than would occur under mildly or strongly reducing conditions. These experiments will therefore provide conservative results. In this study we are reporting on the results in J-13 water.

The maximum temperature of the host rock in which liquid water is present is expected to be limited by the boiling point of water at Yucca Mountain (95°C). The solubility experiments that use Well J-13 water were conducted at temperatures between 25 and 90°C. This span covers the range from pre-emplacement temperatures to the maximum temperature at which solubility would be important.

3. CONCEPT OF SOLUBILITY STUDIES

Solubility establishes an upper limit for the dissolved components in the source term for radionuclide migration from a repository. Studies of the solubility of radionuclides in groundwaters from a repository horizon will provide limits on their potential concentrations in those waters. Such limits are important for (1) validating an essential part of the radionuclide transport calculations and (2) providing guidance in choosing the maximum starting concentrations for radionuclide sorption experiments. Compared with multi-parameter transport models, laboratory solubility experiments are controlled by

fewer variables. If geochemical codes such as EQ3/6, are to be included in the transport model, the model should be capable of predicting the results of solubility experiments.

Complete solubility experiments should provide detailed knowledge of (1) the nature and chemical composition of the solubility-controlling solid, (2) the concentration of the components in solution, and (3) the identity and electrical charge of the species in the solution phase.

Meaningful thermodynamically defined solubility studies must satisfy four criteria: (1) attainment of equilibrium conditions, (2) determination of accurate solution concentrations, (3) attainment and identification of a well-defined solid phase, and (4) knowledge of the speciation/oxidation state of the soluble species at equilibrium.

3.1. Oversaturation and Undersaturation

Ideally, solubility experiments should approach solution equilibrium from both oversaturation and undersaturation. The approach from oversaturation consists of adding an excess amount of the element in soluble form to the aqueous solution and then monitoring the precipitation of insoluble material until equilibrium is reached. The solid formed must then be isolated and characterized. The approach from undersaturation consists of dissolving a well-defined solid in an aqueous solution until equilibrium is reached. In both cases, the solution concentration is measured as a function of time until equilibrium is reached.

Kinetic processes will control the equilibration speed in solubility experiments. Some solutions equilibrate rapidly, others more slowly. It must be demonstrated that equilibrium is reached. This can be accomplished by experimentally determining (for both oversaturation and undersaturation experiments) the solution concentration as a function of time. When the concentration stays constant for several weeks, it is assumed that equilibrium has been established. Because this assumption is based on judgment, the term "steady state" instead of "equilibrium" is more precise. The U.S. Nuclear

Regulatory Commission (U.S. NRC) defines "steady state" as "the conditions where measurable changes in concentrations are not occurring over practical experimental times." [2] At steady state, thermodynamic forces may still change the solution composition: solids may become less soluble as they change from a higher to a lower free energy. The change may be very slow and may require very long or even infinite experimental times, which are not practical.

Despite this constraint, time-limited laboratory solubility experiments can supply valuable information. They provide good estimates on the upper limit of radionuclide concentrations in solution because the experimentally determined steady-state concentrations are higher than the equilibrium concentrations.

A reliable method of proving that a steady state has been reached is to approach equilibrium from both oversaturation and undersaturation. When these two experimental approaches independently produce equal solution concentrations, the data are considered reliable. For unknown solubility systems, one should first perform experiments approaching steady-state concentration from oversaturation and then characterize the solids. This has the advantage of not specifying the solid that controls solubility but of allowing the system under investigation to determine the solid that will precipitate. These solids should be synthesized for use in confirmation experiments that approach steady state from undersaturation. In this study we are reporting results for the oversaturation experiments.

3.2. Phase Separation

The second criterion for meaningful solubility experiments is the derivation of accurate solution concentrations. This requires that phase separations must be as complete as possible. The separation of the solid from the solution often represents a significant practical problem in measuring solubility. Apparently higher or lower solubilities, compared with the steady-state values, can result from incomplete phase separation or from

sorption of solute during and after the separation. Incomplete phase separations (leaving some of the solid with the solution phase) lead to higher radionuclide solubilities. Lower solubilities are measured if constituents of the steady-state solution have been sorbed on filters during a filtration and on container walls after the separation.

Experimentally, the solids and solutions are separated on the basis of differences in size (via filtration) or density (via sedimentation or centrifugation). Filtration is the more commonly applied technique because it physically partitions the solute and solids. Ultrafiltration (i.e., filtration using membranes ≤ 0.1 μm) can effectively remove solids and colloidal particles from aqueous solution. A potential problem with ultrafiltration is adsorption of soluble species on ultrafiltration membranes. Effective filters for solubility studies must pass soluble species quantitatively; that is, either the filter should have no active sorption sites at all or any such sites should be irreversibly blocked. Filters are adequate if they have a small enough pore size to retain the solids and colloids and if they also show no sorption or only minimal sorption during multiple filtrations. Because adsorption of soluble radionuclide species on filters can be dependent on the solution's pH and on the solution species, it is mandatory to verify that possible sorption sites are indeed blocked. Usually the sorptive sites on a filter and filter housing are blocked by preconditioning of these materials. The filter is preconditioned by filtering a volume of the respective radionuclide solution through it and then discarding the filtrate. The volume required for preconditioning is determined experimentally. Details for this procedure are given in Section "4.5 Phase Separation."

3.3. Solid Phase

Solubility depends strongly on the state of the solid phase. Thermodynamically meaningful results require the existence of a well-defined solid phase, which ideally consists of crystalline material. The solids formed from the oversaturation in solubility tests must be clearly identified by physical or chemical characterization methods. Only when

identified unambiguously can the solid be synthesized for use in undersaturation solubility tests. Radionuclide solids formed in laboratory experiments and in nature are often thermodynamically ill-defined amorphous precipitates. Most amorphous solids, however, will become more crystalline with time. Freshly precipitated microcrystalline solids can also convert in time to a macrocrystalline material. Improved bonding at the lattice surface results in decreasing surface area. Thus the crystalline solid of higher free energy changes to one of lower free energy (Ostwald ripening, Ostwald step rule) and become less soluble.[4,5,6,7]

5.4. Determination of Oxidation States and Speciation

Information on oxidation states and speciation of the radionuclides in steady-state solubility solution is important for transport models simulating migration and sorption along the flow path to the accessible environment. The charge and speciation of radionuclides will control their sorption and transportation in the geologic host. Speciation measurements identify complexes that may form between radionuclides and complexing ions present in the groundwater near the repository. The oxidation state in solution describes the charge of soluble species, and speciation describes their chemical nature. Radionuclides can have a single or several different oxidation states in solution. They can be present as simple ions or as complexes. When the ions react with one or several other solution components, they can form soluble complexes.

Oxidation states and speciation in solution are commonly determined by (1) adsorption spectrophotometry, (2) ion exchange chromatography, (3) solvent extraction, (4) coprecipitation, (5) potentiometry and (6) electrochemistry. Of these methods, only absorption spectrophotometry can provide information on speciation, while the others identify only the oxidation state in solution.

Absorption spectrophotometry in J-13 water has a detection limit of about 10^{-4} M. This relatively high concentration limits the application of spectrophotometry for

speciation determination in solutions from radionuclide solubility studies because the solubilities can be several orders of magnitude below 10^{-6} M. Photoacoustic Spectroscopy (PAS) provides much greater sensitivity, approaching 10^{-8} to 10^{-9} M. [8,9,10,11,12]

The methods listed above as 2 through 6 determine only the oxidation state in solution because they cannot determine species. They detect the oxidation state of ions indirectly. This process is different from absorption spectrophotometry, which detects the solution species directly. The indirect methods, however, detect very small concentrations (10^{-10} M and below), which is useful for radionuclide solubility studies. Solvent extraction and coprecipitation are often used successfully to determine the oxidation states of ions in very dilute solutions.[13] Ion exchange chromatography is less reliable for this purpose because the exchange resin often reduces the solution ions, which gives incorrect results for the oxidation state distribution. Electrochemical detection reduces or oxidizes the solution ions and measures the potentials of the reduction and oxidation reactions, respectively. The potential then identifies the individual ion. Electrochemistry needs fast kinetics and reversible thermodynamics for the reduction or oxidation step. These experiments greatly limit the method because many radionuclide ion redox reactions are irreversible and slow (e.g., the reactions of NpO_2^+/Np^{4+}, PuO_2^+/Pu^{4+}).

The oxidation state of plutonium and americium species in solution were determined by a solvent extraction and coprecipitation technique.[13] The neptunium solution species were determined by spectrophotometry because the solution concentration was greater than 10^{-6} M.

The sensitivity of the available analytical methods for plutonium limits this part of our study. PAS is needed to determine directly the species in the supernatant solutions of the solubility experiments at submicromolar concentrations. A related activity is currently developing this capability for the YMP. Once PAS becomes available, it will be used.

4. EXPERIMENTAL DETAILS

We studied the solubilities of neptunium, plutonium, and americium at 25°, 60°, and 90°C and respective pH values of 5.9, 7.0, and 8.5. Measurements were made in an inert-atmosphere box to avoid contamination of solutions by atmospheric CO_2. The solubilities were studied from oversaturation by injecting a small amount, usually between 0.5 and 1 ml, of actinide stock solution into 80 ml of groundwater obtained from Well J-13. The analysis of the water composition is listed in Table IV. The J-13 groundwater was sampled at the site by Los Alamos personnel. It was filtered at Los Alamos before it was shipped to LBL. The water's natural carbondioxide partial pressure (p_{CO2}) could not be preserved during filtration and shipping. For the experiments, however, the natural state was induced by re-equilibrating the water with CO_2 gas. Details of this procedure are described in paragraphs "4.3. Pressure Control System," and "4.4. Solutions." Details of the filtration are described in paragraph "4.4. Solutions." The polyethylene shipping bottle was leached with acid and distilled water prior to its use for the groundwater. The leaching removes possible trace-level contaminants that may alter the composition of the J-13 water.

4.1. Controlled-Atmosphere Glove Box

Due to the radiation hazard of the actinide elements under investigation, all experimental work was performed in glove boxes. External CO_2 control of the experimental solutions requires the exclusion of atmospheric CO_2. To satisfy both conditions, we used a controlled-atmosphere glove box.

Table IV. Well J-13 water composition.[3]

Species	Concentration mM
Ca	0.29
Mg	0.072
Na	1.96
K	0.136
Li	0.009
Fe	0.0008
Mn	0.00002
Al	0.0010
SiO_2	1.07
F^-	0.11
Cl^-	0.18
SO_4^{2-}	0.19
NO_3^-	0.16
Alkalinity	2.34 mequiv/L
Total carbonate	2.81
pH	7.0
Eh	700 mV

4.2. Control System for pH and Temperature

Because the solubilities are highly sensitive to pH and temperature changes, close control of these parameters is necessary. We designed a computer-operated control system (pH-stat) to maintain the aqueous actinide solutions at constant temperatures and pH values for the solubility experiments.[14] The pH-stat records and adjusts the pH values of the experimental solutions (J-13 water) at the target values with standard deviations not exceeding 0.1 pH unit. It uses small amounts (usually between 5 to 50 microliters) of dilute (0.05–0.1 M) $HClO_4$ or NaOH solution for the pH adjustments. The water chemistry was not substantially affected by this adjustment. Temperatures from 25° to 90°C were controlled within less than 1°C.

4.3. Pressure Control System

We designed and manufactured a pressure regulation system to maintain the well waters used in experiments at their nominal carbonate concentrations when their temperatures and pH values are adjusted to conditions differing from their natural state. The system also ensured that no significant evaporative loss of the solutions occurred at elevated temperatures.

4.4. Solutions

The actinide stock solutions were prepared by using established methods.[15] $^{237}Np(V)$ and $^{243}Am(III)$ stock solutions were prepared by dissolving their oxides in HCl. Stable neodymium(III) was used on several occasions as an analogue for americium(III). It was prepared by dissolving Nd_2O_3 in $HClO_4$. The solution was then spiked with purified $^{241}Am(III)$ tracer to enable the use of nuclear counting for the determination of the neodymium solution concentrations. Further details for these $^{241}Am/Nd$ mixtures are given in section 5.3. $^{239}Pu(IV)$ stock was prepared from plutonium metal. The actinide solutions were purified from possible metal contaminants by ion exchange

chromatography. For neptunium and plutonium, anion exchange was used, while cation exchange was employed for americium. The purity of these stock solutions was tested by spark emission spectroscopy, and no contaminants were found above the detection limits of the method. The solutions were converted to a non-complexing perchlorate system. The neptunium and plutonium stock solutions were in the oxidation state +6 after their conversion to perchlorate and were reduced electrolytically to NpO_2^+ and Pu^{4+}, respectively.[16,17,18] Valence purity was established by absorption spectrophotometry.[19,20]

The groundwater, was filtered through 0.05 μm polycarbonate membrane filters (Nuclepore Corp., Pleasanton, CA). This filtration was carried out by Los Alamos personnel prior to shipping the J-13 water sample to LBL. The actinide stock solutions, and all other solutions utilized in this experiment were filtered through 0.22 μm polyvinylidene difluoride syringe filter units (Millipore Corp., Bedford, MA). Filtration was used to remove suspended particulate material, e.g., dust or silica, that could absorb the actinide ions to form pseudocolloids. Before the addition of actinide stock solutions to the J-13 water, a small amount of CO_2-free sodium hydroxide solution was added in order to keep the pH values at or above the desired solution pH. Letting the pH drop below the target value would necessitate addition of concentrated base to the system while the actinide ion is already present in the solution. Addition of strong base can result in unpredictable microprecipitation and formation of microcolloids.

The well water's total dissolved carbonate (2.81×10^{-3} M) was preserved at each individual pH and temperature by equilibrating the solution with mixtures of CO_2 in argon.[3] The amount of CO_2 at a given pH and temperature was calculated from Henry's constant and the dissociation constants of carbonic acid from literature data.[21] If the value at the given ionic strength and temperature was not available, the number was derived by interpolation of adjacent values. The concentrations of the equilibration gas mixtures are given in Table V.

Table V. Concentrations (in percent) of carbon dioxide gas in argon to maintain a total dissolved carbonate concentration of 2.81×10^{-3} M in J-13 groundwater at different pH and temperatures.

	25°C	60°C	90°C
pH 5.9	6.06	9.67	18.58
pH 7.0	1.57	2.35	4.05
pH 8.5	0.0573	0.0877	0.142

The test solutions were kept in 90 ml cells that were made of either Teflon Perfluoralkoxy (TPFA) or Polyether etherketone (PEEK). The PEEK cells were for the ^{243}Am experiments because PEEK is more radiation resistant than TPFA. All cells had sealed ports at the top that accommodate the permanent emplacement of a pH electrode, an opening to draw samples, and three 1/16" diameter Teflon lines for addition of acid, base, and the CO_2-argon mixture. The temperature was controlled by placing the test cells in a heated aluminum block of LBL design. The electric heater was mounted on an orbital shaker (Lab-Line Inc., Melrose Park, IL), and all solutions were shaken continuously at approximately 100 rpm. The solutions' pH values were controlled by a computer-operated pH control system (pH-stat).[14] The pH-stat was designed and assembled at LBL. It records and adjusts the pH values automatically over the required long periods of time with standard deviations generally not exceeding 0.1 pH unit. We could not use the pH-stat for the 90°C experiments. The combination pH electrodes (Beckman Instr. Inc., Model 39522), used at 25° and 60°C to monitor the solutions pH values, deteriorated rather rapidly when in contact with the 90°C solutions. The deterioration is mainly due to the dissolution of the Ag/AgCl layer of the reference electrode wire and also of the wire used in the pH sensing compartment itself; the solubility of AgCl increases approximately 240 times when the temperature changes from 10° to 100°C. Although the manufacturer claims the working range of these electrodes is up to 100°C, we were unable to use the electrodes continuously with the pH-stat. Therefore, we performed the pH adjustment every day by hand: the Beckman pH electrodes were removed from the individual experimental solutions after each adjustment and reintroduced for each new measurement. Before measuring the pH, the electrodes were calibrated and remained in the solutions for several hours to come to temperature equilibrium. For the americium solubility experiments, we used Ross combination electrodes (Orion). These electrodes are stable at 95°C because they have a $I_2/2I^-$ internal reference electrode instead of a Ag/AgCl electrode. The electrolyte bridge of the Ross electrodes however,

leaked substantially more than those of the Beckman electrodes. Placing them permanently into the test solutions would have altered the composition of the J-13 water. Therefore, we also had to adjust the pH for this experiment by hand in the same manner as we did with the Beckman pH electrodes.

4.5. Phase Separation

Achievement of steady-state conditions for the solubility measurements was monitored by sampling aliquots of the solution phases and analyzing for the respective radioisotope as a function of time. We used Centricon-30 centrifugal filters (Amicon Corp., Danvers, MA) for separating the phases of the neptunium, plutonium, and americium solutions. For the separations, the centrifuge (High-speed centrifuge, Model HSC-1000, Savant Instruments Inc.) was heated with a circulating water bath to the appropriate temperature. The filters contain a YM-type membrane with a calculated pore size of 4.1 nm. To ascertain that we achieved complete phase separation and minimal adsorption on the filters during the preparation of the solution assays, we conducted a series of filtration tests.

For each solution, these tests were done at different times during the equilibration period. We used one filter per solution and filtered consecutive portions of 500 µL solution through it. Each filtrate was acidified to minimize sorption in the filtrate-collection container and an assay was taken. Then another 500 µL were filtered through the same filter, collected in a new container, and assayed. This is repeated until the assays show a constant concentration. The volume necessary to saturate the filter was the cumulative amount of volumes used until the assay concentration remained constant. The presaturation volume was radionuclide-dependent.

We determined and used the following preconditioning volumes: 500 µL, 1000 µL, and 2000 µL for the neptunium, plutonium, and neodymium/americium solutions, respectively.

4.6. Analysis

After separation of the solution and the solid phases, the two components were analyzed separately. Concentration measurements of the supernatants were made by counting liquid aliquots with a germanium low-energy counting system (LBL design). For ^{237}Np, ^{241}Am, and ^{243}Am the 29.38 keV, 59.54 keV, and 74.67 keV γ-ray lines were used, respectively. A waiting period of at least 30 days was required for the ^{243}Am samples before they could be assayed because the ^{243}Am was not at secular equilibrium with the ^{239}Np daughter at sampling. After this time, the 74.67 keV γ-line was resolved from the large Compton edge of the plutonium *K* x-rays and the 106.13 keV γ-line from the ^{239}Np decay.

^{239}Pu was analyzed by utilizing the U *L* x-rays coming from the α-decay of the plutonium. Possible contributions to the *L* x-rays from the decays of other radionuclides, also present in small amounts, were corrected by subtraction.[22] In selected cases, liquid scintillation counting was also used for plutonium concentration determinations (Packard Instr. Co., Dowers Grove, Ill., model Tri-Carb 460C). The two energy windows of the counter were set to discriminate properly between possible β-emitting solution contaminants and the plutonium α-radiation. Repeated sample counting and the observation of a constant count rate in the α-window ensured no β-contribution to the α-count.

4.7 Criteria for Steady-State Concentrations

Constant concentrations over time with minimal deviation during that time span are the criteria for determining the average steady-state concentration from the individual concentration measurements.

These limits depend on the solubility of the nuclide involved and the temperature of the experiment. High solubilities yield precise concentrations within short counting times; whereas, low solubilities yield concentration with large errors, even after very long counting times. Experiments at ambient temperatures lead to very consistent

concentrations. Elevated temperatures, however, lead to greater deviations in concentration because of the difficulties involved in maintaining elevated temperature during phase separation and sample preparation.

4.8. Eh Measurements

At the end of each solubility experiment, we measured the Eh with a platinum electrode versus a Ag/AgCl/sat. NaCl reference. We cleaned the platinum electrode with 6 M HNO_3 before and after each measurement. Readings were stable within 30 to 60 minutes. The electrode setup was checked with "Zobell Solution" before and after each measurement.[23,24] We measured the Eh values to supply future chemical modeling efforts (neptunium, plutonium, and americium solubilities in J-13 water solutions) with a reference value. Without modeling, however, the Eh measurements are only of limited value, because they may represent a combination of many different redox reactions for each individual solubility solution.

4.9. Identification of Solids

The solid compounds were analyzed by x-ray powder diffraction measurements. A few micrograms of each actinide precipitate were placed in a 0.33 mm diameter quartz capillary tube, and the tube was sealed with an oxy-butane microtorch. The tube was mounted in an 11.46 cm diameter Debye-Scherrer camera and then irradiated with x-rays from a Norelco III x-ray generator (Phillips Electronics, Inc.). Copper K_α radiation filtered through nickel was used. When the solids did not produce any pattern or when the pattern could not be assigned to any known compound, Fourier transform infrared-spectroscopy (FTIR) was applied. A small amount of each solid was placed between two pre-fabricated polished KBr windows, and the windows were then sealed at the rim with epoxy. Great care was taken to keep the outside of the KBr windows free of contamination. These samples were then analyzed by FTIR (Mattson Instr., Inc., Madison, WI,

model Sirius 100).

5. RESULTS AND DISCUSSION

5.1. Neptunium

5.1.1. Solubility

Results of the neptunium solubility studies are shown in Figure 1. The neptunium was initially introduced as NpO_2^+ into the J-13 groundwater. The steady-state concentrations and the solutions' Eh values are given in Table VI. Concentration profiles as a function of equilibration time and pH for 25°, 60°, and 90°C are shown in Figures 2, 3, and 4, respectively. The individual measurements are listed in Appendix A. At each temperature the neptunium solubility decreased with increasing pH. No significant temperature dependence was found within each individual temperature studied.

5.1.2. Speciation

The supernatant solutions were analyzed by absorption spectrophotometry to determine the oxidation state and speciation. The spectra are shown in Figures 5, 6, and 7 for 25°, 60°, and 90°C, respectively. The supernatant samples from the experiments at pH 6, 25° and 60°C were diluted with J-13 water to keep the absorbance value within the sensitivity limit of the spectrophotometer used. With the exception of the spectra at 90°C and pH 6 and 7, all other spectra show the NpO_2^+ main absorption band at 980 nm and an additional band at 992 nm that increases with pH due to the increasing carbonate complexation. The band at 980 nm is characteristic for uncomplexed NpO_2^+. The band at 992 nm is typical for neptunyl(V) carbonate complexation.[25]

From the difference between the total amount of neptunium (determined by γ-spectroscopy) and the free NpO_2^+ (determined from the 980 nm peak), we calculated the amount of neptunium present as carbonate complex. The results for the amount of carbonate complexation in the steady-state solutions are given in Table VII. Because the

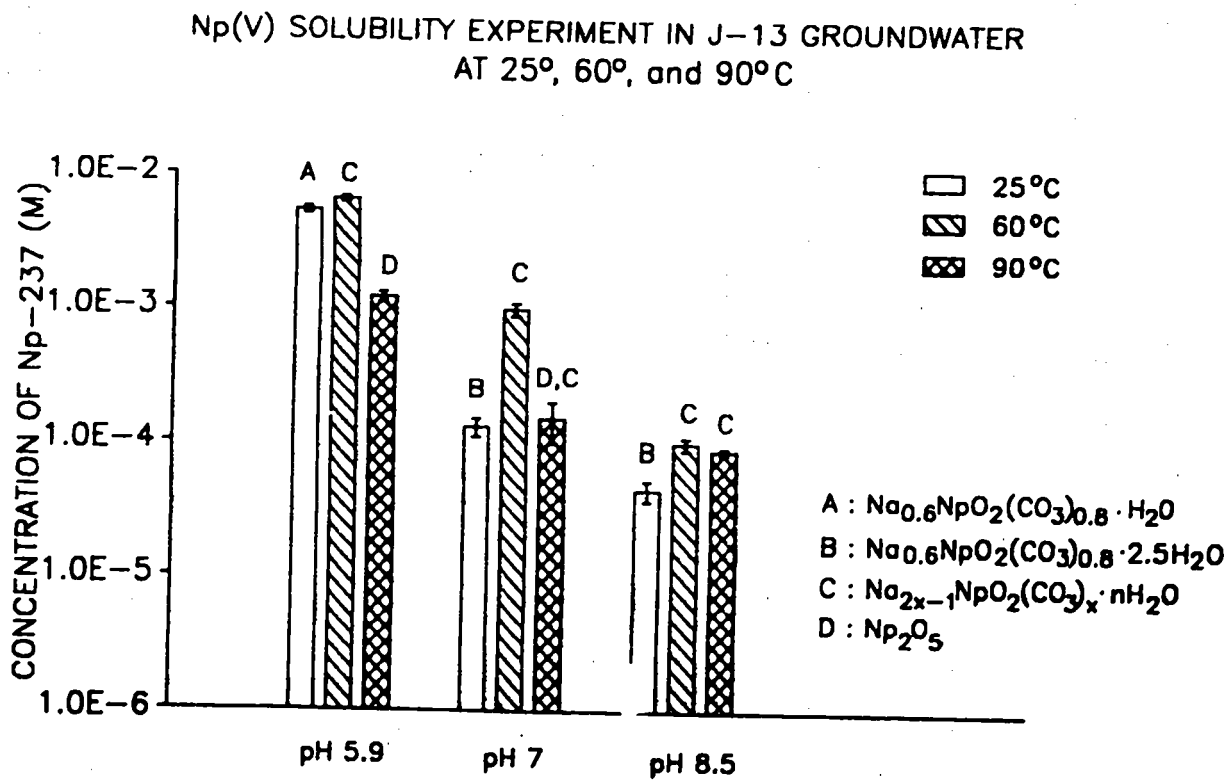

Figure 1. Results for NpO_2^+ solubility experiments in J-13 groundwater as a function of pH and temperature.

Table VI. Comparison of steady-state solution concentrations for neptunium in J-13 groundwater at 25°, 60°, and 90°C.

Np	25°C	
pH	conc. (M)	Eh (mV vs. NHE)
5.9 ± 0.1	$(5.3 \pm 0.3) \times 10^{-3}$[c]	588 ± 10
6.9 ± 0.1	$(1.3 \pm 0.2) \times 10^{-4}$[b]	482 ± 10
8.5 ± 0.1	$(4.4 \pm 0.7) \times 10^{-5}$[d]	497 ± 10

Np	60°C	
pH	conc. (M)	Eh (mV vs. NHE)
5.9 ± 0.1	$(6.4 \pm 0.4) \times 10^{-3}$[a]	440 ± 10
7.1 ± 0.1	$(9.8 \pm 1.0) \times 10^{-4}$[a]	325 ± 10
8.5 ± 0.1	$(1.0 \pm 0.1) \times 10^{-4}$[b]	215 ± 10

Np	90°C	
pH	conc. (M)	Eh (mV vs. NHE)
5.9 ± 0.2	$(1.2 \pm 0.1) \times 10^{-3}$[b]	392 ± 10
7.2 ± 0.2	$(1.5 \pm 0.4) \times 10^{-4}$[a]	299 ± 10
8.4 ± 0.1	$(8.9 \pm 0.4) \times 10^{-5}$[c]	159 ± 10

(a-e): the steady-state values were determined from the last a) 5, b) 6, c) 9, d) 12, e) 15 samplings.

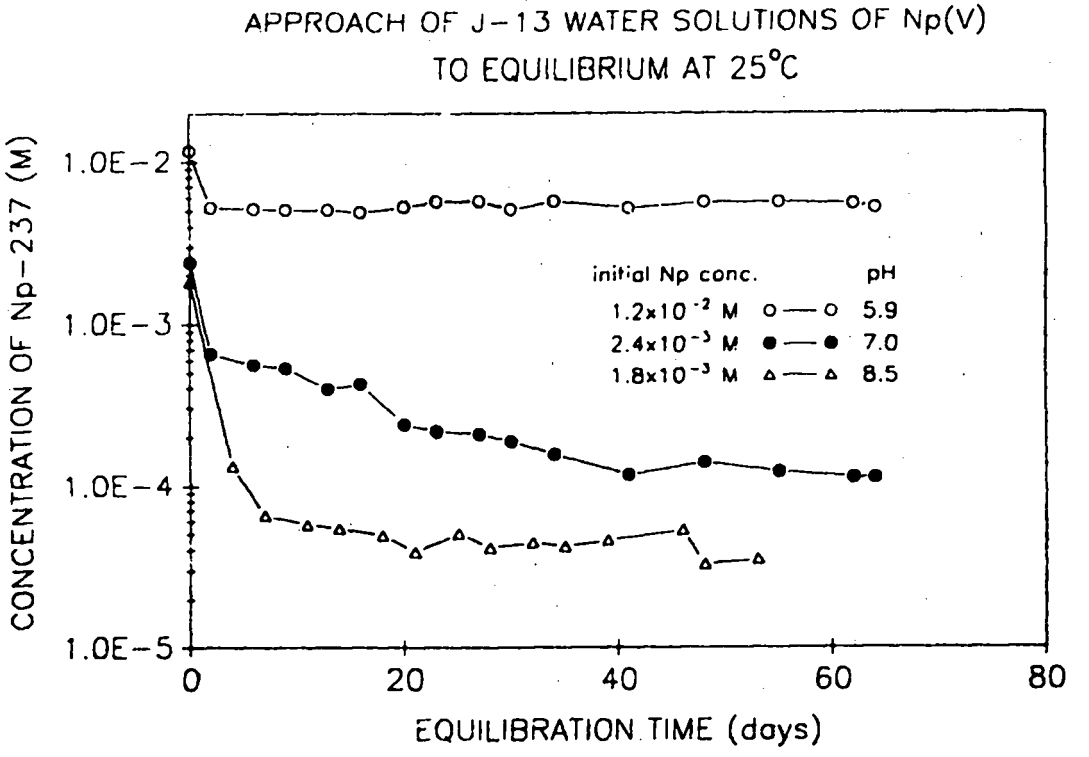

Figure 2. Solution concentations of ^{237}Np in contact with precipitate obtained from supersaturation of J-13 groundwater at 25°C as a function of time. pH 5.9 ± 0.1 (open circles), pH 6.9 ± 0.1 (filled circles), and pH 8.5 ± 0.1 (triangles). The neptunium was added initially (day 0) as NpO_2^+; initial concentrations were 1.2×10^{-2} M (pH 5.9), 2.4×10^{-3} M (pH 7), and 1.8×10^{-3} M (pH 8.5).

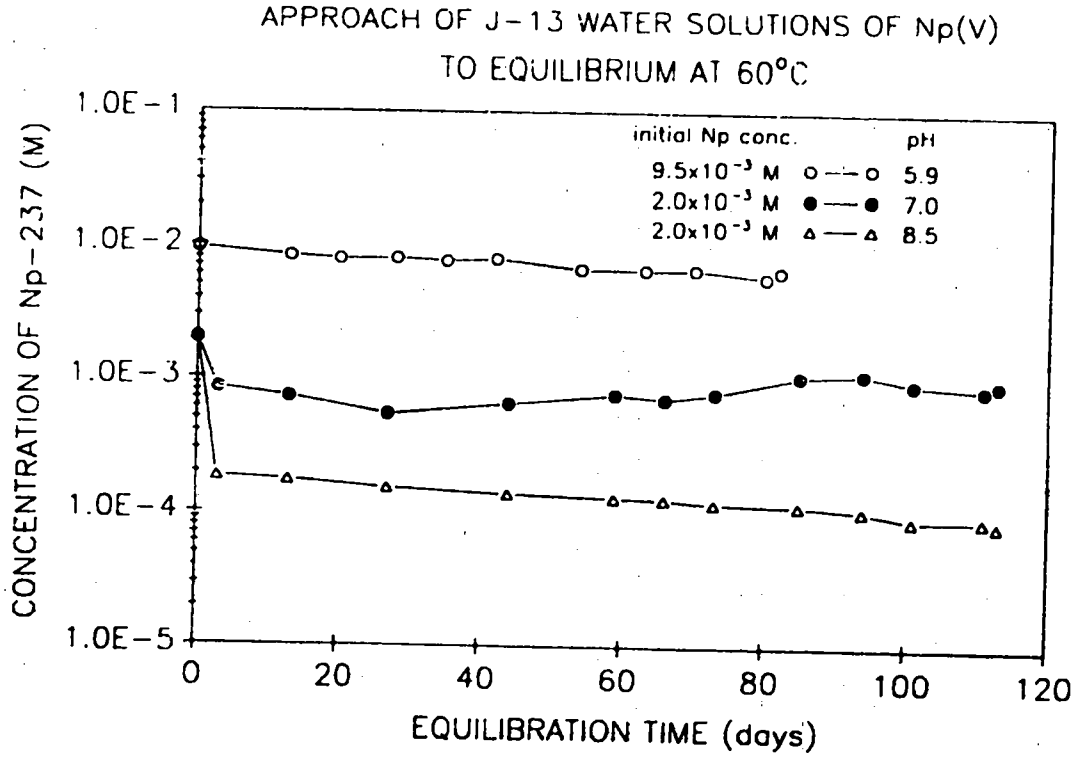

Figure 3. Solution concentrations of ^{237}Np in contact with precipitate obtained from supersaturation in J-13 groundwater at 60°C as a function of time. pH 5.9 ± 0.1 (open circles), pH 7.1 ± 0.1 (filled circles), and pH 8.5 ± 0.1 (triangles). The neptunium was added initially (day 0) as NpO_2^+; initial concentrations were 9.5×10^{-3} M (pH 5.9) and 2.0×10^{-3} M (pH 7 and 8.5).

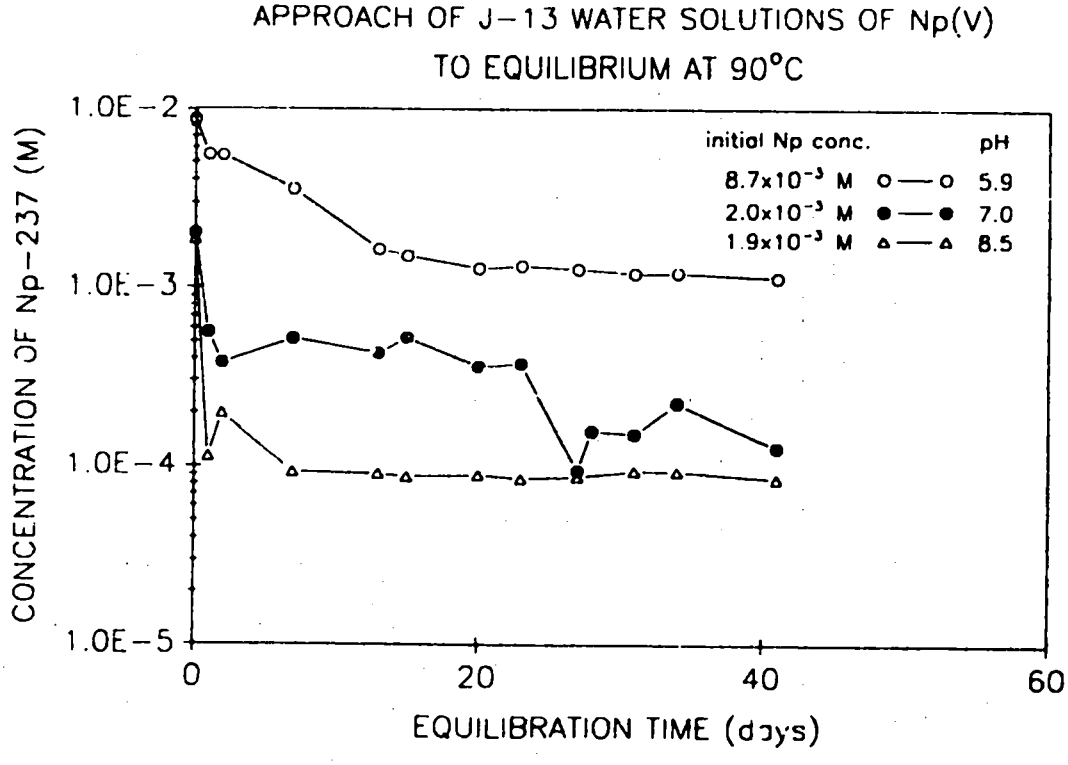

Figure 4. Solution concentrations of ^{237}Np in contact with precipitate obtained from supersaturation in J-13 groundwater at 90°C as a function of time. pH 5.9 ± 0.2 (open circles), pH 7.2 ± 0.2 (filled circles), and pH 8.4 ± 0.1 (triangles). The neptunium was added initially (day 0) as NpO_2^+; initial concentrations were 8.7×10^{-3} M (pH 5.9), 2.0×10^{-3} M (pH 7.2), and 1.9×10^{-3} M (pH 8.5).

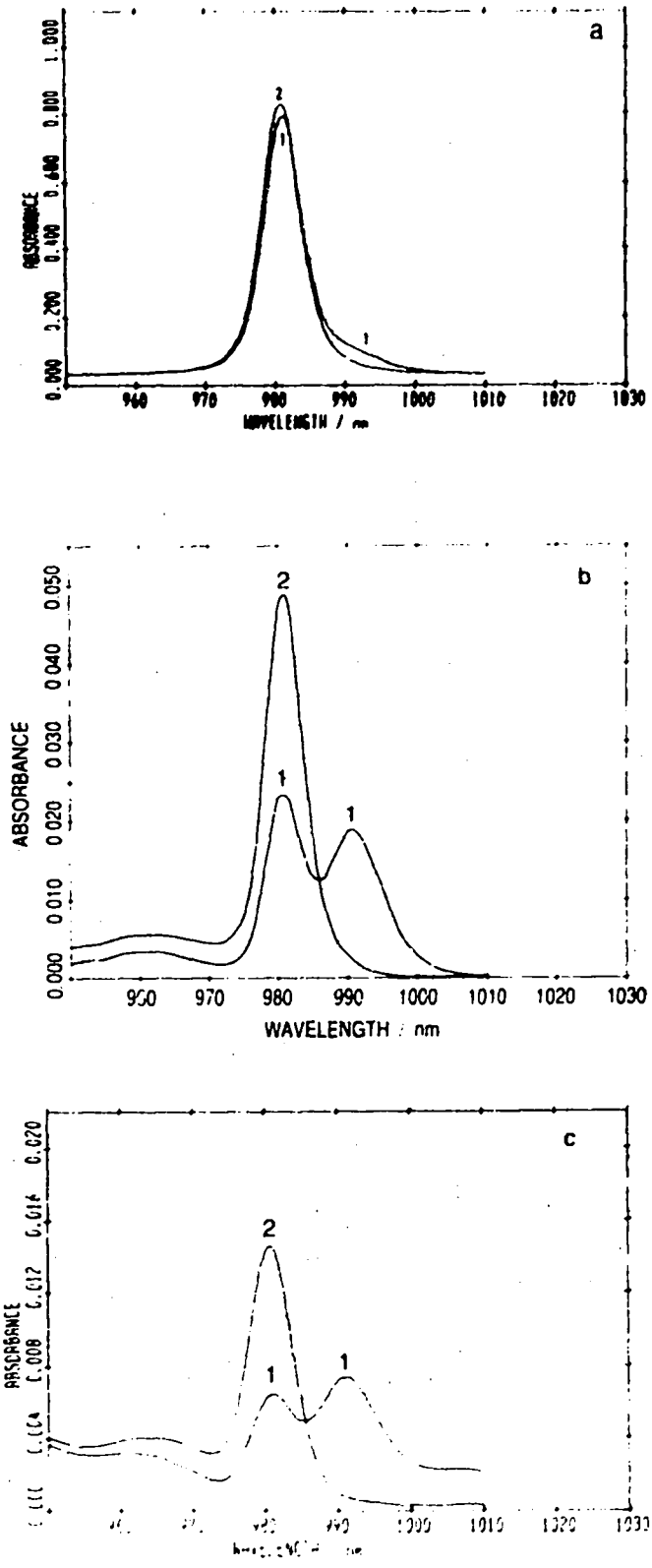

Figure 5. Near-IR absorption spectra of Np supernatant solutions at steady state formed in J-13 groundwater at 25°C in (a) pH 5.9, (b) pH 6.9, (c) pH 8.5: (a) at the experimental pH; (2) after acidification with $HClO_4$ to pH 0.

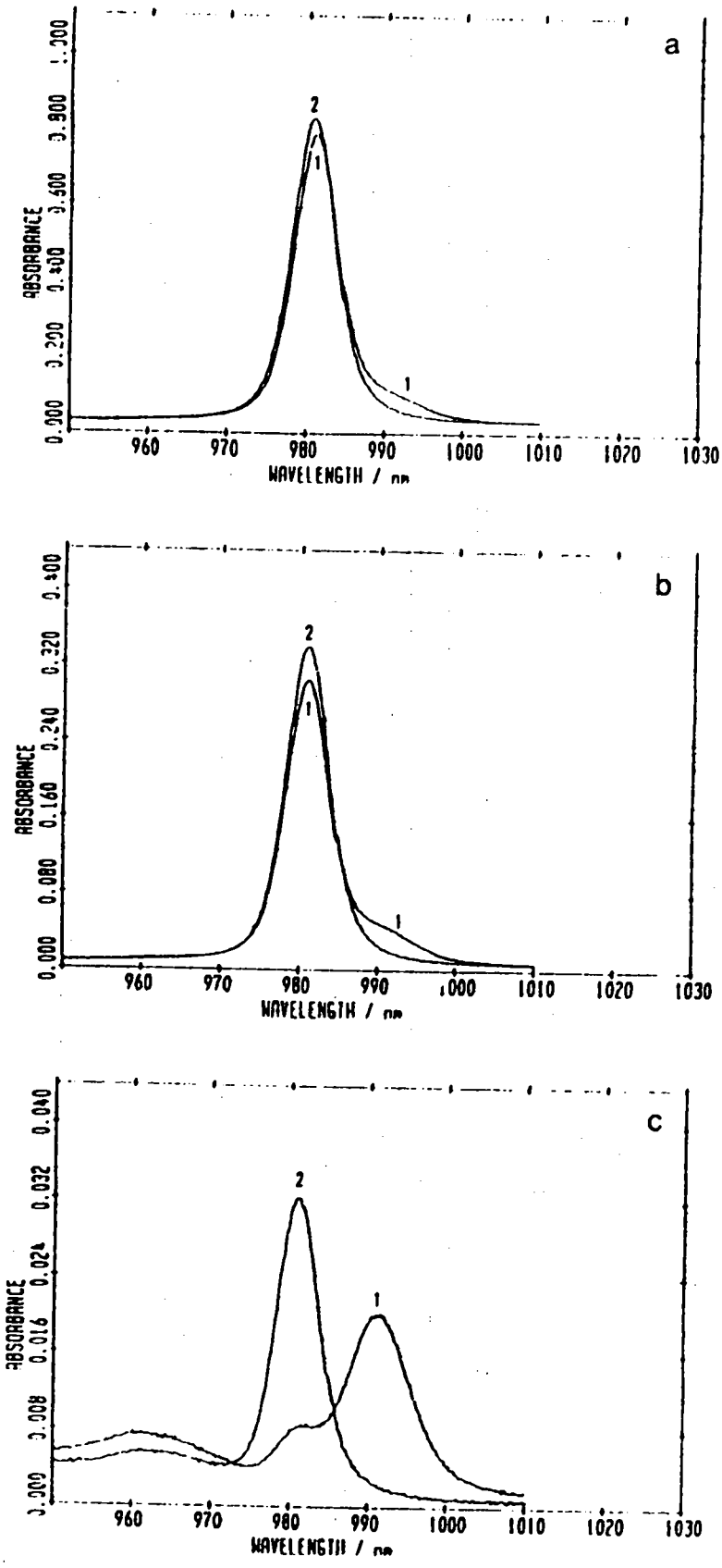

Figure 6. Near-IR absorption spectra of Np supernatant solutions at steady state formed in J-13 groundwater at 60°C in (a) pH 5.9, (b) pH 7.2, (c) pH 8.4: (1) at the experimental pH; (2) after acidification with $HClO_4$ to pH 0.

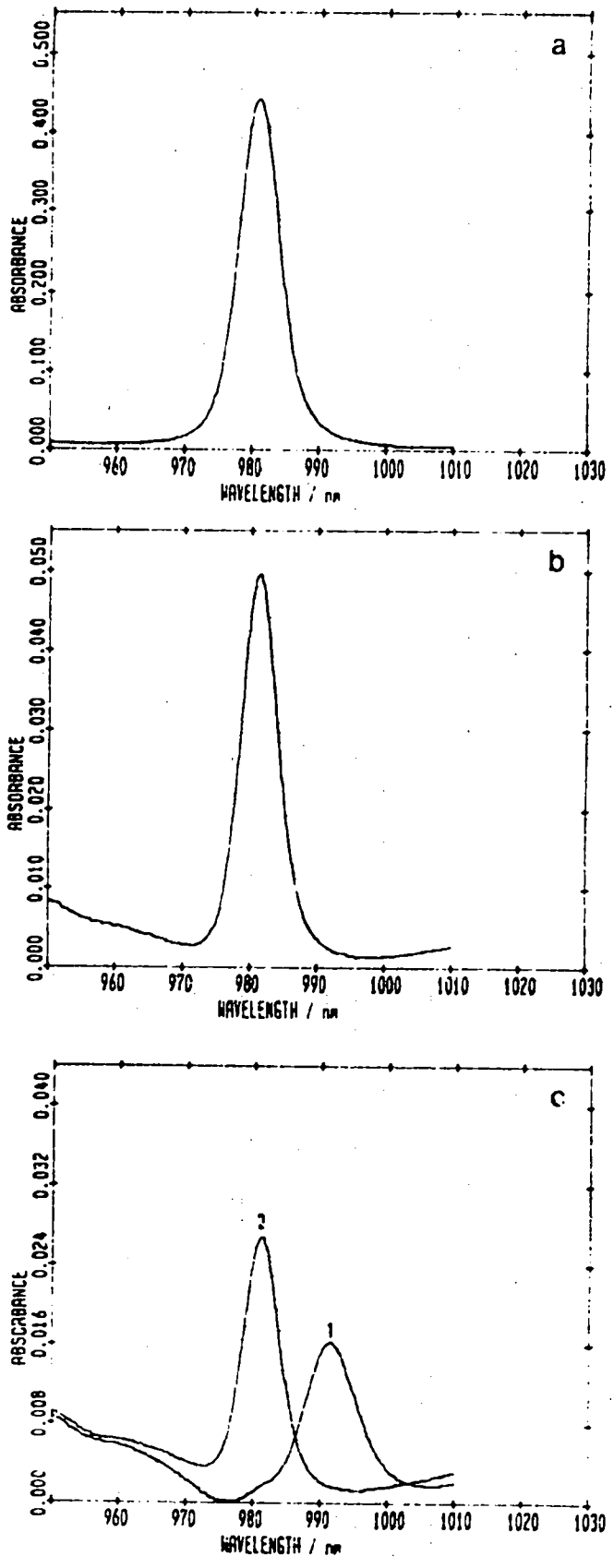

Figure 7. Near-IR absorption spectra of Np supernatant solutions at steady state formed in J-13 groundwater at 90°C in (a) pH 5.9, (b) pH 7.2, (c) pH 8.4: (1) at the experimental pH; (2) after acidification with $HClO_4$ to pH 0.

Table VII. Comparison of extent of carbonate complexation for steady-state solutions of neptunium in J-13 groundwater at 25°, 60°, and 90°C.

Np Carbonate Complexation								
25°C			60°C[a]			90°C[a]		
pH	NpO_2^+(%)	$NpO_2CO_3^-$(%)	pH	NpO_2^+(%)	$NpO_2CO_3^-$(%)	pH	NpO_2^+(%)	NpO_2CO_3(%)
5.9 ± 0.1	91	9	5.9 ± 0.1	92	8	5.9 ± 0.1	100	0
6.9 ± 0.1	46	54	7.1 ± 0.1	85	15	7.2 ± 0.1	100	0
8.5 ± 0.1	38	62	8.5 ± 0.1	16	84	8.4 ± 0.1	0	100

(a): distribution determined at ambient temperature

spectra of the 90°C and 60°C solutions were taken without controlling the temperature, the solubility and speciation may have possibly been perturbed. Therefore, the derived speciation results may be more semiquantitative.

After each solution was acidified with $HClO_4$ to pH 0, the absorption at 992 nm disappeared, and only the band at 980 nm was present. These facts show increased carbonate complexation with increasing pH for the 25° and 60°C series. The amount of carbonate complexing increased with increasing temperature for the pH 8.5 solutions. It decreased with increasing temperature for the pH 7 solutions. Very little carbonate complexation occurred for the pH 5.9 solutions at each temperature. In the 90°C experiments only the pH 8.4 solution contained carbonate complexes.

5.1.3. Identification of Solids

The precipitates formed in the neptunium solutions were collected by centrifugation, washed with a small amount of CO_2–free water, and dried with an argon jet. All precipitates at 25°C and 60°C had a bright lime green color. The precipitates formed in the solutions at 90°C had the following colors:

pH 5.9 – dark brown to black

pH 7.2 – light brown

pH 8.4 – light green

From the solution at pH 8.4, two different precipitates were isolated by fractionated centrifugation, because the wet solid appeared to be composed of a tan and a green phase. When dried, these solids became identically light green. X-ray powder diffraction patterns taken from the precipitates produced distinct lines; d-spacings and relative intensities are listed in Tables VIII, IX, and X for 25°, 60°, and 90°C, respectively.

A comparison of the 25°C solids with published patterns of $Na_{0.6}Np(O)_2(CO_3)_{0.8}\cdot 2.5H_2O$, $Na_{0.6}Np(O)_2(CO_3)_{0.8}\cdot nH_2O$, and $Na_3Np(O)_2(CO_3)_2\cdot nH_2O$ are

Table VIII. X-ray powder diffraction patterns of neptunium solid phases in J-13 groundwater at 25°, 60°, and 90°C and pH 5.9.

25°C		60°C		90°C	
d(Å)	I[a]	d(Å)	I[a]	d(Å)	I[a]
9.80	w	7.47	w	8.85	s
7.31	t	7.11	w–	7.55	w
6.22	t	5.09	s	7.15	m
4.93	w	4.81	w+	5.64	w+
4.80	w	4.46	m+	4.16	s
4.31	s	4.34	w	3.45	vs
3.96	s–	4.05	vs	3.27	w+
3.21	s–	3.72	w–	2.66	vs
3.05	w	3.34	s	2.58	w+
2.94	t	3.22	w	2.09	w–
2.71	m	2.93	w+	2.05	w
2.40	t	2.69	m+	1.93	m–
2.16	t	2.55	s+	1.84	w+
2.10	t	2.41	w–	1.80	m
2.06	t	2.28	m–	1.76	m
1.99	vs	2.21	w	1.74	w+
1.94	s	2.16	s	1.65	w–
1.73	m–	2.10	w–	1.61	m+
		2.02	w+	1.54	w
		1.98	t	1.51	t
		1.90	t	1.47	w+
		1.85	m–	1.43	m–
		1.80	m–	1.40	t
		1.65	m	1.34	s
		1.38	w–	1.30	w
		1.31	t	1.29	w–
		1.29	w–	1.28	w
		1.27	w	1.26	t
		1.24	t	1.23	w
		1.22	w–	1.21	w–
		1.19	w–	1.19	t
		1.15	t		

(a) Relative intensities visually estimated: vs = very strong, s = strong, m = medium, w = weak, t = trace.

* denotes diffuse bands.

Table IX. X-ray powder diffraction patterns of neptunium solid phases in J-13 groundwater at 25°, 60°, and 90°C and pH 7.

25°C		60°C		90°C	
d(Å)	I[a]	d(Å)	I[a]	d(Å)	I[a]
9.03	w	9.94	s	8.82*	s
8.53	w	9.14	t	7.05*	m–
6.92	s	7.52	w–	5.01	w–
4.91	m	6.27	w+	4.19	m
4.27	m	5.12	m+	4.04	m
4.01	m–	4.98	s	3.46	vs
3.63	w+	4.82	t	3.30	m–
		4.36	vs		
3.45	w	4.05	vs	2.67	s
3.22	s	3.33	m+	2.59	w–
2.92	m	3.23	m–	2.55	w+
2.82	w	3.08	w	2.27	w–
2.44	t	2.96	t	2.15	w
2.36	t	2.82	t	2.09	t
2.30	t	2.71	m+	2.05	t
2.16	t	2.63	t	2.02	t
2.13	t	2.55	s	1.94	w–
2.09	t	2.48	t	1.84	w+
2.03	w	2.42	w–	1.80	w+
1.99	t	2.35	w–	1.76	w
1.88	t	2.27	w+	1.74	w–
1.81	t	2.21	t	1.64	w
		2.16	s–	1.61	w
		2.11	t	1.59	t
		2.06	w	1.50	w+
		2.02	w+	1.34	m–
		1.94	w+	1.27	w–
		1.84	s–		
		1.80	m		
		1.65	m–		
		1.62	t		
		1.59	w–		
		1.50	m		
		1.47	w–		
		1.45	w–		
		1.41	w		
		1.37	w		
		1.34	t		
		1.29	w+		
		1.27	w+		
		0.79	w–		

(a) Relative intensities visually estimated: vs = very strong, s = strong, m = medium, w = weak, t = trace.

* denotes diffuse bands.

Table X. X-ray powder diffraction patterns of neptunium solid phases in J-13 groundwater at 25°, 60°, and 90°C and pH 8.5.

25°C		60°C		90°C (green phase)		90°C (tan phase)		(cont'd)	
d(Å)	I[a]	d(Å)	I[a]	d(Å)	I[a]	d(Å)	I[a]	d(Å)	I[a]
6.88	s	8.67	m	10.38	t	9.99	s–	1.84	m+
4.87	s–	7.85	m	8.59	w+	9.72	s	1.79	m
4.35	s	6.63	s	7.00	w	8.63	w+	1.75	t
4.04	s	5.12	w	6.41	w–	8.37	m	1.65	m+
3.65	m	5.01	s–	5.04	m–	4.99	s	1.59	w
3.47	w	4.75	s	4.65	t	4.90	w+	1.57	w–
3.35	w	4.31	vs	4.43	m	4.64*	w	1.49	m
3.24	s	4.03	vs	4.23	w–	4.41	m+	1.47	w+
2.93	s	3.86	w–	4.05	vs	4.23	m–	1.42	w
2.71	t	3.62	w	3.34	w+	4.04*	vs	1.40	t
2.56	m	3.32	m+	2.68	w–	3.66*	w	1.37	t
2.37	t	3.19	s	2.55	m	3.50	t	1.34	w–
2.31	t	3.11	t	2.28	w–	3.32	s	1.29	w
2.15	t	3.00	w	2.16	w	3.20	w+	1.27	w+
2.04	w	2.87	w+	2.03	w–	3.12	w–	1.24	w–
1.99	w	2.67	w	1.84	w	3.04	t	1.22	w
1.89	t	2.54	s–	1.80	w	2.91	w	1.15	w–
1.82	t	2.38	w–	1.65	w+	2.81	t	1.14	w
		2.27	w–	1.49	w	2.77	t		
		2.16	s	1.22	t	2.67	m–		
		2.08	w+	1.19	t	2.55	s		
		2.02	w			2.51	m–		
		1.97	w–			2.46	w–		
		1.89	w–			2.27	m		
		1.84	w			2.21	w		
		1.79	w			2.16	m+		
		1.65	w+			2.12	w		
		1.60	t			2.02	m–		
		1.58	t			1.99	t		
		1.49	w+			1.96	t		
		1.47	w						
		1.41	w						
		1.29	t						
		1.27	w–						
		1.23	t						
		1.22	t						

(a) Relative intensities visually estimated: vs = very strong, s = strong, m = medium, w = weak, t = trace.

* denotes diffuse bands.

given in Tables XI, XII, and XIII, respectively.[26,27,28,29] The d-spacings of the solid formed at pH 5.9 agreed well with d-spacings of $Na_{0.6}NpO_2(CO_3)_{0.8}\cdot 2.5H_2O$. Eleven of the 18 measured lines matched the reference pattern with a tolerance of 0.01 Å, and 17 lines matched within 0.03 Å. For the pH 7.0 solid, 5 lines of this pattern matched the 21-line pattern of $Na_{0.6}NpO_2(CO_3)_{0.8}\cdot nH_2O$ within 0.01 Å, and 13 lines within 0.03 Å. This solid better matched the patterns of $NaNpO_2CO_3\cdot 3.5H_2O$ and $NaNpO_2CO_3\cdot 2H_2O$; 5 and 10 lines agreed within 0.01 Å, and 13 and 16 lines matched within 0.03 Å, respectively.[28] The d-spacings for the pH 8.5 solid agreed relatively well with the $Na_{0.6}NpO_2(CO_3)_{0.8}\cdot 2.5H_2O$; 11 of the 18 measured lines matched within 0.03 Å, but only three matched within 0.01 Å.

The x-ray diffraction patterns of solids formed at 60°C at pH 7.0 and pH 8.5 agreed well with the pattern of $Na_{0.6}NpO_2(CO_3)_{0.8}\cdot 2.5H_2O$. All lines matched within 0.03 Å, and 17 and 15 lines matched within 0.01 Å for pH 7.0 and 8.5, respectively. The pH 5.9 solid compared best with $Na_{0.6}NpO_2(CO_3)_{0.8}\cdot 2.5H_2O$ and with $Na_3NpO_2(CO_3)_2\cdot nH_2O$. Within 0.03 Å tolerance, all the diffraction lines of the solid matched with those of $Na_{0.6}NpO_2(CO_3)_{0.8}\cdot 2.5H_2O$; 24 lines matched with $Na_3NpO_2(CO_3)_2\cdot nH_2O$. Within 0.01 Å 18 lines matched with $Na_{0.6}NpO_2(CO_3)_{0.8}\cdot 2.5H_2O$, and 13 lines with $Na_3NpO_2(CO_3)_2\cdot nH_2O$. We viewed these solids also under a microscope to further identify them. The solids from the pH 7 and the pH 8.5 solutions appeared microcrystalline and of an approximate size of 1 to 10 μm. The pH 5.9 precipitate contained two separate phases: bright-green flat shingles of up to 200 μm were interlayered by white spherical particles that were up to 250 μm in size. Comparison of the aggregate's powder pattern with those of $NaClO_4$, Na_2CO_3, $NaHCO_3$ (as possible non-actinide solid phases) proved the absence of such compounds.

The d-spacings of the solids formed in the 90°C solutions are compared in Tables XIV and XV with Np_2O_5 [30] and $KNpO_2CO_3$ [31] patterns. The pH 5.9 solid was conclusively identified as Np_2O_5. Although the powder pattern of Np_3O_8 is being reported

Table XI. X-ray powder diffraction patterns of neptunium solid phases in J-13 groundwater at 25°, pH 5.9, pH 7.0, and pH 8.5 compared with the pattern of $Na_{0.6}NpO_2(CO_3)_{0.8} \cdot 2.5\ H_2O$.[26]

pH 5.9		pH 7.0		pH 8.5		$Na_{0.6}NpO_2(CO_3)_{0.8} \cdot 2.5\ H_2O$	
d(Å)	I[a]	d(Å)	I[a]	d(Å)	I[a]	d(Å)	I[a]
						13.64	t
						9.96	s–
9.80	w						
		9.03	w				
		8.53	w				
7.31	t						
		6.92	s	6.88	s		
6.22	t					6.22	w
4.93	w	4.91	m			4.96	s–
				4.87	s–		
4.80	w					4.82	w
4.31	s			4.35	s	4.33	vs
		4.27	m				
		4.01	m–	4.04	s		
3.96	s–					3.97	s
						3.73	t
		3.63	v/+	3.65	m		
		3.45	w	3.47	w	3.44	t
				3.35	w	3.30	t
3.21	s–	3.22	s	3.24	s	3.22	s–
3.05	w					3.06	m–
2.94	t	2.92	m	2.93	s	2.89	t
		2.82	w			2.80	w–
						2.72	w–
2.71	m			2.71	t	2.70	m+
				2.56	m	2.62	w+
		2.44	t			2.47	w
2.40	t			2.37	t	2.40	w+
		2.36	t			2.34	w–
		2.30	t	2.31	t	2.30	t
2.16	t	2.16	t	2.15	t	2.16	m–
2.10	t	2.13	t			2.11	w
2.06	t	2.09	t	2.04	w	2.06	m
1.99	vs	2.03	w	1.99	w	1.98	w–
		1.99	t			1.96	w–
1.94	s			1.89	t	1.94	t
		1.88	t			1.83	w–
		1.81	t	1.82	t	1.80	t
1.73	m–					1.77	w

(a) Relative intensities visually estimated: vs = very strong, s = strong, m = medium, w = weak, t = trace.

(b) The $Na_{0.6}NpO_2(CO_3)_{0.8} \cdot 2.5H_2O$ reference pattern has an additional 26 lines (w and t) not listed here, ranging from 1.70 Å to 1.11 Å.

Table XII. X-ray powder diffraction patterns of neptunium solid phases in J-13 groundwater at 25°, pH 5.9, pH 7.0, and pH 8.5 compared with the pattern of $Na_{0.6}NpO_2(CO_3)_{0.8} \cdot nH_2O$.[26]

pH 5.9		pH 7.0		pH 8.5		$Na_{0.6}NpO_2(CO_3)_{0.8} \cdot nH_2O$[b]	
d(Å)	I[a]	d(Å)	I[a]	d(Å)	I[a]	d(Å)	I[a]
9.80	w						
		9.03	w				
		8.53	w				
7.31	t						
		6.92	s	6.88	s		
						6.54	m–
6.22	t						
4.93	w	4.91	m	4.87	s–		
4.80	w					4.80	m–
4.31	s	4.27	m	4.35	s	4.32	m–
3.96	s–	4.01	m–	4.04	s		
						3.87	m–
		3.63	w+	3.65	m	3.60	m–
		3.45	w	3.47	w		
				3.35	w		
				3.24	s	3.27	w
3.21	s–	3.22	s			3.20	w
3.05	w						
2.94	t	2.92	m	2.93	s	2.88	vs
		2.82	w				
2.71	m			2.71	t	2.70	w–
				2.56	m	2.60	w–
2.40	t	2.44	t	2.37	t	2.40	w
		2.36	t				
		2.30	t	2.31	t	2.29	w–
						2.25	t
2.16	t	2.16	t	2.15	t	2.16	w+
2.10	t	2.13	t			2.10	w
2.06	t	2.09	t	2.04	w	2.05	w–
		2.03	w				
1.99	vs	1.99	t	1.99	w	1.99	w
						1.97	w–
1.94	s					1.93	w
		1.88	t	1.89	t	1.88	w–
		1.81	t	1.82	t	1.80	m–
1.73	m–					1.76	w–
						1.69	w–

(a) Relative intensities visually estimated: vs = very strong, s = strong, m = medium, w = weak, t = trace.

(b) The $Na_{0.6}NpO_2(CO_3)_{0.8} \cdot nH_2O$ reference pattern has an additional 19 lines (w and t) not listed here, ranging from 1.63 Å to 1.11 Å.

Table XIII. X-ray powder diffraction patterns of neptunium solid phases in J-13 groundwater at 25°, pH 5.9, pH 7.0, and pH 8.5 compared with the pattern of $Na_3NpO_2(CO_3)_2 \cdot nH_2O$.[27]

pH 5.9		pH 7.0		pH 8.5		$Na_3NpO_2(CO_3)_2 \cdot nH_2O$.[b]	
d(Å)	I[a]	d(Å)	I[a]	d(Å)	I[a]	d(Å)	I[a]
9.80	w						
		9.03	w				
		8.53	w				
7.31	t						
		6.92	s	6.88	s		
6.[illegible]	t						
						6.07	w
						5.75	w+
4.93	w	4.91	m	4.87	s–		
4.80	w						
				4.35	s	4.39	vs
4.31	s	4.27	m			4.29	w–
3.96	s–	4.01	m–	4.04	s	4.00	w+
		3.63	w+	3.65	m		
		3.45	w	3.47	w		
				3.35	w		
3.21	s–	3.22	s	3.24	s		
						3.11	w–
3.05	w					2.99	w–
2.94	t	2.92	m	2.93	s	2.91	w–
		2.82	w			2.80	w–
2.71	m			2.71	t	2.71	t
				2.56	m	2.53	m
2.40	t	2.44	t				
		2.36	t	2.37	t	2.34	t
		2.30	t	2.31	t		
						2.19	m–
2.16	t	2.16	t	2.15	t	2.14	t
		2.13	t				
2.10	t	2.09	t			2.10	t
2.06	t	2.03	w	2.04	w	2.00	w–
1.99	vs	1.99	t	1.99	w	1.97	w–
1.94	s					1.94	w–
		1.88	t	1.89	t	1.90	w–
				1.82	t	1.84	t
		1.81	t			1.80	t
1.73	m–					1.74	t
						1.70	t

(a) Relative intensities visually estimated: vs = very strong, s = strong, m = medium, w = weak, t = trace.

(b) The $Na_3NpO_2(CO_3)_2 \cdot nH_2O$ reference pattern has an additional 11 lines (w and t) not listed here, ranging from 1.67 Å to 1.27 Å.

Table XIV. X-ray powder diffraction patterns of neptunium solid phases in J-13 groundwater at 90°C, pH 5.9, and pH 7.2 compared with the pattern of Np_2O_5.[30]

Np_2O_5		pH 5.9		pH 7.2	
d(Å)	I[a]	d(Å)	I[a]	d(Å)	I[a]
		8.85	s	8.82*	s
		7.55	w	7.05*	m–
		7.15	m		
		5.64	w+	5.01	w–
4.18	90	4.16	s	4.19	m
				4.04	m
3.47	100	3.45	vs	3.46	vs
3.30	90	3.27	w+	3.30	m–
2.678	100	2.66	vs	2.67	s
2.666	100				
2.586	90	2.58	w+	2.59	w–
				2.55	w+
				2.27	w–
				2.15	w
2.092	60	2.09	w–	2.09	t
2.043	90	2.05	w	2.05	t
				2.02	t
1.934	90	1.93	m–	1.94	w–
1.841	60	1.84	w+	1.84	w+
1.831	60				
1.796	60	1.80	m	1.80	w+
1.790	60				
1.766	40				
1.757	60	1.76	m	1.76*	w
1.754	60				
1.736	60	1.74	w+	1.74	w–
		1.65	w–	1.64	w
1.616	40	1.61	m+	1.61	w
1.607	40				
1.600	40			1.59	t
1.531	40	1.54	w		
		1.51	t	1.50	w+
1.464	20	1.47	w+		
1.456	20	1.43	m–		
1.421	20				
1.418	20				
1.396	20	1.40	t		
1.340	20	1.34	s	1.34	m–
1.333	20	1.30	w	1.27	w–
1.334	20	1.29	w–		
		1.28	w		
		1.26	t		
		1.23	w		
		1.21	w–		
		1.19	t		

(a) Relative intensities visually estimated: vs = very strong, s = strong, m = medium, w = weak, t = trace.

* denotes diffuse bands

Table XV. X-ray powder diffraction patterns of neptunium solid phases in J-13 groundwater at 90°C, pH 7.2 (phase 2), and pH 8.4 (green phase 3 and tan phase 4) compared with the pattern of $KNpO_2CO_3$.[31]

$KNpO_2CO_3$		pH 7.2		pH 8.4 (green)		pH 8.4 (tan)		(cont'd)	
d(Å)	I^a	d(Å)	I^a	d(Å)	I^a	d(Å)	I^a	d(Å)	I^a
		8.82*	s	10.08	t	9.99	s–	1.84	m+
		7.05*	m–	8.59	w+	9.72	s	1.79	m
5.01	s	5.01	w–	7.00	w	8.63	w+	1.75	t
4.44	m	4.19	m	6.41	w–	8.37	m	1.65	m+
4.06	vs	4.04	m	5.04	m–	4.99	s	1.59	w
		3.46	vs	4.65	t	4.90	w+	1.57	w–
3.31	s	3.30	m–	4.43	m	4.64*	w	1.49	m
2.66	m	2.67	s	4.23	w–	4.41	m+	1.47	w+
2.56	s	2.59	w–	4.05	vs	4.23	m–	1.42	w
2.49	m	2.55	w+	3.34	w+	4.04*	vs	1.40	t
2.28	m	2.27	w–	2.68	w–	3.66*	w	1.37	t
2.22	w	2.15	w	2.55	m	3.50	t	1.34	w–
2.16	s	2.09	t	2.28	w–	3.32	s	1.29	w
		2.05	t	2.16	w	3.20	w+	1.27	w+
2.02	m	2.02	t	2.03	w–	3.12	w–	1.24	w–
		1.94	w–	1.84	w	3.04	t	1.22	w
1.85	m–	1.84	w+	1.80	w	2.91	w	1.15	w–
1.82	m–	1.80	w+	1.65	w+	2.81	t	1.14	w
1.79	m	1.76*	w	1.49	w	2.77	t		
		1.74	w–	1.22	t	2.67	m–		
1.65	m+	1.64	w	1.19	t	2.55	s		
		1.61	w			2.51	m–		
1.59	w	1.59	t			2.46	w–		
1.56	w–	1.50	w+			2.27	m		
1.50	w	1.34	m–			2.21	w		
1.48	w	1.27	w–			2.16	m+		
						2.12	w		
						2.02	m–		
						1.99	t		
						1.96	t		

(a) Relative intensities visually estimated: vs = very strong, s = strong, m = medium, w = weak, t = trace.

* denotes diffuse bands

as nearly identical to that of Np_2O_5, the Np_3O_8 contains a 2:1 ratio of Np(V) to Np(VI). Spectrophotometry on the dissolved pH 5.9 precipitate established the absence of Np(VI), thereby identifying the solid formed as pure Np_2O_5. This finding agrees with the results of Cohen and Walter.[30] These investigators found only the NpO_2^+ ions when they dissolved Np_2O_5 in mineral acid; whereas NpO_2^+ and NpO_2^{2+} ions were found in the ratio of 2:1 when Np_3O_8 was dissolved under similar conditions. This phase was also present in the pH 7.2 precipitate together with another phase it had in common with the pH 8.4 precipitates; the x-ray diffraction lines are listed in Table XV. The other phase corresponds well to the published pattern of $KNpO_2CO_3$. We exclude the existence of this compound in J-13 groundwater because the potassium content of this water is far lower than the sodium content.[3] The formation of an isostructural sodium analogue is more likely under these conditions. However, none of the published patterns of sodium neptunyl(V) carbonates with varying stoichiometry and hydration number can unequivocally provide a complete match for this phase.[26–29] From microscopic viewing of the 90°C solids contained in the x-ray capillaries, we confirmed that the solid formed at pH 7.2 was composed of multiple phases. Three phases were distinguishable: the major phase was light brown and finely crystalline, another one was dark brown and coarsely crystalline, and a minor phase was bright green.

To gain additional information on the nature of the neptunium precipitates, we treated a small portion of the 60° and 90°C precipitates with 1 M $HClO_4$ to test for the presence of carbonate. This test is positive if the solid dissolves with the evolution of gas, which can only be CO_2. The 60°C solids showed increased gas evolution with increasing pH. This may indicate increasing carbonate content, but the varying crystallite size may also influence the rate of gas release. Near-IR spectrophotometry of the dissolved solids showed the neptunium present in the +5 state, assuming that no change in oxidation state occurred during the dissolution.

We also tested the 90°C solids for carbonate. The pH 5.9 precipitate dissolved sparingly with no detectable gas evolution, as was expected of Np_2O_5. The pH 7.2 solid released some gas, and the pH 8.4 precipitate produced significant amounts of gas; both solids dissolved completely. The findings that the pH 7.2 and pH 8.4 solids contained carbonate are supported by their FTIR spectra given in Figures 8, 9, and 10. In particular the characteristic C-O stretching bands between approximately 1300 and 1500 cm^{-1} indicate the presence of coordinated carbonate in the pH 7.2 and pH 8.4 solids.[32] The pH 5.9 solid is too opaque to obtain an interpretable transmission spectrum in this wavelength region, as shown in Figure 11. Furthermore, the absorptions in all three FTIR spectra at approximately 830 cm^{-1} are characteristic of the asymmetric neptunyl(V) stretch, which proves that the neptunium remained pentavalent in solid phases.[33] This is also supported by the electronic near-IR absorption spectra of the dissolved solids. The only feature observed in these spectra is the 980 nm absorption, characteristic of NpO_2^+. The FTIR spectra for the 25°C solids are shown in Figures 12, 13, and 14. All three spectra display the characteristic C-O stretching frequencies between about 1300 and 1500 cm^{-1}. Additionally, C-O frequencies between 693 and 865 cm^{-1} are also present. The 830 cm^{-1} band, which is characteristic for the asymmetric neptunyl(V) stretch, is present in the spectra for the samples at all pH values.

In summary, except for the 90°C experiment at pH 5.9, all solids contained sodium neptunium carbonate hydrates with different stoichiometry and water content. It appears that many of the corresponding solids described in the literature are metastable and therefore difficult to reproduce.[26–29] At pH 5.9, the 90°C solid formed was neptunium pentoxide; at pH 7, the solids were a mixture of sodium neptunium carbonate hydrate and neptunium pentoxide. The formation of Np_2O_5 under these conditions is quite surprising, because higher temperatures are normally required to produce this solid.[30] The solubility decrease with increasing pH is clearly connected to the increased formation of CO_3^{2-} with increasing pH. This in turn results in the formation of more insoluble sodium neptunium

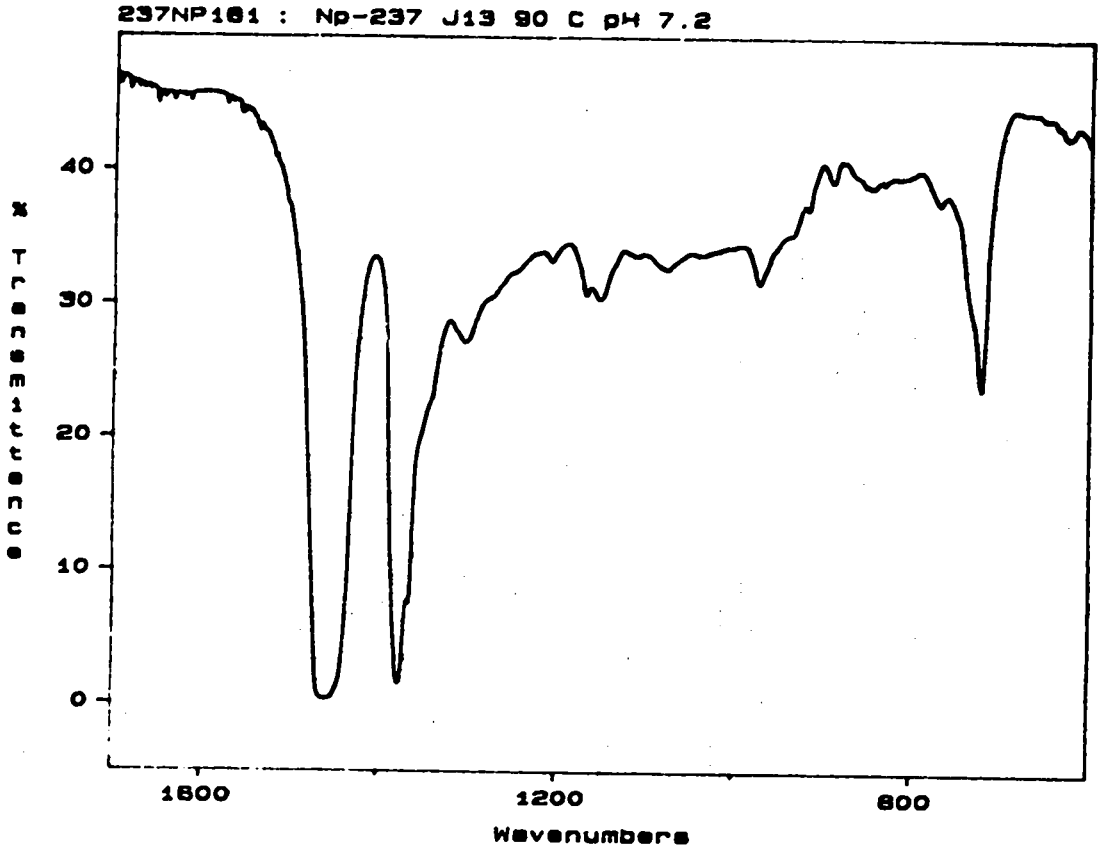

Figure 8. FTIR spectrum of Np solid phase formed at pH 7.2 and 90°C in J-13 groundwater.

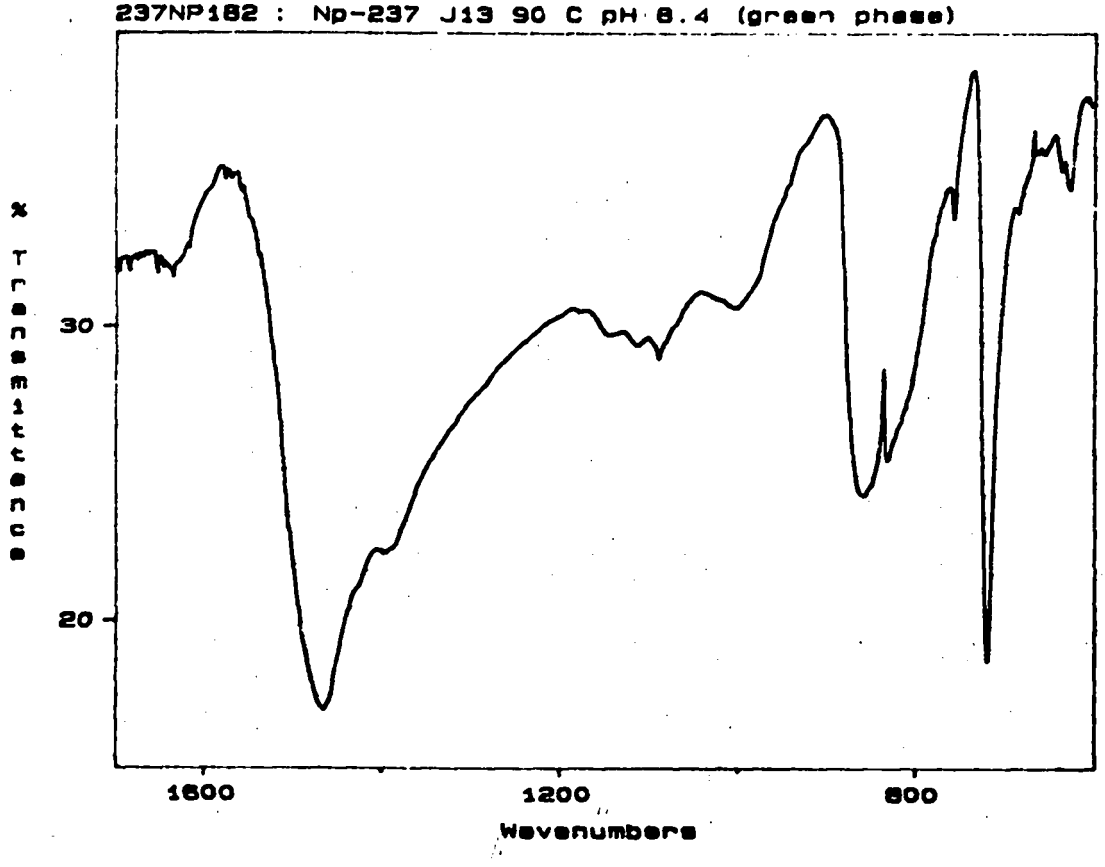

Figure 9. FTIR spectrum of Np solid (green phase) formed at pH 8.4 and 90°C in J-13 groundwater.

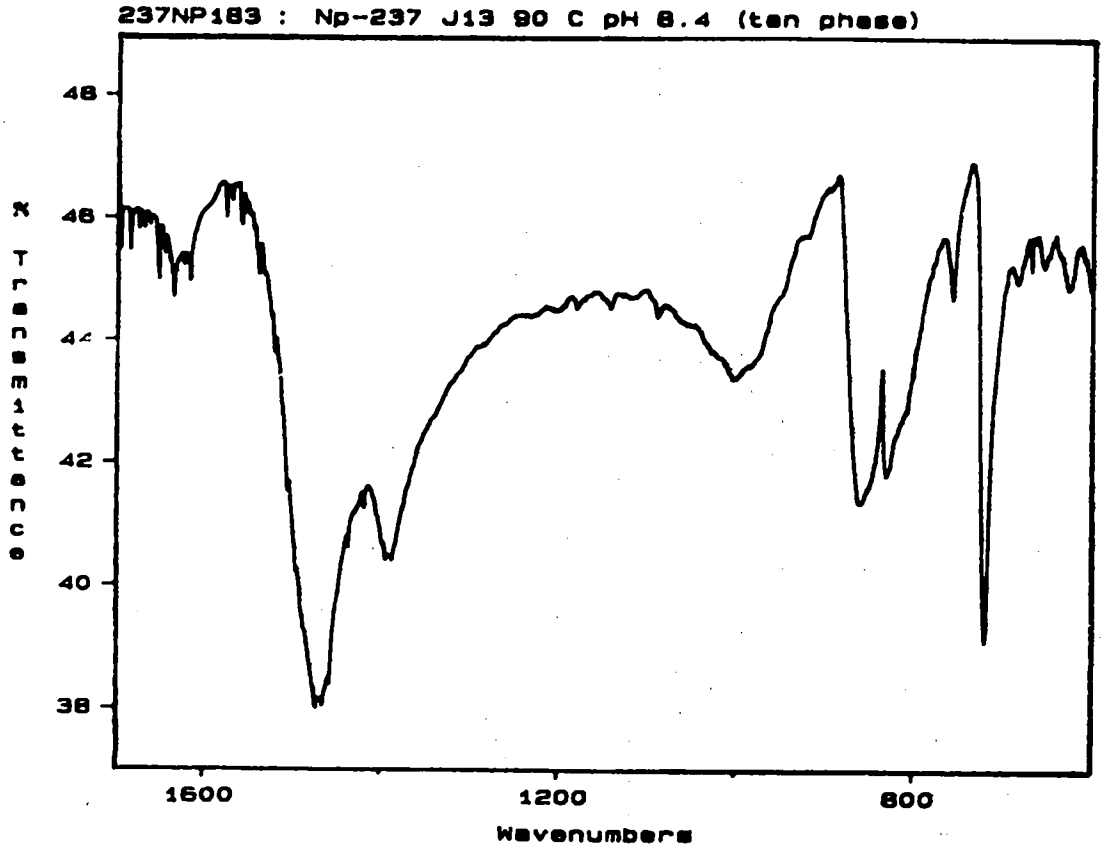

Figure 10. FTIR spectrum of Np solid (tan phase) formed at pH 8.4 and 90°C in J-13 groundwater.

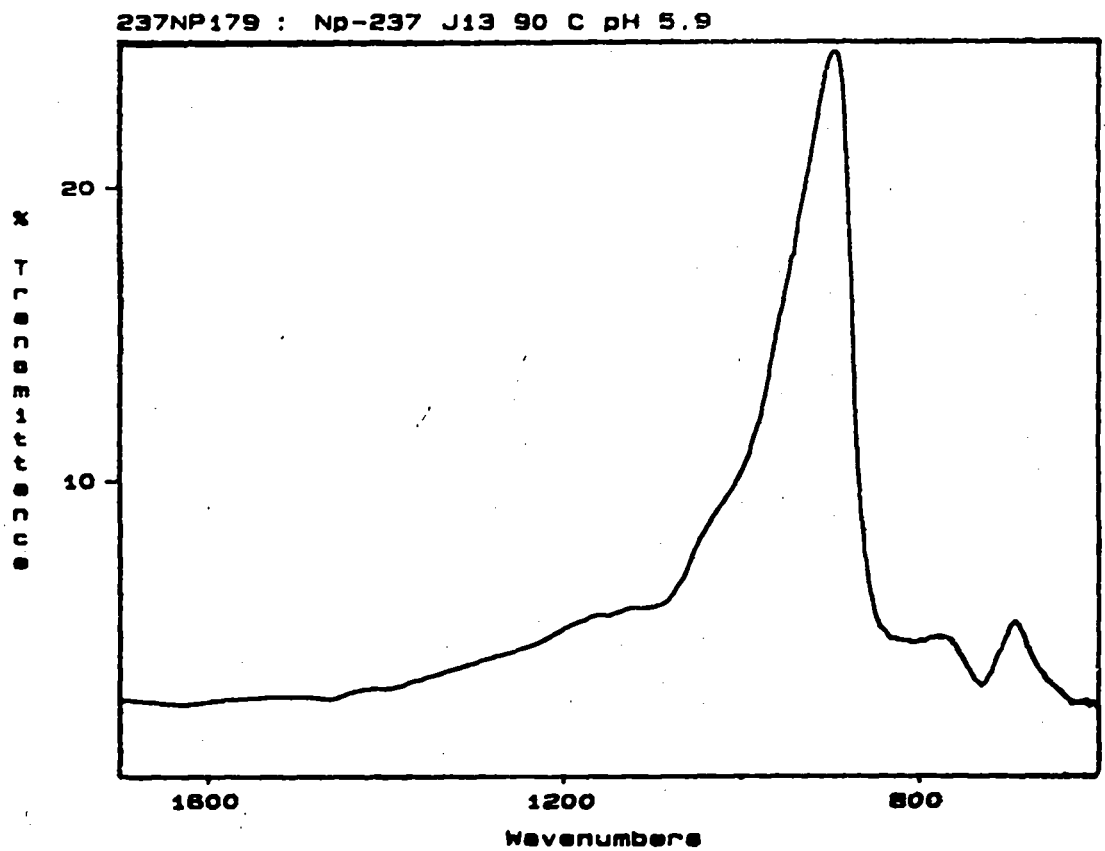

Figure 11. FTIR spectrum of Np solid phase formed at pH 5.9 and 90°C in J-13 groundwater.

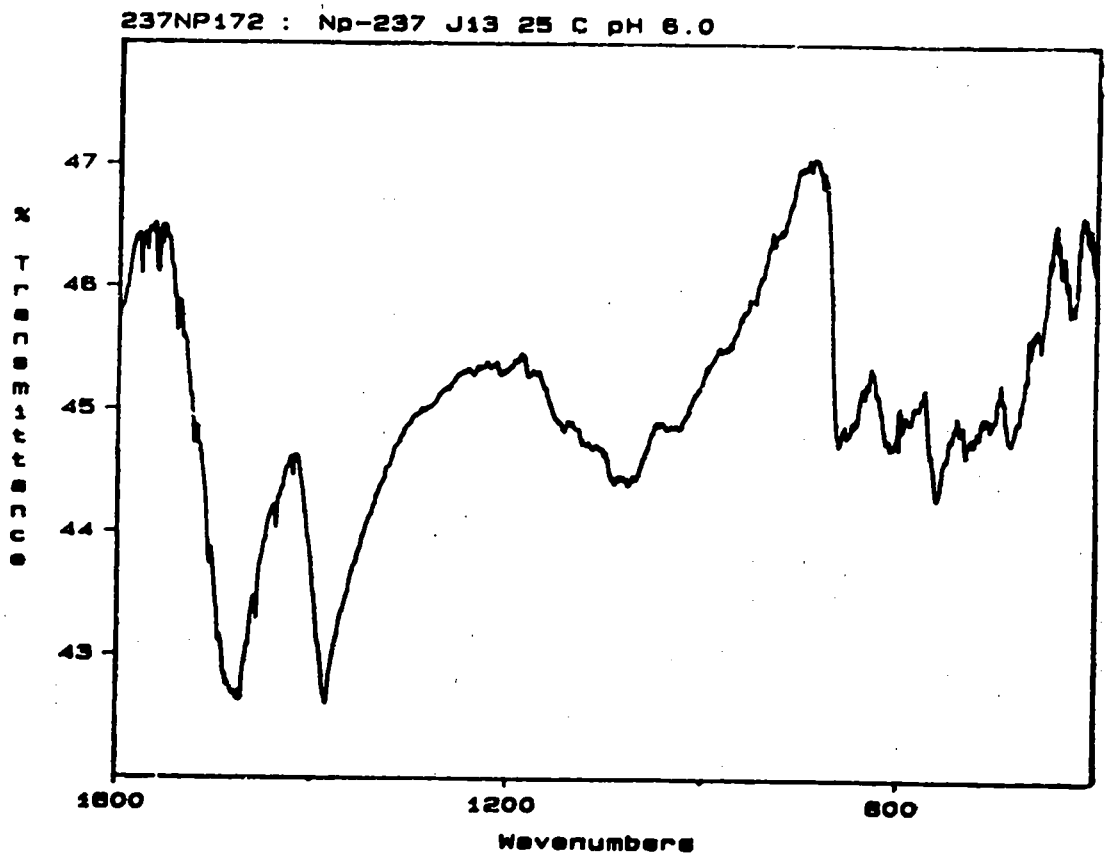

Figure 12. FTIR spectrum of Np solid phase formed at pH 5.9 and 25°C in J-13 groundwater.

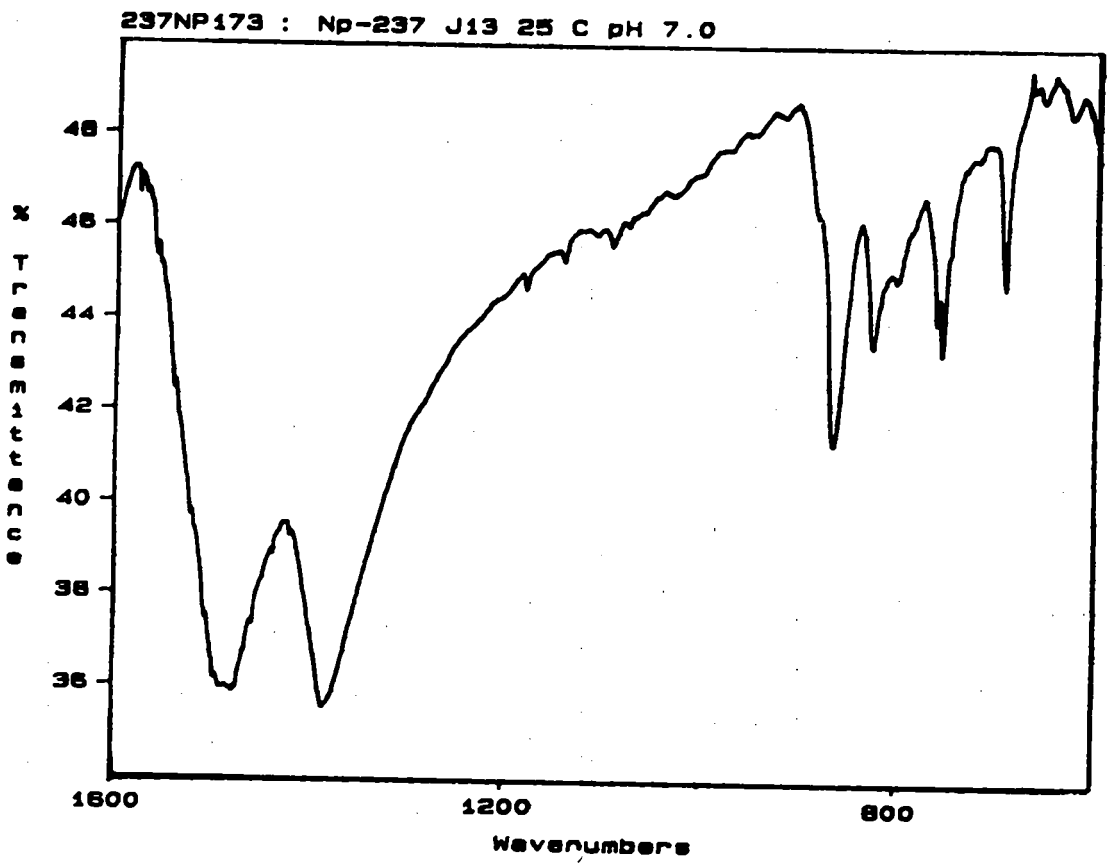

Figure 13. FTIR spectrum of Np solid phase formed at pH 7.0 and 25°C in J-13 groundwater.

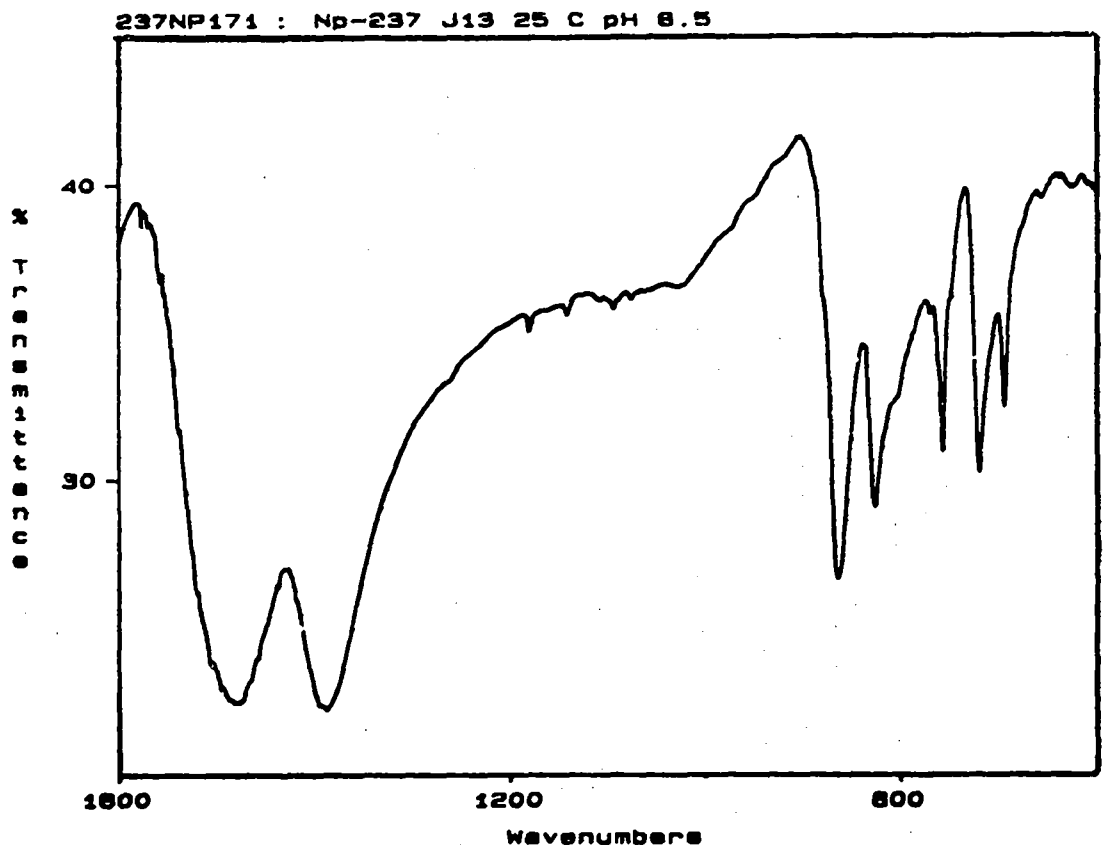

Figure 14. FTIR spectrum of Np solid phase formed at pH 8.5 and 25°C in J-13 groundwater.

carbonate hydrates and in lower solubilities.

5.2. Plutonium

5.2.1. Solubility

Results of the plutonium solubility studies are shown in Figure 15. The plutonium was initially introduced as Pu^{4+} into the J-13 groundwater. The steady-state concentrations and the solutions' Eh values are given in Table XVI. Concentration profiles as a function of equilibration time and pH for 25°, 60°, and 90°C are shown in Figures 16, 17, and 18, respectively. The individual measurements are listed in Appendix B. No clear trend with increasing pH was observed. But the solution concentrations decreased drastically with increasing temperature.

5.2.2. Oxidation State Determination

The plutonium supernatant solutions at steady state were analyzed for their oxidation state distributions. The speciation studies are made difficult by the low solubility of plutonium. The solutions' concentration levels lie below the sensitivity range of methods such as absorption spectrophotometry, which would allow the direct measurement of the species present. Therefore, we developed a method to determine the oxidation states indirectly. The method involves a combination of solvent extractions and coprecipitation. It was tested on solutions of known plutonium oxidation state mixtures with both high-level and trace-level concentrations.[13] Results of this study for 25°, 60°, and 90°C are given in Table XVII. They are also displayed in Figures 19, 20, and 21, for pH 5.9, 7.0, and 8.5, respectively. Because the oxidation state determinations for the 90°C and 60° solutions were made at ambient temperature, the solubility and speciation may have possibly been perturbed. Therefore, the derived results for the oxidation state determinations may be more semiquantitative.

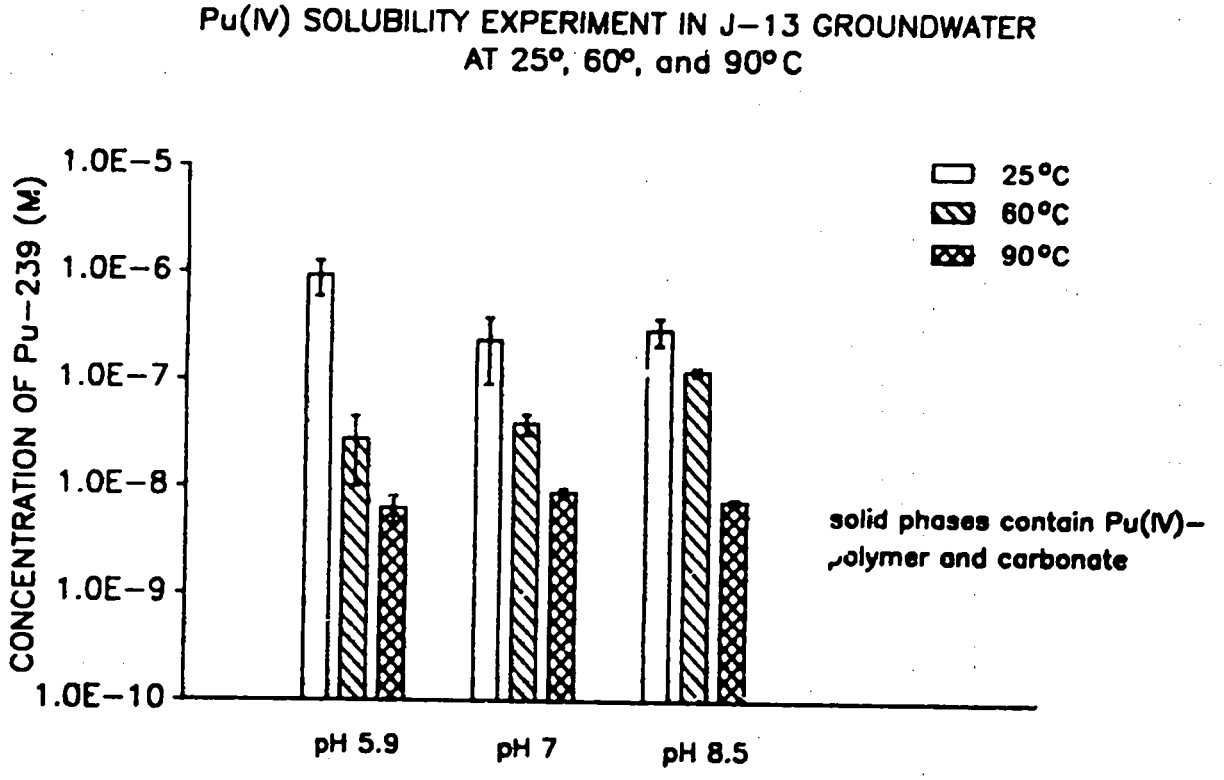

Figure 15. Results for Pu^{4+} solubility experiments in J-13 groundwater as a function of pH and temperature.

Table XVI. Comparison of steady-state solution concentrations for plutonium in J-13 groundwater at 25°C, 60°C and 90°C.

Pu	25°C	
pH	conc. (M)	Eh (mV vs. NHE)
5.9 ± 0.1	$(1.1 \pm 0.4) \times 10^{-6}$[f]	342 ± 10
7.0 ± 0.1	$(2.3 \pm 1.4) \times 10^{-7}$[e]	126 ± 10
8.4 ± 0.1	$(2.9 \pm 0.8) \times 10^{-7}$[e]	259 ± 10

Pu	60°C	
pH	conc. (M)	Eh (mV vs. NHE)
5.9 ± 0.1	$(2.7 \pm 1.1) \times 10^{-8}$[a]	451 ± 10
7.0 ± 0.1	$(3.8 \pm 0.9) \times 10^{-8}$[a]	386 ± 10
8.5 ± 0.1	$(1.2 \pm 0.1) \times 10^{-7}$[b]	241 ± 10

Pu	90°C	
pH	conc. (M)	Eh (mV vs. NHE)
5.9 ± 0.3	$(6.2 \pm 1.9) \times 10^{-9}$[c]	360 ± 10
7.2 ± 0.2	$(8.8 \pm 0.8) \times 10^{-9}$[d]	376 ± 10
8.5 ± 0.1	$(7.3 \pm 0.4) \times 10^{-9}$[d]	133 ± 10

(a-f):The steady-state values were determined from a) all, the last b) 5, c) 6, d) 8, e) 13, f) 14 samplings.

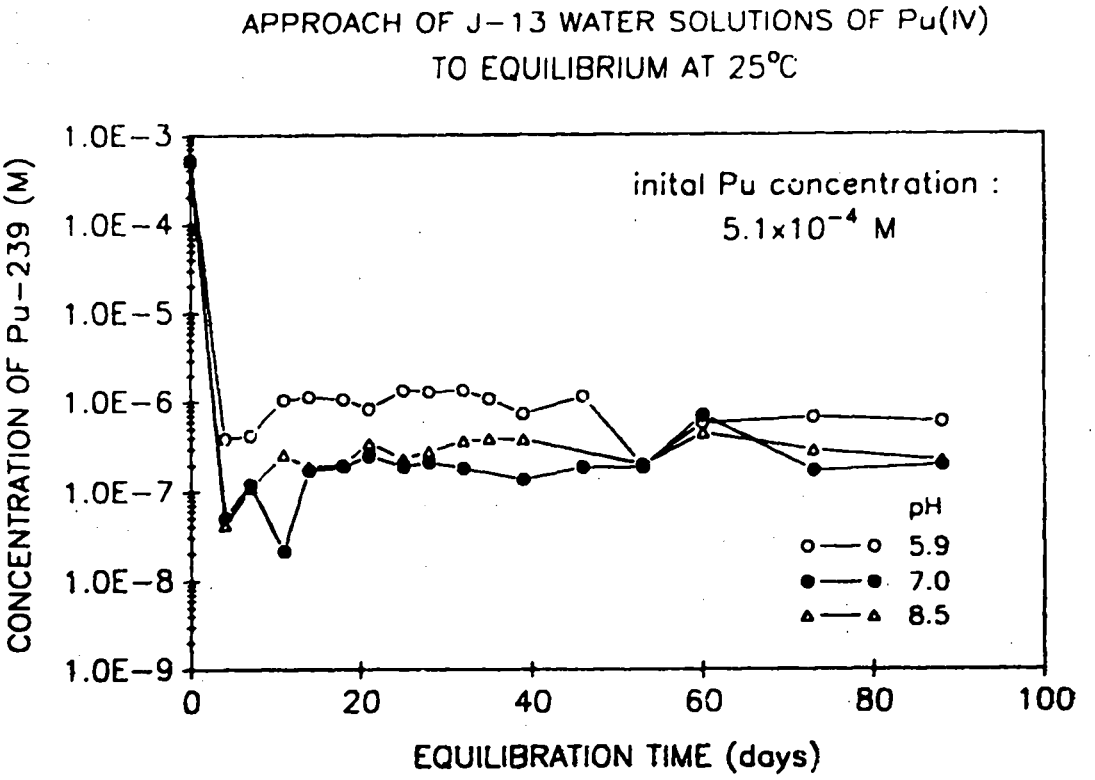

Figure 16. Solution concentrations of ^{239}Pu in contact with precipitate obtained from supersaturation in J-13 groundwater at 25°C as a function of time. pH 5.9 ± 0.1 (open circles), pH 7.0 ± 0.1 (filled circles), and pH 8.4 ± 0.1 (triangles). The plutonium was added initially (day 0) as Pu^{4+} at initial concentrations of 5.1×10^{-4} M.

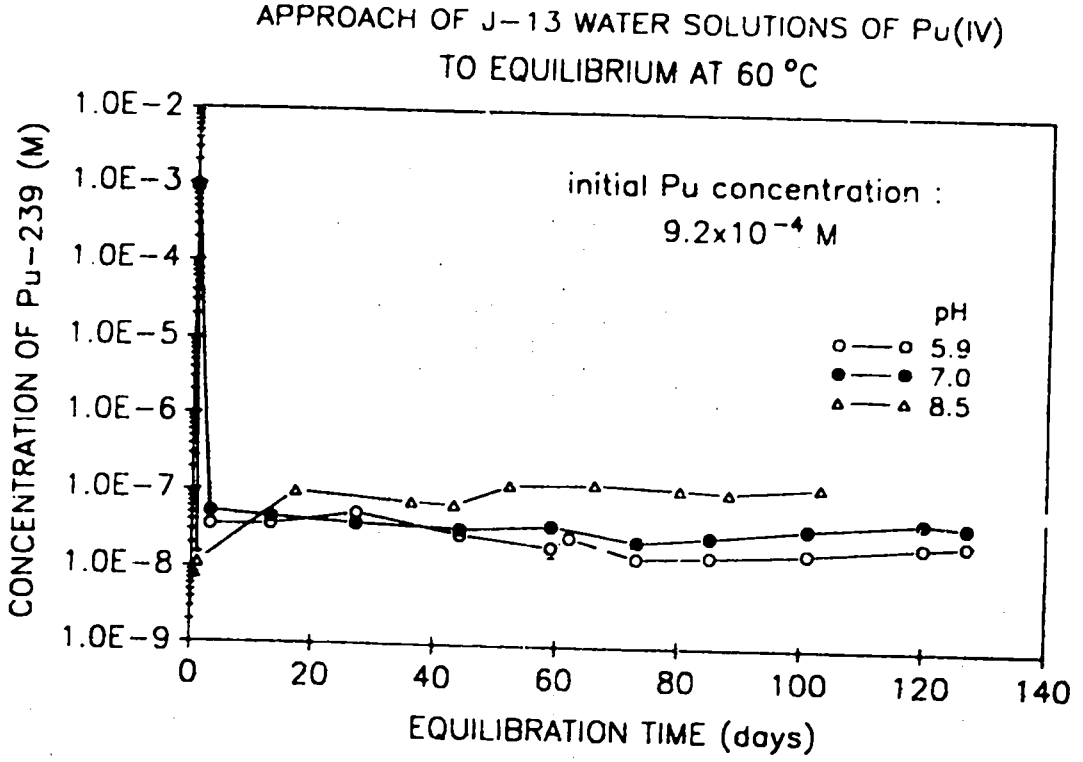

Figure 17. Solution concentrations of ^{239}Pu in contact with precipitate obtained from supersaturation in J-13 groundwater at 60°C as a function of time. pH 5.9 ± 0.1 (open circles), pH 7.0 ± 0.1 (filled circles), and pH 8.5 ± 0.1 (triangles). The plutonium was added initially (day 0) as Pu^{4+} at initial concentrations of 9.2×10^{-4} M.

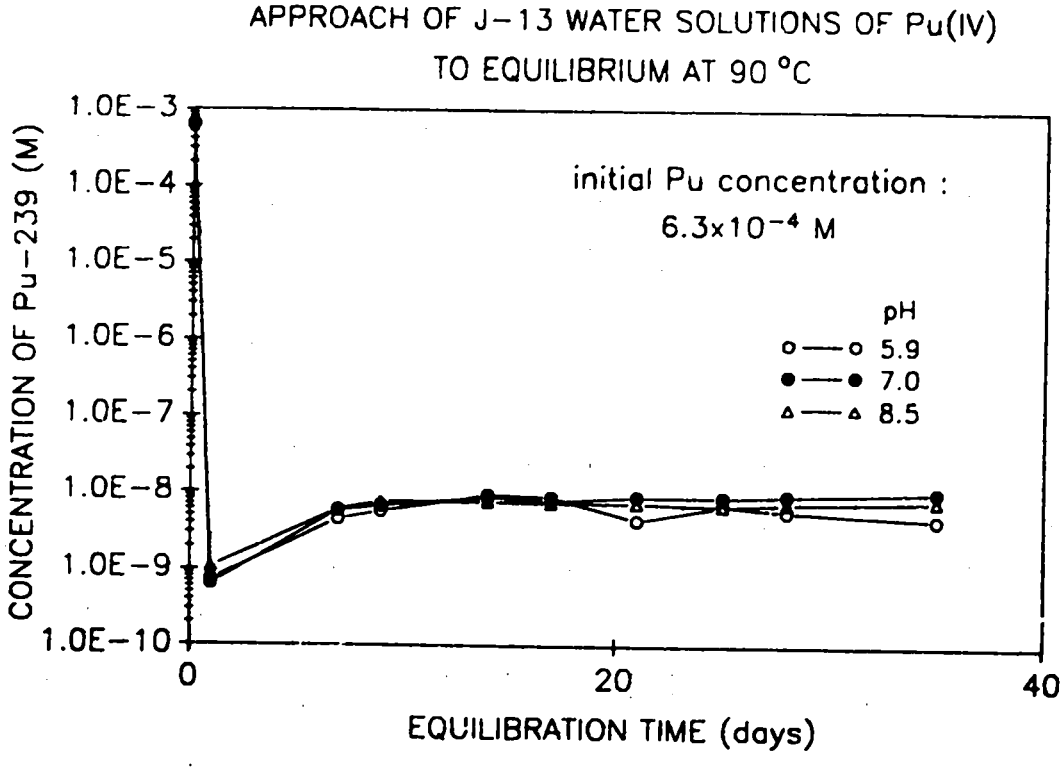

Figure 18. Solution concentrations of ^{239}Pu in contact with precipitate obtained from supersaturation in J-13 groundwater at 90°C as a function of time. pH 5.9 ± 0.1 (open circles), pH 7.0 ± 0.1 (filled circles), and pH 8.5 ± 0.1 (triangles). The plutonium was added initially (day 0) as Pu^{4+} at initial concentrations of 6.3×10^{-4} M.

Table XVII. Distribution of plutonium oxidation states in J-13 groundwater solutions at steady state and various pH values and temperatures of 25°, 60° and 90°C.

pH	Oxidation States (%)											
	Pu(IV)			Pu(V)			Pu(VI)			Pu(III + poly.)		
	25°C	60°C[d]	90°C[d]	25°C	60°C[d]	90°C[d]	25°C	60°C[d]	90°C[d]	25°C	60°C[d]	90°C[d]
5.9[a]	5 ± 1	2 ± 1	6 ± 5	68 ± 7	17 ± 5	79 ± 7	29 ± 3	72 ± 5	7 ± 5	3 ± 1	10 ± 2	9 ± 5
7.0[b]	6 ± 1	2 ± 1	13 ± 1	73 ± 7	44 ± 9	48 ± 3	18 ± 2	52 ± 4	3 ± 3	5 ± 1	3 ± 1	45 ± 2
8.5[c]	6 ± 1	13 ± 1	10 ± 2	63 ± 6	58 ± 2	85 ± 4	27 ± 3	24 ± 1	3 ± 3	3 ± 1	5 ± 4	11 ± 2

poly. = Pu(IV) polymer

[a] 25°C: 5.9 ± 0.1; 60°C: 5.9 ± 0.1; 90°C: 5.9 ± 0.3;

[b] 25°C: 7.0 ± 0.1; 60°C: 7.0 ± 0.1; 90°C: 7.2 ± 0.2;

[c] 25°C: 8.4 ± 0.1; 60°C: 8.5 ± 0.1; 90°C: 8.5 ± 0.1.

[d] distribution determined at ambient temperature

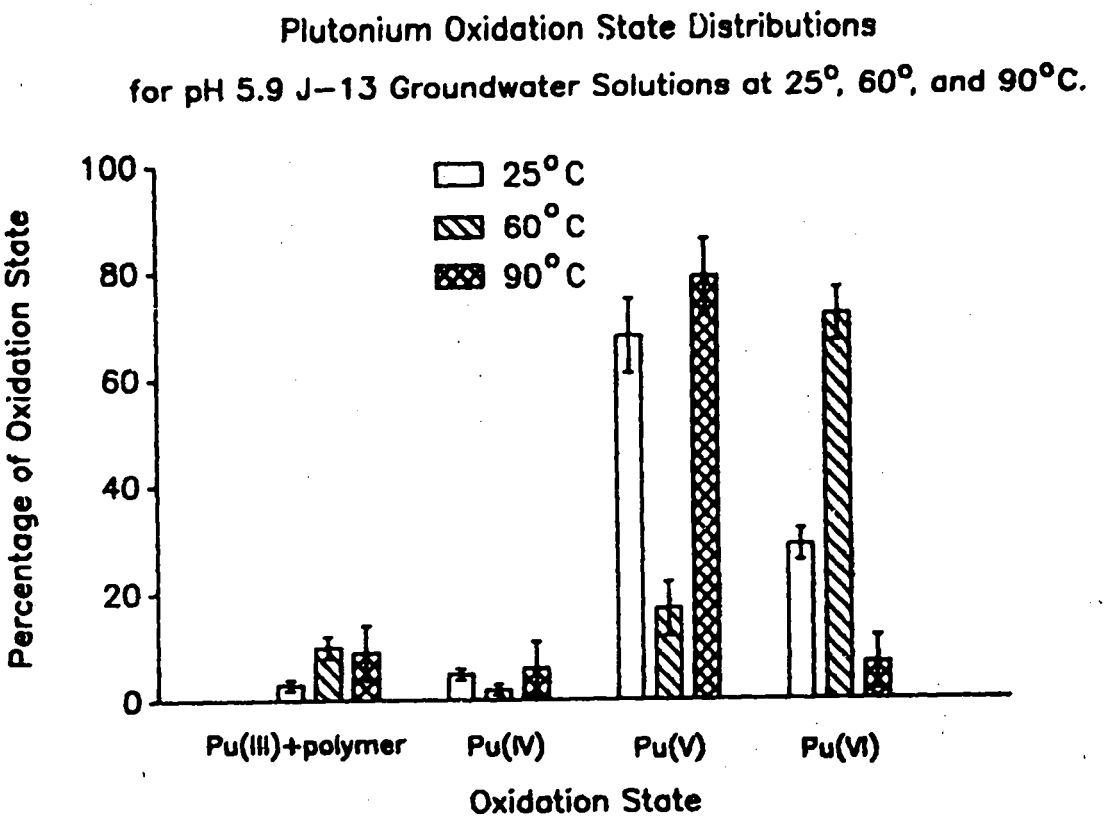

Figure 19. Plutonium oxidation state distributions of the supernatant at steady state for Pu^{4+} solubility experiments in J-13 groundwater at pH 5.9 and 25°C, 60°C, and 90°C. The solutions were filtered through 4.1-nm filters.

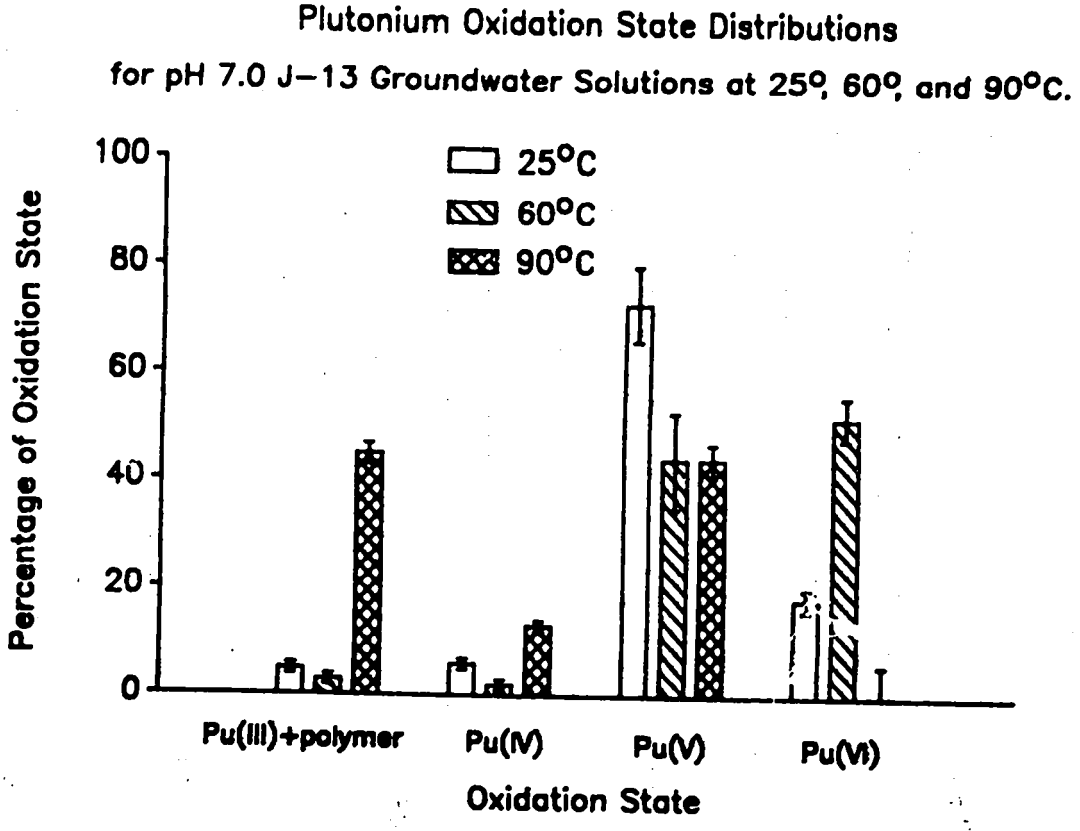

Figure 20. Plutonium oxidation state distributions of the supernatant at steady state for Pu^{4+} solubility experiments in J-13 groundwater at pH 7.0 and 25°C, 60°C, and 90°C. The solutions were filtered through 4.1-nm filters.

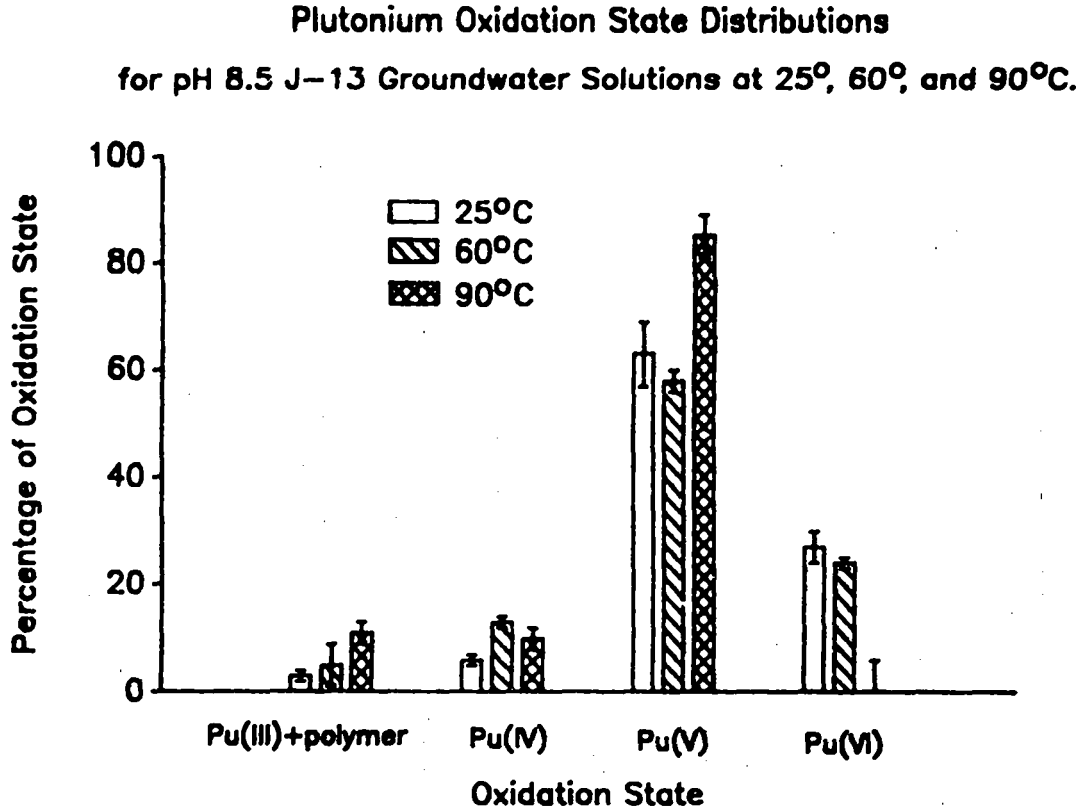

Figure 21. Plutonium oxidation state distributions of the supernatant at steady state for Pu^{4+} solubility experiments in J-13 groundwater at pH 8.5 and 25°C, 60°C, and 90°C. The solutions were filtered through 4.1-nm filters.

All solutions, except the 90°C solution at pH 7, contained predominately Pu(V) and Pu(VI), whereas Pu(III), Pu(IV), and Pu(IV) polymer are present only in small or insignificant quantities. These observed valence distributions cannot be explained by disproportionation equilibria and complex stabilization.[34] It is possible that oxidation products formed by α-radiolysis of the water may cause the predominance of high oxidation states in the plutonium solutions. It is noteworthy that the solutions were filtered through a 4.1-nm filter prior to the oxidation state determination because we wanted to determine only the true soluble plutonium fraction without any colloidal or polymeric plutonium being present. This treatment separates all Pu(IV) polymer larger than 4.1-nm from the solution. Therefore, we refer to Pu(IV) polymer in the context of this determination as to the fraction that is smaller than 4.1 nm.

At pH 7 and 90°C, Pu(V) is measured to be equal to the sum of Pu(III) and Pu(IV) polymer. We explain this measured decrease of Pu(V) and the increase of Pu(III + poly.) by leakage of the 4.1-nm Amicon filter used for phase separation. Such leakage would introduce more polymer and change the relative oxidation state distribution. This explanation is supported by comparison of the assay taken as a reference standard for the extraction at pH 7 and 90°C, with a parallel sampling for the solubility determination; the extraction sample contained 2.36 times more plutonium. Unfortunately, we could not repeat this experiment, because not enough supernatant was left for the test. From the other distribution results, we see no reason to doubt that this solution, too, contained probably mostly Pu(V) and Pu(VI).

5.2.3. Identification of Solids

The plutonium precipitates found in the solutions at 25° 60°, and 90°C were collected by centrifugation, washed with a small amount of CO_2-free water, and dried with an argon jet. All precipitates had a dark green appearance similar to that of Pu(IV) polymer. D-spacings and relative intensities of the x-ray powder diffraction patterns from the

precipitates are listed in Tables XVIII, XIX, and XX. Most of the few lines observed were rather diffuse, indicating at most a low degree of crystallinity. As these patterns show, some phases have several diffuse lines in common, but we found no reference pattern in the literature to assign the lines. They were compared to patterns of crystalline PuO_2[35], $PuO_3 \cdot 0.8H_2O$[36], PuO_2CO_3[36], $NH_4PuO_2CO_3$[37], and PuO_2CO_3[38].

Therefore, we tested all plutonium precipitates for carbonates. When treated with 1 M HCl, each precipitate dissolved partially with the evolution of gas. The amount of gas evolution increased from the pH 5.9 to the pH 8.5 precipitates. The pH 8.5 solids showed vigorous bubbling of gas. Much less gas was produced by the pH 7 solids, and an even lesser amount by the pH 5.9 solids. The non-dissolved residues of the precipitates were dissolved further with 6 M HCl/NaF, filtered through 220-nm pore size filters, and analyzed by absorption spectrophotometry. The spectra showed the characteristic absorption bands for Pu(IV) polymer. The presence of carbonate in these solids can be explained in several ways. Pu(IV) polymer absorbs CO_2, which converts on the polymer surface to carbonate.[39] The identification of the precipitates as Pu(IV) polymer is not confirmed by the x-ray data, because aged Pu(IV) polymer yields a pattern with diffuse lines at the same spacings as PuO_2.[40] In spite of the x-ray data, the sparing solubility in 6 M HCl and the need to use of NaF as a catalyst to dissolve the solids suggests that at least one component of the precipitates is Pu(IV) polymer. Another component could be a plutonium carbonate that would also test positive for carbonate. To further elucidate this matter, we viewed the solids contained in x-ray capillaries with a microscope.

We found no evidence for multicomponent solids for 25° and 60°C. The 90° solids, however, contained at least two phases. The pH 5.9 precipitate contained a yellow-green powdery phase, probably non-crystalline, that was mixed with a smaller fraction of darker green clumps. Such a combination of crystalline and amorphous materials in this solid can explain the observed powder pattern, which is composed of both very sharp and diffuse lines. The pH 7.2 solid was a yellow-green powder similar to the major phase at

Table XVIII. X-ray powder diffraction patterns of plutonium solid phases in J-13 groundwater at 25°, 60°, and 90°C and pH 5.9.

25°C		60°C		90°C	
d(Å)	I[a]	d(Å)	I[a]	d(Å)	I[a]
		10.5*	m		
				6.61*	s–
		6.43*	w+		
		4.20*	s	4.15*	vs
		3.15*	t	3.15*	m
				2.34	vs
1.99	s	1.99*	vs	2.03	s
				1.94*	s
				1.90*	w
1.73	w	1.75*	t	1.70*	vs
				1.64*	w
				1.40	w+
1.24	t			1.18	m–
0.87	m				
0.84	m–				

(a) Relative intensities visually estimated: vs = very strong, s = strong, m = medium, w = weak, t = trace.

* denotes diffuse bands.

Table XIX. X-ray powder diffraction patterns of plutonium solid phases in J-13 groundwater at 25°, 60°, and 90°C and pH 7.

25°C		60°C		90°C	
d(Å)	I[a]	d(Å)	I[a]	d(Å)	I[a]
		18.4*	w–		
				10.56*	s
				6.58*	m
		4.20*	s		
				4.13*	m
1.98	s	1.98	vs		
1.73	w	1.73*	w+		

(a) Relative intensities visually estimated: vs = very strong, s = strong, m = medium, w = weak, t = trace.

* denotes diffuse bands.

Table XX. X-ray powder diffraction patterns of plutonium solid phases in J-13 groundwater at 25°, 60°, and 90°C and pH 8.5.

25°C		60°C		90°C	
d(Å)	I[a]	d(Å)	I[a]	d(Å)	I[a]
				10.07	s
		4.17*	vs	4.17*	w+
		3.03*	m		
		2.41*	t		
1.98	s	1.99*	vs	1.95*	m
				1.92*	t
1.72	t	1.73*	w+	1.69*	m
				1.62*	t
1.23	t				
0.85	t				

(a) Relative intensities visually estimated: vs = very strong, s = strong, m = medium, w = weak, t = trace.

* denotes diffuse bands.

pH 5.9. The precipitate formed at pH 8.5 was a mixture of a similar-appearing yellow-green powder in which some lighter green pellets were embedded. The low crystallinity and the dominant yellow-green color of all three precipitates suggest that the solids consist mainly of polymeric Pu(IV). Further characterization of the 25° and 90°C solids was accomplished by FTIR spectroscopy. The spectra are depicted in Figures 22 to 27. All spectra show absorptions that can be assigned to carbonate-containing aged Pu(IV) polymer.[39] The split bands between 1350 cm^{-1} and 1650 cm^{-1} are characteristic of coordinated CO_3^{2-} (ν_3). The absorptions between 1000 cm^{-1} and 1100 cm^{-1} are correlated to aged Pu(IV) polymer. The solubility behavior of the plutonium experiments further indicates that the solubility-controlling solids contain mainly polymeric Pu(IV) mixed with some plutonium carbonates. No clear trend in solubility with increasing pH was observed. But the solution concentrations decreased drastically with increasing temperature. Such behavior can be expected from Pu(IV) polymer that is rather unaffected by changes in pH in the near-neutral region. With increasing temperature, however, the polymer peptizes to become more thermodynamically stable and therefore less soluble; over long times it may possibly convert to crystalline PuO_2 of much lower solubility.

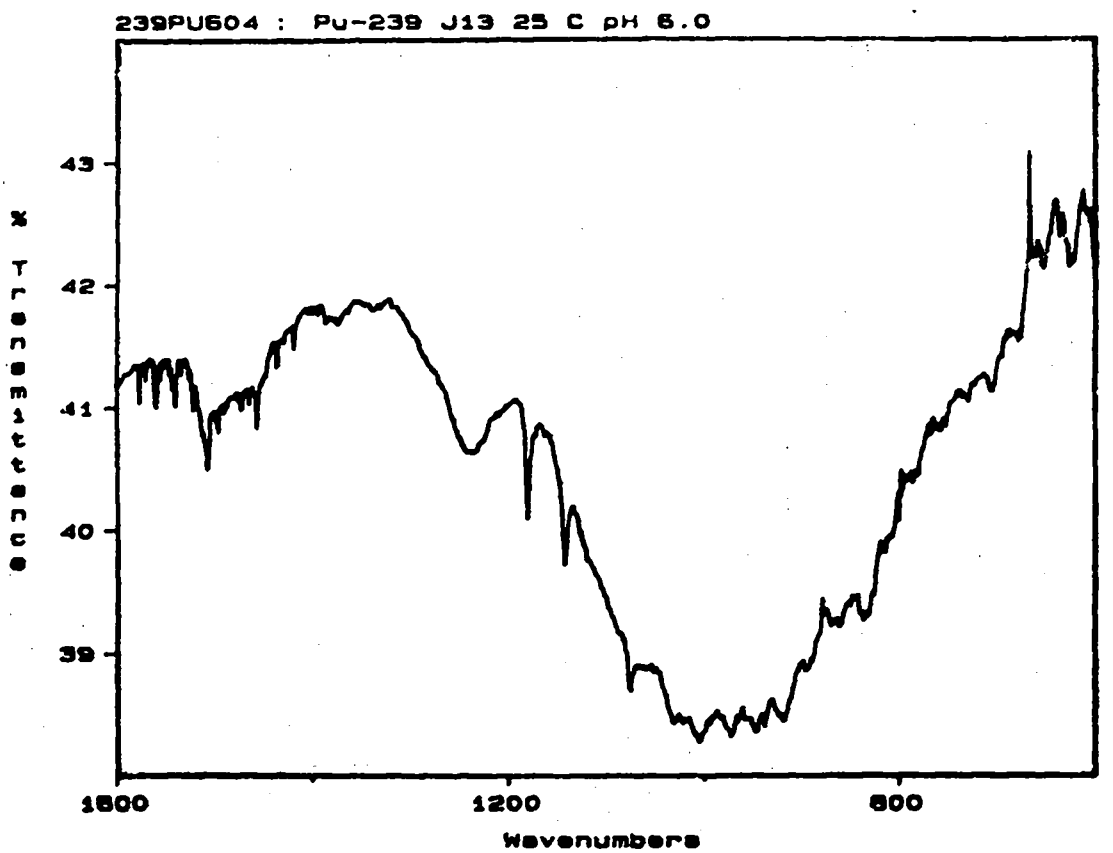

Figure 22. FTIR spectrum of Pu solid phase formed at pH 5.9 and 25°C in J-13 groundwater.

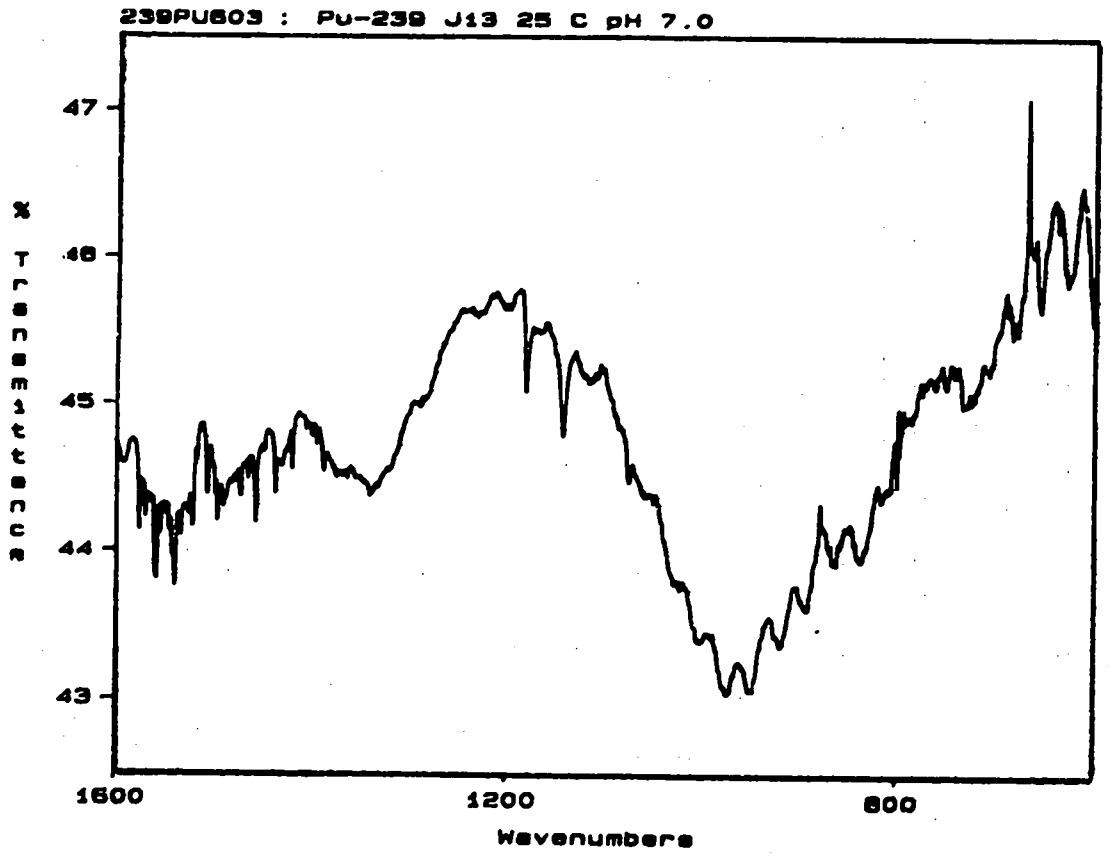

Figure 23. FTIR spectrum of Pu solid phase formed at pH 7.0 and 25°C in J-13 groundwater.

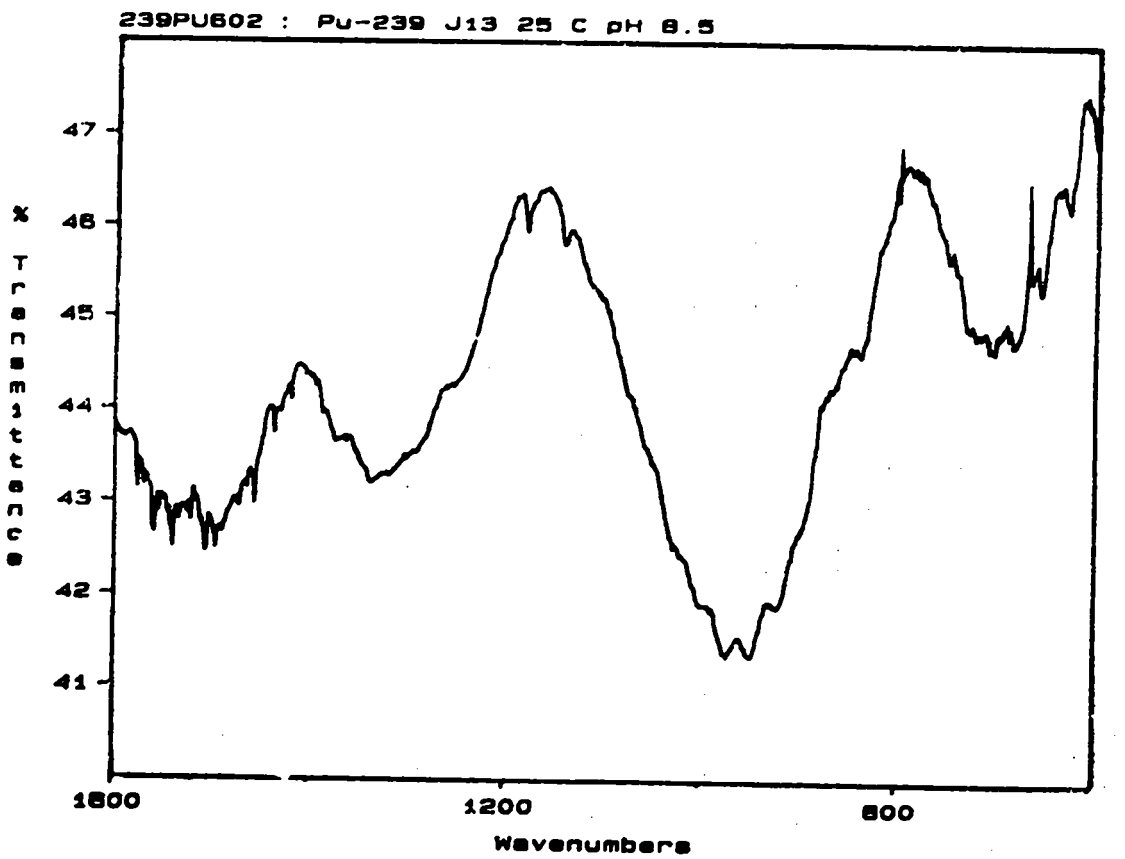

Figure 24. FTIR spectrum of Pu solid phase formed at pH 8.5 and 25°C in J-13 groundwater.

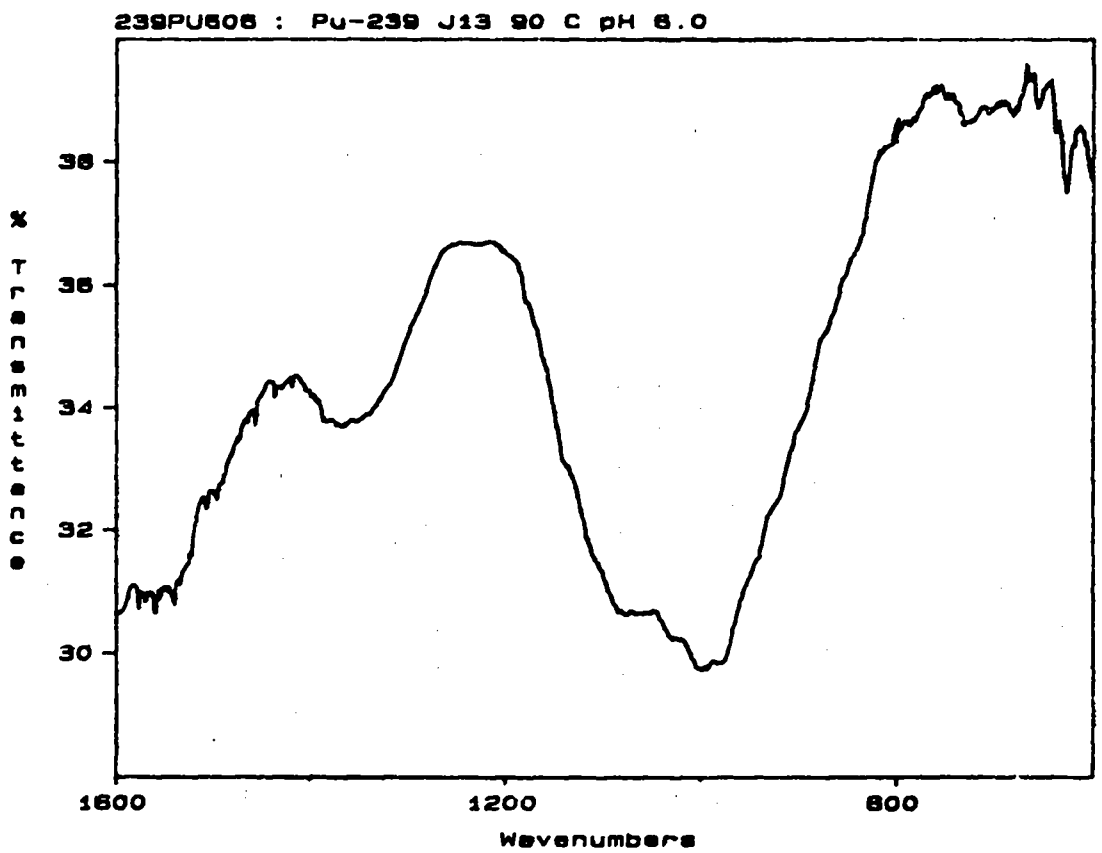

Figure 25. FTIR spectrum of Pu solid phase formed at pH 5.9 and 90°C in J-13 groundwater.

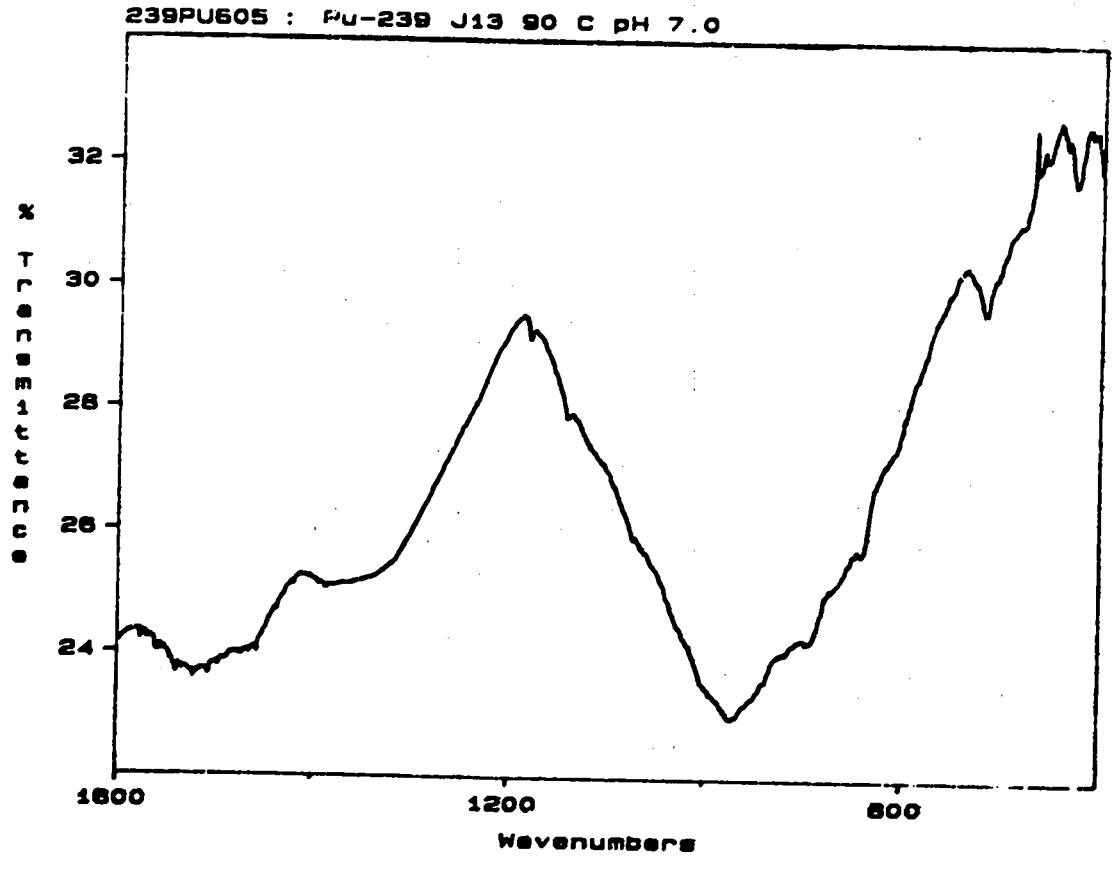

Figure 26. FTIR spectrum of Pu solid phase formed at pH 7.2 and 90°C in J-13 groundwater.

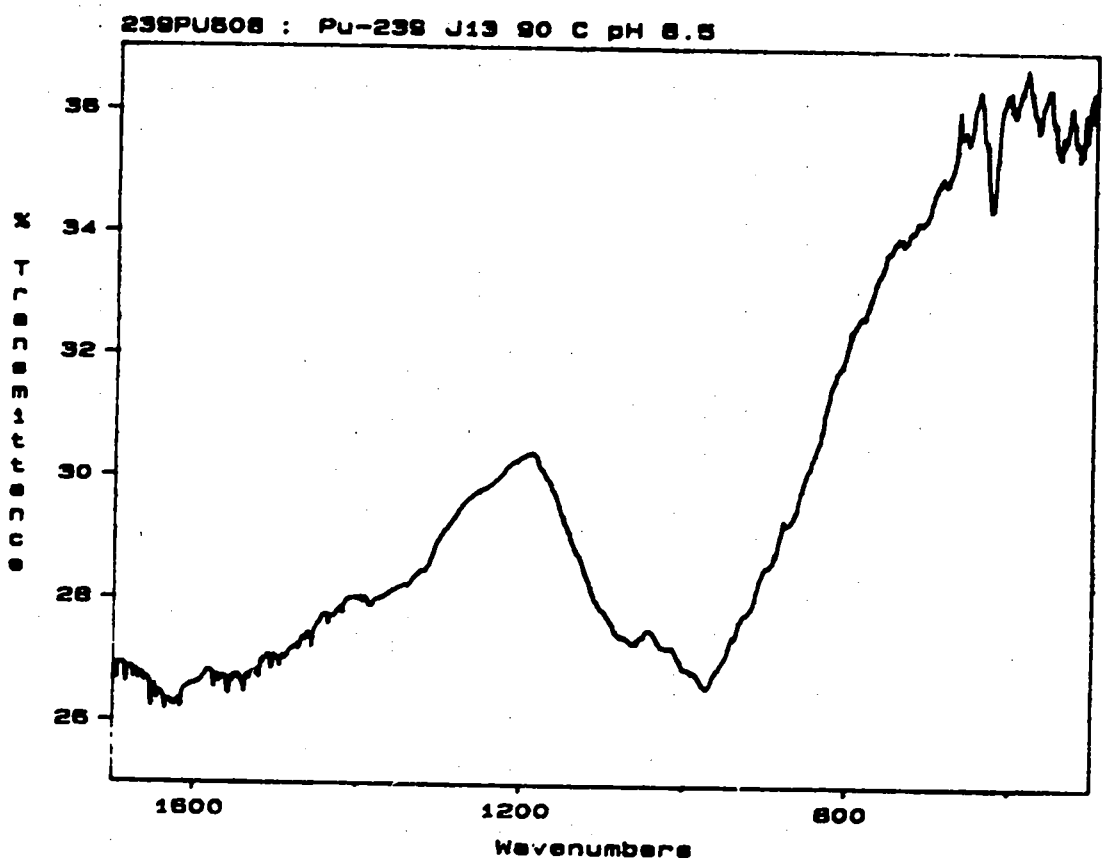

Figure 27. FTIR spectrum of Pu solid phase formed at pH 8.5 and 90°C in J-13 groundwater.

5.3. Americium

We used non-radioactive neodymium in place of americium to minimize radiation-induced degradation of the solubility cell made of Teflon perfluoralkoxy copolymer (TPFA, Savillex Corporation, Minnetonka, MN). The high α-radiation field of americium-243 can cause pitting in the test container, and the dislodged teflon container particles can possibly serve as nucleation centers for americium to form pseudocolloids. Neodymium is chemically similar to americium.[41] It has an ionic radius of 0.983 Å that is very close to that of 0.975 Å for trivalent americium.[42] The neodymium was spiked with a small amount of ^{241}Am to facilitate sample counting using the 59.54-keV photo-peak. The use of the neodymium spiked with ^{241}Am tracer reduced the alpha-radiation to a fraction of the radiation that would have been present if we had used pure ^{243}Am instead. The radiation levels were reduced to 21%, 29%, and 90% for the 25°, 60°, and 90°C experiments, respectively. To determine whether the substitution of americium with the neodymium analogue is acceptable, we measured the solubility of a neodymium solution that was spiked with ^{241}Am (Nd/^{241}Am) and that of pure ^{243}Am in J-13 ground-water at 60°C and pH 6, 7, and 8.5. The ^{243}Am solubility tests were carried out in special cells that were made of the highly radiation-resistant material polyether etherketone (PEEK).[43] The results of this study, shown in Figure 28, give excellent evidence that neodymium is indeed a good stand-in element for americium. The differences between the solubilities of Nd/^{241}Am and pure ^{243}Am are insignificant at each of the studied pH values. This validates our solubility tests in J-13 groundwater at 25°, 60°, and 90°C where we used neodymium mixed with trace amounts of americium-241 as a substitute for americium-243.

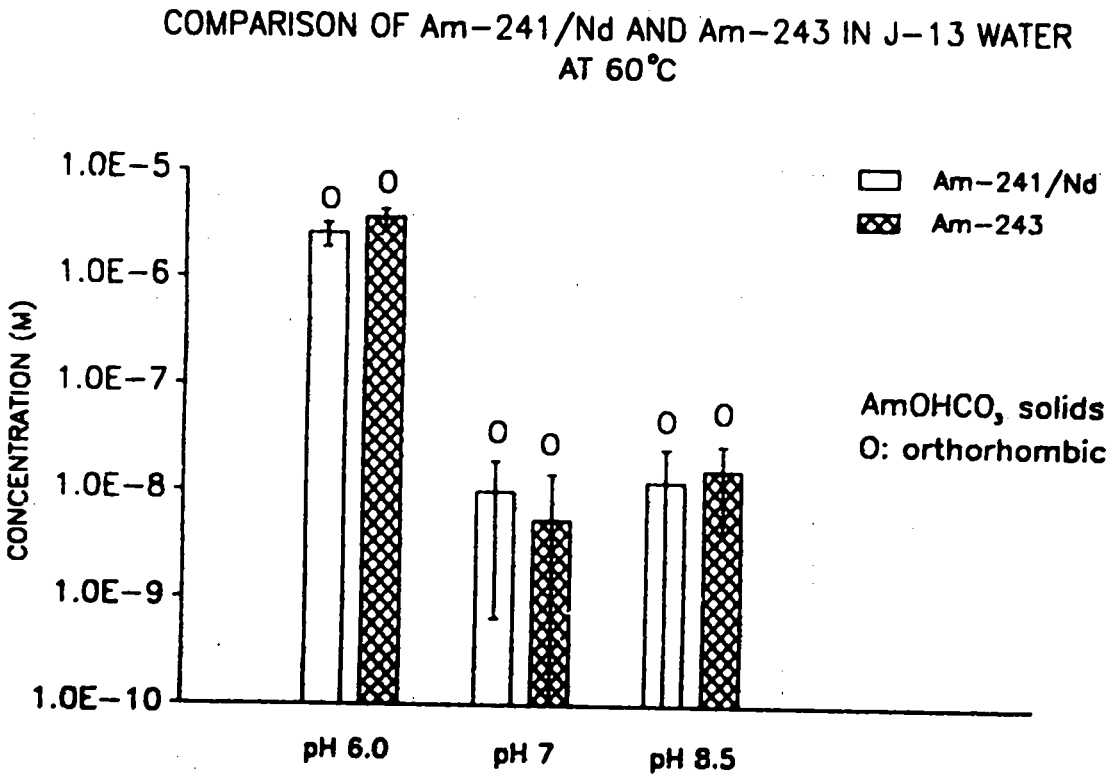

Figure 28. Comparison of results for $^{241}Am^{3+}$ and $^{243}Am^{3+}/Nd^{3+}$ solubility experiments in J-13 groundwater as a function of pH.

5.3.1. Solubility

Results of the solubility studies are shown in Figure 29. The steady-state concentrations and the solutions' Eh values are listed in Table XXI. Concentration profiles as a function of equilibration time and pH for 25°, 60°, and 90°C are shown in Figures 30, 31, and 32, respectively. Figure 33 shows the concentration profiles for the ^{243}Am solubility study at 60°C. No clear trend for the americium solubility was found with increasing temperature and increasing pH. Much higher solubilities were found for 60°C compared with 25°C and 90°C. The individual measurements are listed in Appendix C.

5.3.2. Speciation

Speciation measurements could not be carried out because of the low solution concentrations. The trivalent neodymium cannot change its oxidation state. We determined for the 25°C solutions whether the ^{241}Am tracer undergoes a change in oxidation state. We used extractions with 0.5 M TTA at pH 0 and coprecipitations with LaF_3 for this test. The TTA extracts the oxidation state IV and leaves the oxidation state III, V, and VI in the aqueous solution. The lanthanium fluoride (with holding oxidant) coprecipitates the americium oxidation states III and IV, and leaves the V and VI in the supernatant. As could be expected for the experimental conditions, we found no higher americium oxidation states. The trivalent americium did not change its oxidation state.

5.3.3. Identification of Solids

The precipitates formed in the americium-241/neodymium solutions at 25°, 60°, and 90°C, and the ones formed in the americium-243 solutions at 60° were analyzed by x-ray powder analysis to identify the unknown solids. The d-spacings and relative intensities of the americium-241/neodymium solids are listed in Tables XXII, XXIII, XXIV, for 25°, 60°, and 90°C together with published literature patterns of orthorhombic and hexagonal $NdOHCO_3$.[44,45] It was shown in the literature that americium hydroxycarbonates

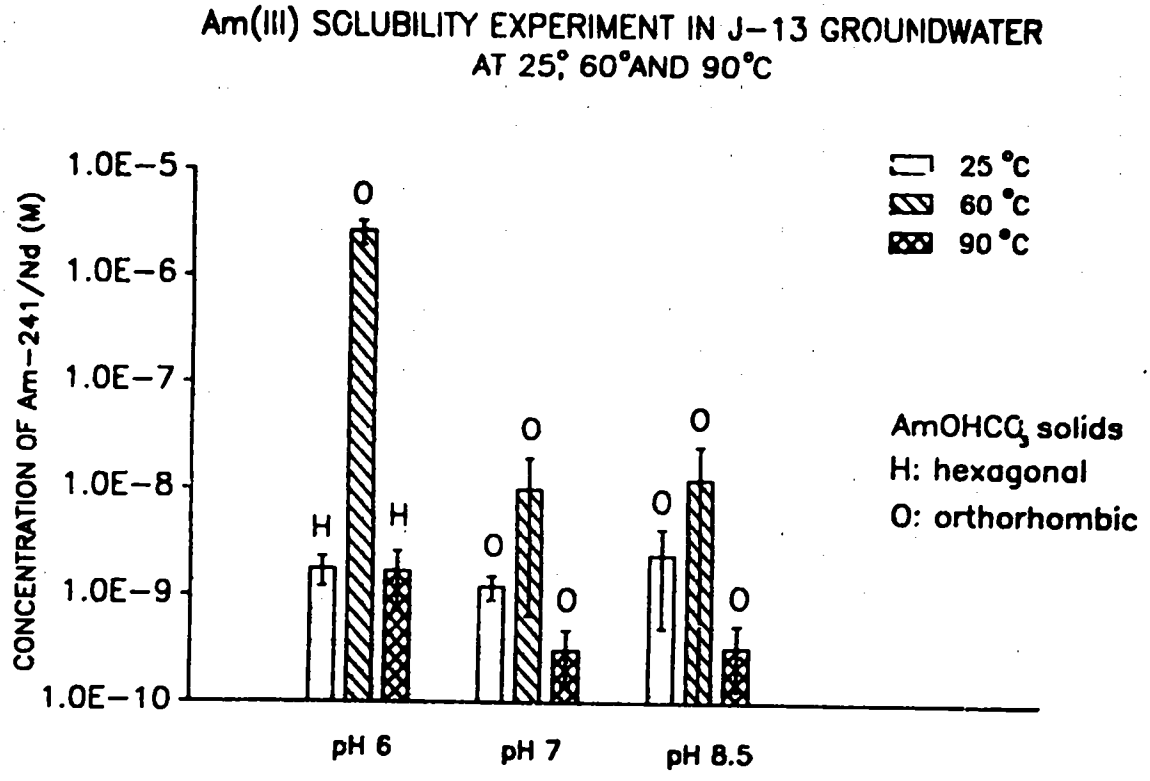

Figure 29. Results for $^{241}Am^{3+}/Nd^{3+}$ solubility experiments in J-13 groundwater as a function of pH and temperature.

Table XXI. Comparison of steady-state solution concentrations for americium–241/neodymium and americium–243 in J-13 groundwater at 25°, 60°, and 90°C.

^{241}Am/Nd	25°C	
pH	conc. (M)	Eh (mV vs. NHE)
5.9 ± 0.1	$(1.8 \pm 0.6) \times 10^{-9}$[b]	331 ± 10
7.0 ± 0.1	$(1.2 \pm 0.3) \times 10^{-9}$[a]	361 ± 10
8.5 ± 0.2	$(2.4 \pm 1.9) \times 10^{-9}$[g]	182 ± 10

	60°C			
	^{241}Am/Nd		^{243}Am	
pH	conc. (M)	Eh (mV vs. NHE)	Conc.(M)	Eh(mV vs. NHE)
5.9 ± 0.1	$(2.5 \pm 0.7) \times 10^{-6}$[d]	392 ± 10	$(3.6 \pm 0.7) \times 10^{-6}$[c]	328 ± 10
7.0 ± 0.1	$(9.9 \pm 9.2) \times 10^{-9}$[e]	385 ± 10	$(5.5 \pm 8.9) \times 10^{-9}$[e]	407 ± 10
8.4 ± 0.1	$(1.2 \pm 1.3) \times 10^{-8}$[e]	343 ± 10	$(1.6 \pm 1.1) \times 10^{-8}$[c]	241 ± 10

^{241}Am/Nd	90°C	
pH	conc. (M)	Eh (mV vs. NHE)
pH 6.0 ± 0.1	$(1.7 \pm 0.9) \times 10^{-9}$[g]	NA
pH 7.0 ± 0.1	$(3.1 \pm 1.7) \times 10^{-10}$[h]	NA
pH 8.5 ± 0.1	$(3.4 \pm 2.1) \times 10^{-10}$[f]	NA

(a-h):The steady-state values were determined from the last

a) 3, b) 4, c) 6, d) 7, e) 9, f) 11, g) 12, h) 13 samplings.

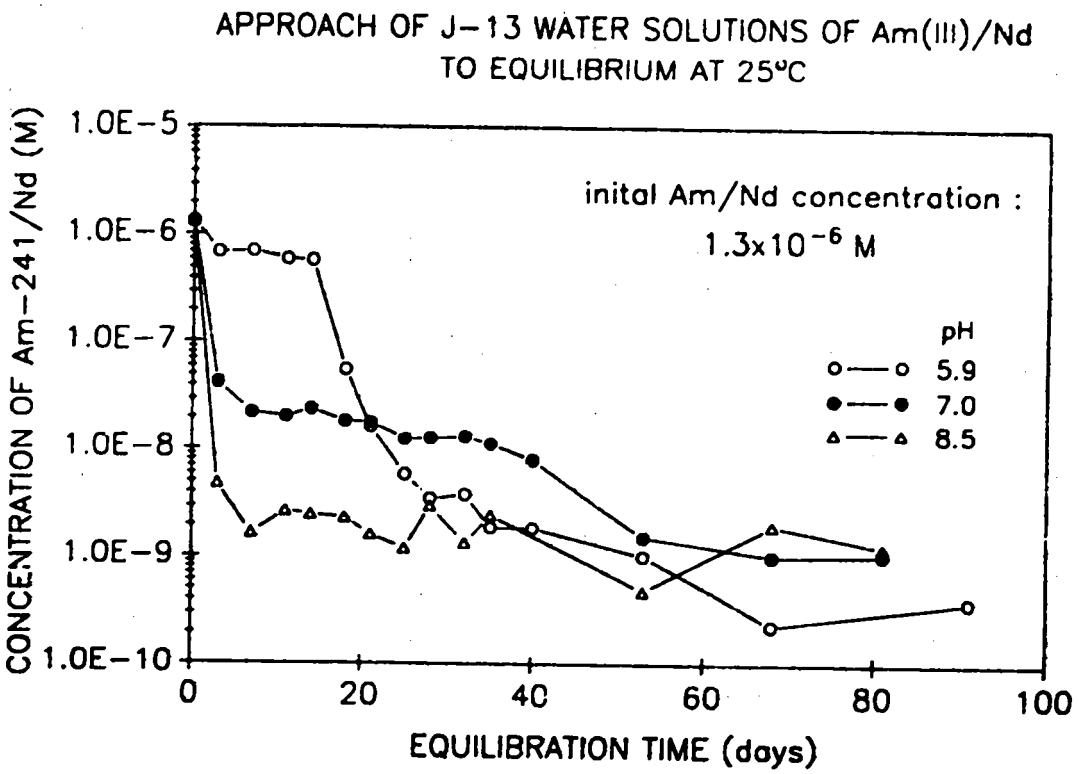

Figure 30. Solution concentration of $^{241}Am/Nd$ in contact with precipitate obtained from supersaturation in J-13 groundwater at 25°C as a function of time. pH 5.9 ± 0.1 (open circles), pH 7.0 ± 0.1 (filled circles), and pH 8.5 ± 0.2 (triangles). The americium/neodymium was added (day 0) as Am^{3+}/Nd^{3+}.

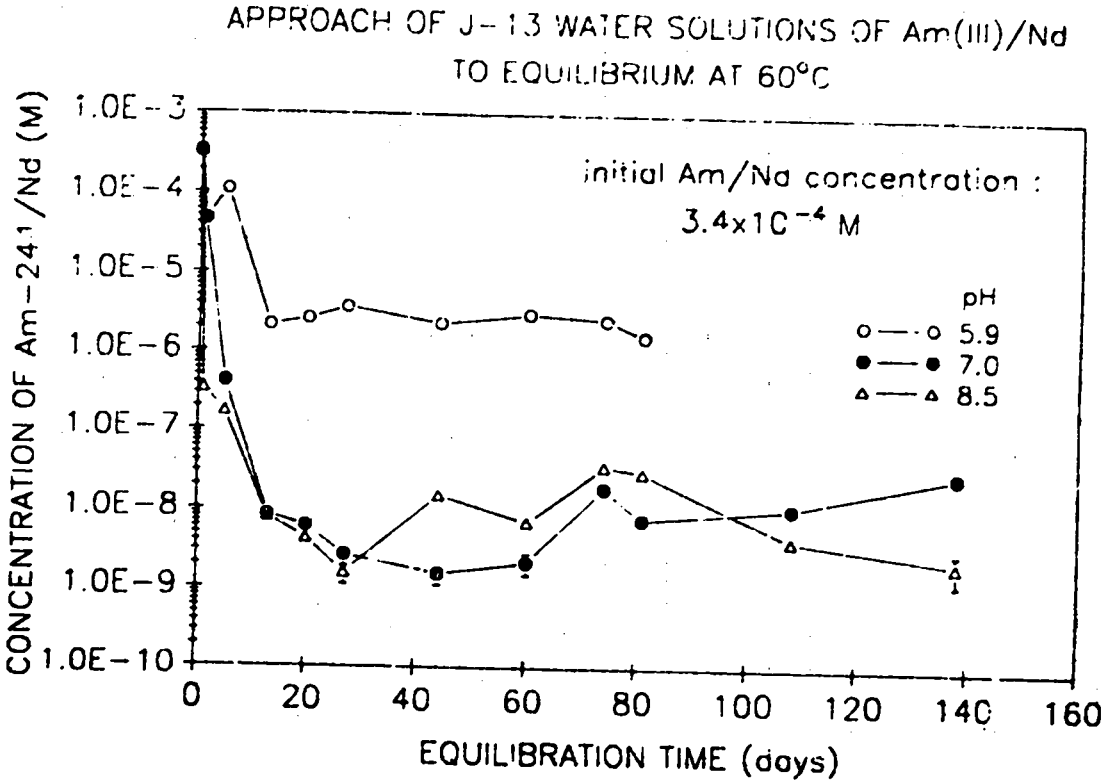

Figure 31. Solution concentration of $^{241}Am/Nd$ in contact with precipitate obtained from supersaturation in J-13 groundwater at 60°C as a function of time. pH 6.0 ± 0.1 (open circles), pH 7.0 ± 0.1 (filled circles), and pH 8.5 ± 0.2 (triangles). The americium/neodymium was added (day 0) as Am^{3+}/Nd^{3+}.

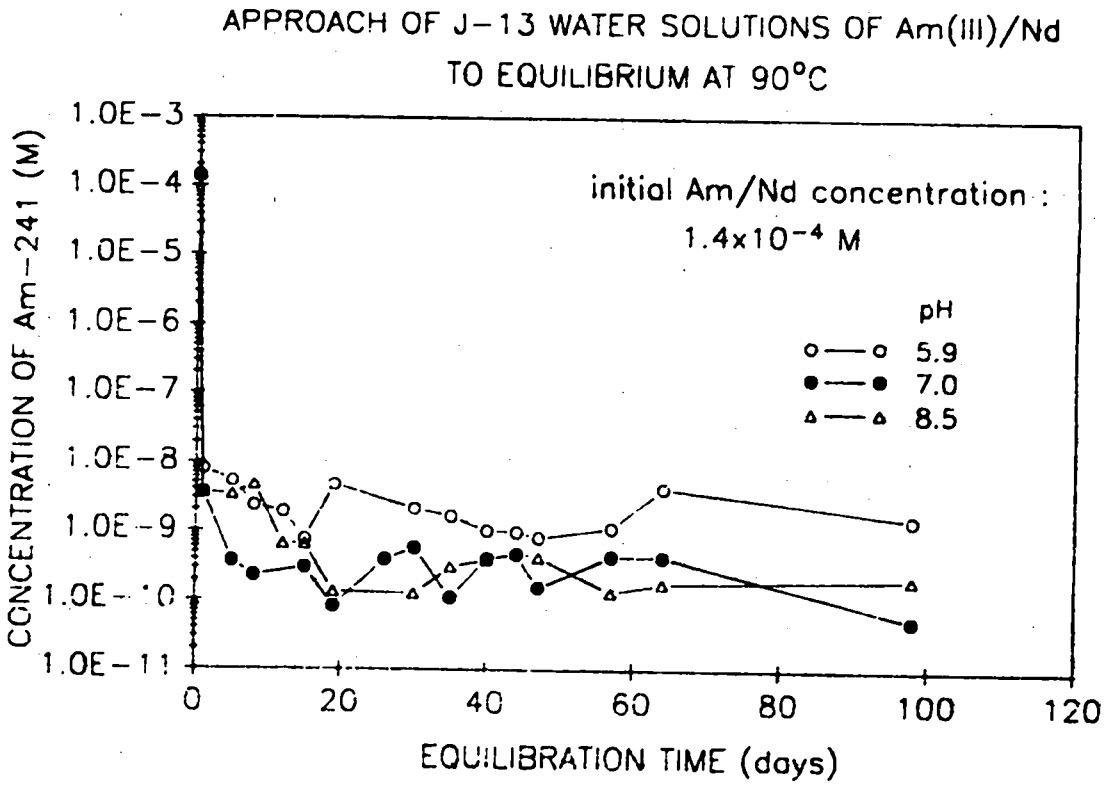

Figure 32. Solution concentration of ^{241}Am/Nd in contact with precipitate obtained from supersaturation in J-13 groundwater at 90°C as a function of time. pH 5.9 ± 0.1 (open circles), pH 7.0 ± 0.1 (filled circles), and pH 8.4 ± 0.1 (triangles). The americium/neodymium was added (day 0) as Am^{3+}/Nd.

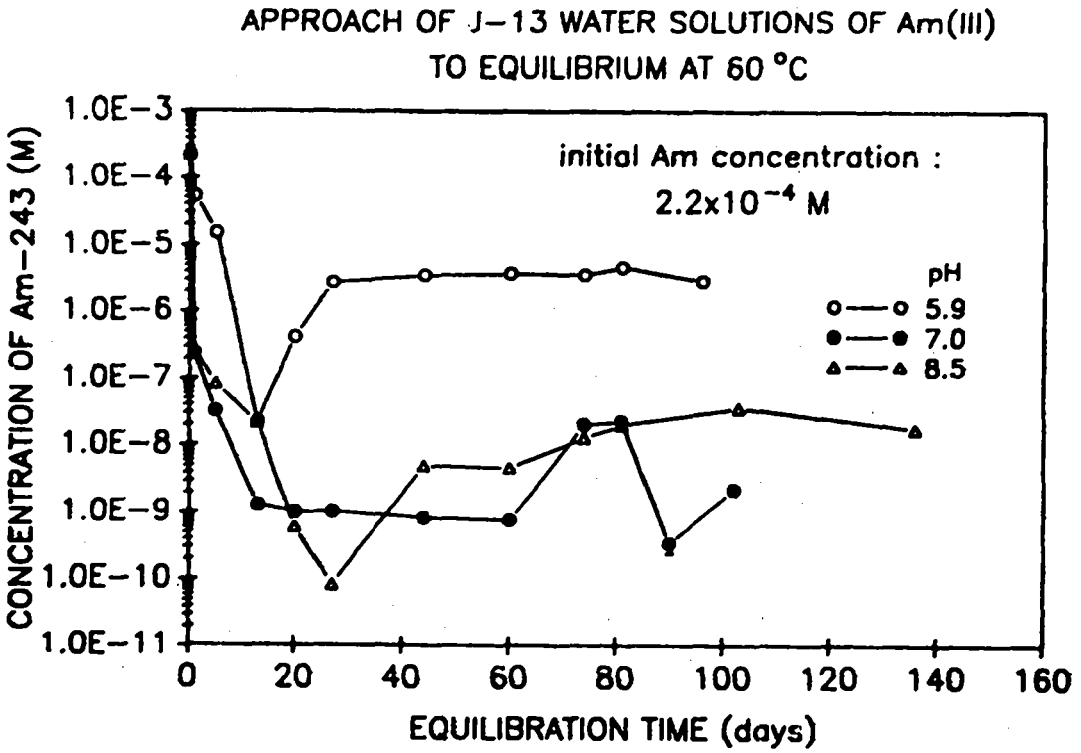

Figure 33. Solution concentration of ^{243}Am in contact with precipitate obtained from supersaturation in J-13 groundwater at 60°C as a function of time. pH 5.9 ± 0.1 (open circles), pH 7.0 ± 0.1 (filled circles), and pH 8.4 ± 0.1 (triangles). The americium/neodymium was added (day 0) as Am^{3+}.

Table XXII. X-ray powder diffraction patterns of ^{241}Am/Nd solid phases in J-13 groundwater at 25°, 60°, and 90°C and pH 5.9 compared with the patterns of hexagonal and orthorhombic $NdOHCO_3$.[44,45]

25°C		60°C		90°C		$NdOHCO_3$-hexagonal		$NdOHCO_3$-orthorhombic	
d(Å)	I[a]	d(Å)	I[a]	d(Å)	I[a]	d(Å)	I[a]	d(Å)	I[a]
		5.49	t					5.50	w+
4.92	m			4.91	m–	4.96	m+		
		4.26	m					4.28	m
								4.24	vs
3.50	m+	3.66	t	3.53	s–	3.57	s–	3.68	w–
		3.30	t					3.65	m–
		3.09	t					3.32	m–
2.86	w+			2.86	vs	2.90	vs	2.94	w–
				2.43	t	2.49	w	2.91	m
								2.75	w
								2.63	m
2.27	w–	2.32	t					2.48	s
								2.40	w–
								2.32	w
								2.31	w+
								2.14	w
								2.12	s
						2.06	m	2.10	t
2.03	;	2.04	w+	2.04	w+	2.04	s–	2.05	w
1.99	s	1.99	s	2.00	w+			2.03	w+
1.87	t	1.83	t	1.88	w	1.90	m–	1.96	w
								1.93	w
1.73	t	1.73	w–	1.77	t	1.78	w–	1.88	w–
								1.83	s
								1.81	w
								1.72	w–
1.65	t			1.66	w–	1.68	w	1.69	w–
								1.66	w–
								1.62	w–
				1.56	t	1.59	w	1.60	w
								1.58	t
								1.57	w–
				1.47	t	1.50	w	1.54	m
								1.52	w
								1.50	w–
				1.43	t	1.45	w–	1.47	m–
								1.46	m+
								1.44	w–
								1.42	w–
								1.40	w–
				1.33	t	1.35	w–	1.37	w–
				1.29	t	1.30	w	1.31	w+
						1.29	w+	1.30	w–
		1.24	t					1.28	w–
								1.27	w–
								1.25	w
								1.24	w+
								1.23	w+
								1.21	w–
								1.20	w

(a) Relative intensities visually estimated: vs = very strong, s = strong, m = medium, w = weak, t = trace.

* denotes diffuse bands.

Table XXIII. X-ray powder diffraction patterns of ^{241}Am/Nd solid phases in J-13 groundwater at 25°, 60°, and 90°C and pH 7 compared with the pattern of orthorhombic $NdOHCO_3$.[44]

25°C		60°C		90°C		$NdOHCO_3$-orthorhombic	
d(Å)	I[a]	d(Å)	I[a]	d(Å)	I[a]	d(Å)	I[a]
		5.53	w	5.47	w+	5.50	w+
				4.34	s		
		4.28	s	4.28	vs	4.28	m
						4.24	vs
		3.66	s–	3.68	m	3.68	w–
						3.65	m–
		3.33	m	3.32	w+	3.32	m–
		2.92	m+	2.93	m–	2.94	w–
				2.83	m	2.91	m
						2.75	w
		2.63	w	2.62	t	2.63	m
		2.45	w–	2.49	w-	2.48	s
		2.40	t	2.41	t	2.40	w–
		2.32	m	2.33	m	2.32	w
						2.31	w+
						2.14	w
						2.12	s
						2.10	t
		2.05	w+	2.04	w+	2.05	w
						2.03	w+
1.99	s	1.99	s	1.99	m–	1.96	w
		1.93	t	1.93	w–	1.93	w
		1.88	t	1.89	t	1.88	w–
		1.83	t	1.84	t	1.83	s
		1.80	t			1.81	w
1.73	w					1.72	w–
						1.68	w–
		1.66	t			1.66	w–
						1.62	w–
						1.60	w
						1.58	t
						1.57	w–
						1.54	m
						1.52	w
						1.50	w–
						1.47	m–
						1.46	w+
						1.44	w–
						1.42	w–
						1.40	w–
						1.37	w–
						1.31	w+
						1.30	w–
						1.28	w–
						1.27	w–
						1.25	w
1.24	t					1.24	w+
						1.23	w+
						1.21	w–
						1.20	w

(a) Relative intensities visually estimated: vs = very strong, s = strong, m = medium, w = weak, t = trace.

Table XXIV. X-ray powder diffraction patterns of ^{241}Am/Nd solid phases in J-13 groundwater at 25°, 60°, and 90°C and pH 8.5.

25°C		60°C		90°C		$NdOHCO_3$-orthorhombic	
d(Å)	I[a]	d(Å)	I[a]	d(Å)	I[a]	d(Å)	I[a]
5.49	t	5.47	m	5.47	w+	5.50	w+
4.93	t						
4.27	s	4.25	s–	4.28	s	4.28	m
						4.24	vs
3.66	w+	3.67	s–	3.68	m	3.68	w–
				3.46	w	3.65	m–
3.32	t	3.32	m–	3.29	w	3.32	m–
				3.06	w–		
2.92	w–	2.91	m+	2.90	w+	2.94	w–
				2.81	vs	2.91	m
				2.71	w–	2.75	w
2.63	t	2.64	w	2.63	w–	2.63	m
2.48	t	2.50	w–	2.48	w–	2.48	s
		2.41	w–			2.40	w–
2.32	t	2.32	m	2.31	t	2.32	w
2.26	s-					2.31	w+
						2.14	w
						2.12	s
						2.10	t
2.05	t	2.07	w	2.05	w	2.05	w
2.00	s			2.00	w+	2.03	w+
1.97	w	2.00	s				
						1.96	w
		1.93	w–			1.93	w
		1.88	t			1.88	w–
		1.82	w–			1.83	s
						1.81	w
1.73	t	1.73	w–				
						1.72	w–
						1.69	w–
						1.66	w–
				1.63	t	1.62	w–
						1.60	w
						1.58	t
						1.57	w–
						1.54	m
						1.50	w–
						1.47	m–
						1.46	w+
						1.44	w–
						1.42	w–
						1.40	w–
1.39	t					1.37	w–
						1.31	w+
						1.30	w+
						1.28	w–
						1.27	w–
						1.25	w
1.24	t					1.24	w
						1.23	w+
						1.21	w–
1.19	t					1.20	w

(a) Relative intensities visually estimated: vs = very strong, s = strong, m = medium, w = weak, t = trace.

are isostructural to the analogous neodymium hydroxy-carbonates.[41,45] Table XXV lists the additional results for the solids formed at 60°C that contained pure ^{243}Am. All solids were $^{241}AmOHCO_3/NdOHCO_3$, with orthorhombic structure for all temperatures at pH 7 and 8.5 and for 60°C at pH 6, and with hexagonal structure for 25°C and 90°C at pH 6. Orthorhombic $AmOHCO_3/NdOHCO_3$ appears to have a much higher solubility at pH 5.9 and 60°C than the hexagonal form at the same pH at 25°C or 90°C. We found the same results for the solutions at 60°C that contained pure ^{243}Am. The $^{243}AmOHCO_3$ precipitates were orthorhombic for all three pH values. In an earlier attempt to measure the solubility of ^{243}Am, however, we isolated a hexagonal $^{243}AmOHCO_3$ precipitate. This experiment was carried out in TPFA cells, and no steady-state conditions were reached because the soluble americium formed pseudocolloids together with Teflon particles that were dislodged from the container material by α-radiation. It is possible that the orthorhombic $AmOHCO_3$ is metastable at pH 5.9 and may with time convert to the hexagonal form with lower solubility.

Table XXV. X-ray powder diffraction patterns of ^{243}Am solid phases in J-13 water at 60°C, and pH 5.9, 7.0 and 8.5 compared with the pattern of orthorhombic $NdOHCO_3$.[44]

pH 6.0		pH 7.0		pH 8.5		$NdOHCO_3$-orthorhombic	
d(Å)	I[a]	d(Å)	I[a]	d(Å)	I[a]	d(Å)	I[a]
		5.51	t			5.50	w+
4.29	s	4.2[illegible]	s	4.27	s	4.28	m
						4.24	vs
3.69	m	3.57	m	3.67	m	3.68	w–
						3.65	m–
3.32	w	3.35	t			3.32	m–
2.93	m–					2.94	w–
		2.91	w	2.91	w	2.91	m
						2.75	w
						2.63	m
2.47	t					2.48	s
						2.40	w–
2.33	t			2.32	t	2.32	w
						2.31	w+
						2.14	w
						2.12	s
						2.10	t
						2.05	w
						2.03	w+
1.99	s	1.99	s	1.98	s	1.96	w
1.95	t					1.93	w
						1.88	w–
						1.83	s
						1.81	w
1.73	t	1.73	t			1.72	w–
						1.69	w–
						1.66	w–
						1.62	w–
						1.60	w
						1.58	t
						1.57	w–
						1.54	m
						1.52	w
						1.50	w–
						1.47	m–
						1.46	w+
						1.44	w–
						1.42	w–
						1.40	w–
						1.37	w–
						1.31	w+
						1.30	w–
						1.28	w–
						1.27	w–
						1.25	w
						1.24	w+
						1.23	w+
						1.21	w–
						1.20	w

(a) Relative intensities visually estimated: vs = very strong, s = strong, m = medium, w = weak, t = trace.

REFERENCES

1. U.S. Department of Energy Yucca Mountain Site Characterization Plan, Yucca Mountain Site, Nevada Research and Development Area, Nevada, Office of Civilian Radioactive Waste Management, Washington, D.C. (1988). HQO.881201.0002

2. D. J. Brooks and J. A. Corrado, "Determination of Radionuclide Solubility in Groundwater for Assessment of High-Level Waste Isolation," U.S. Nuclear Regulatory Commission, Technical Position, Washington, D.C. (1984). NNA.871104.0035

3. A. E. Ogard and J. F. Kerrisk, "Groundwater Chemistry Along the Flow Path between a Proposed Repository Site and the Accessible Environment," report LA-10188-MS, Los Alamos National Laboratory, New Mexico (1984). NNA.870406.0021

4. B. V. Enüstün, J. Turevich, "Solubility of Fine Particles of Strontium Sulfate," J. Amer. Chem. Soc. **82**, 4502–4509 (1960). NNA.930326.0103

5. P. W. Vorhees, "The Theory of Ostwald Ripening" J. Stat. Phys. **38**, 231–252 (1985). NNA.930326.0102

6. J. W. Morse, W. H. Casey, "Ostwald Processes and Mineral Paragenesis in Sediments" Amer. J. Sci. **288**, 537–560 (1980). NNA.930326.0101

7. J. A. Rard, "The Effect of Precipitation Conditions and Aging upon Characteristics of Particles Precipitated from Aqueous Solutions," report UCID-21755, Lawrence Livermore National Laboratory, Livermore, California, U.S.A. (1989). NNA.930406.0024

8. R. Stumpe, J. I. Kim, W. Schrepp, H. Walter, "Speciation of Actinide Ions in Aqueous Solution by Laser-Induced Pulsed Photoacoustic Spectroscopy," Appl. Phys. **B 34**, 203–206 (1984). HQS.880517.2551

9. F. T. Ewart, M. Liezers, J. W. McMillan, P. M. Pollard, H. P. Thomason, "The Development of a Laser Induced Photoacoustic Facility for Actinide Speciation," report NSS/R103, Harwell Laboratory, Oxfordshire, U.K. (1988). HQX.880701.0010

10. J. E. Cross, D. Crossley, J. W. Edwards, P. M. Pollard, S. Turner, "Actinide Speciation. Further Development and Application of Laser Induced Photoacoustic Spectroscopy and Voltammetry," report NSS/R119, Harwell Laboratory, Oxfordshire, U.K. (1989). HQX.891211.0040

11. R. A. Torres, C. E. Palmer, P. A. Baisden, R. E. Russo, R. J. Silva, "A Comparison of Photoacoustic Spectroscopy, Conventional Absorption Spectroscopy, and Potentiometry as Probes of Lanthanide Speciation," report UCRL-101760, Lawrence Livermore National Laboratory, Livermore, California, U.S.A (1989). NNA.930326.0100

12. M. M. Doxtader, V. A. Maroni, J. V. Beitz, M. Heaven, "Laser Photoacoustic Spectroscopy for Trace Level Detection of Actinides in Groundwater," Mat. Res. Soc. Symp. Proc. **84**, 173–185 (1987). NNA.930420.0098

13. H. Nitsche, S. C. Lee, R. C. Gatti, "Determination of Plutonium Oxidation States at Trace Levels Pertinent to Nuclear Waste Disposal," J. Radioanal. Nucl. Chem. **124**(1), 171–185 (1988). NNA.930326.0099

14. D. B. Tucker, E. M. Standifer, H. Nitsche, and R. J. Silva, "Data Acquisition and Feedback Control System for Solubility Studies of Nuclear Waste Elements," Lanthanide and Actinide Research **2**, 279–287 (1988). NNA.930326.0096

15. H. Nitsche and N. M. Edelstein, "Solubilities and Speciation of Selected Transuranium Ions. A Comparison of a Non-Complexing Solution with a Groundwater from the Nevada Tuff Site," Radiochim Acta **39**, 23 (1985). NNA.930326.0097

16. D. Cohen, "Electrochemical Studies of Plutonium Ions in Perchloric Acid Solution," J. Inorg. Nucl. Chem. **18**, 207 (1961). NNA.930326.0098

17. G. A. Burney, R. M. Harbour, "Radiochemistry of Neptunium," NAS-NS 3060, Nuclear Science Series, National Academy of Sciences - National Research Council, 22–25 (1974). NNA.930326.0095

18. T. W. Newton, D. E. Hobart, P. D. Palmer, "The Preparation and Stability of Pure Oxidation States of Neptunium, Plutonium, and Americium," report LA-UR-86-967, Los Alamos National Laboratory, Los Alamos, New Mexico (1986). NNA.930406.0025

19. D. Cohen, "The Absorption Spectra of Plutonium Ions in Perchloric Acid Solution," J. Inorg. Nucl. Chem. **18**, 211 (1961). NNA.930326.0094

20. P. G. Hagan, J. M. Cleveland, "The Absorption Spectra of Neptunium Ions in Perchloric Acid Solution," J. Inorg. Nucl. Chem. **28**, 2905 (1966). NNA.930326.0093

21. S. L. Phillips, C. A. Phillips, and J. Skeen, "Hydrolysis, Formation and Ionization Constants at 25°C, and at High Temperature - High Ionic Strength," Report LBL-14996, Lawrence Berkeley Laboratory, University of California, Berkeley, California (1985). NNA.930430.0016

22. H. Nitsche, R. C. Gatti, and S. C. Lee "Low-level determination of plutonium by gamma and *L*- X-ray spectroscopy," Proceedings of International Topical Conference on Methods and Applications of Radioanalytical Chemistry-II, April 21–27, Kona, Hawaii (in press, 1991). NNA.930326.0092

23. R. M. Garrels, Mineral Equilibria at Low Temperature and Pressure, Harper and Brothers, New York, N.Y. (1960). NNA.930406.0026

24. D. Langmuir, "Eh-pH Determinations," in Procedures in Sedimentary Petrology, R. E. Carver, ed., 597–635, Wiley, New York, N.Y. (1971). Readily Available.

25. H. Nitsche, E. M. Standifer, and R. J. Silva, "Neptunium(V) Complexation with Carbonate," Lanthanide and Actinide Research **3**, 203–211 (1990). NNA.930406.0027

26. Y. F. Volkov, G. I. Visyashcheva, S. V. Tomilin, V. I. Spiryakov, I. I. Kapshukov, and A. G. Rykov, "Carbonate Compounds of Pentavalent Actinides with Alkali Metal Cations VII. Synthesis and Crystal Structure of Hydrate Compounds with the Composition $Na_{0.6}NpO_2(CO_3)_{0.8} \cdot nH_2O$," Sov. Radiochem. (Eng. transl.) **21**.

583–590 (1979). NNA.930420.0098

27. Y. F. Volkov. G. I. Visyashcheva, S. V. Tomilin, I. I. Kapshukov, and R. G. Rykov, "Study of Carbonate Compounds of Pentavalent Actinides with Alkali-Metal Cations. VIII. Synthesis and X-Ray Diffraction Investigation of Several Compounds of Neptunium(V) with Sodium and Rubidium," Sov. Radiochem. (Eng. transl.) **23**, 191–195 (1981). NNA.930326.0091

28. Y. F. Volkov, G. I. Visyashcheva, and I. I. Kapshukov, "Study of Carbonate Compounds of Pentavalent Actinides with Alkali Metal Cations. V. Production and Identification of Hydrate Forms of Sodium Monocarbonato-neptunylate," Sov. Radiochem. (Eng. transl.) **19**, 263–266 (1977). NNA.930326.0089

29. Y. F. Volkov, S. V. Tomilin, G. I. Visyashcheva, and I. I. Kapshukov, "Carbonate Compounds of Pentavalent Actinoids with Alkali-Metal Cations. VI. X-Ray Structure Analysis of $LiNpO_2CO_3$ and $NaNpO_2CO_3$," Sov. Radiochem. (Eng. transl.) **21**, 579–583 (1979). NNA.930326.0090

30. D. Cohen and A. J. Walter, "Neptunium Pentoxide," J. Chem. Soc., 2696–2699 (1964). NNA.930326.0088

31. T. K. Keenan and F. H. Kruse, "Potassium Double Carbonates of Pentavalent Neptunium, Plutonium, and Americium," Inorg. Chem. 3, 1231 (1964). NNA.930326.0086

32. K. Nakamoto, Infrared and Raman Spectra of Inorganic and Coordination Compounds, Wiley, New York, N.Y. (1986). Readily Available.

33. L. H. Jones and R. A. Penneman, "Infrared Spectra and Structure of Uranyl and Transuranium (V) and (VI) Ions in Aqueous Perchloric Acid Solution," J. Chem. Phys. **21**, 542 (1952). NNA.930406.0028

34. G. L. Silver, "Suggestion for the Determination of Plutonium Valencies in Aqueous Solutions," Radiochem. Radioanal. Lett. **9**, 5–6, 315–320 (1972). NNA.930326.0087

35. R. C. L. Mooney and W. H. Zachariasen, The Transuranium Elements Part II, G. T. Seaborg, J. J. Katz, and W. M. Manning, eds., 1442–1447, McGraw-Hill, New York, N.Y. (1949). NNA.930326.0085

36. K. W. Bagnall and J. B. Laidler, "Neptunium and Plutonium Trioxide Hydrates," J. Chem. Soc., 2693–2696 (1964). NNA.930326.0084

37. F. H. Ellinger and W. H. Zachariasen, "The Crystal Structure of $KPuO_2CO_3$, $NH_4PuO_2CO_3$ and $RbAmO_2CO_3$," J. Phys. Chem. **58**, 405–408 (1954). NNA.930326.0082

38. J. Navratil and Bramlet, "Preparation and Characterization of Plutonyl(VI) Carbonate," J. Inorg. Nucl. Chem. **35**, 157–163 (1973). NNA.930326.0083

39. L. M. Toth and H. A. Friedman, "The IR Spectrum of Pu(IV) Polymer," J. Inorg. Nucl. Chem. **40**, 807 (1978). NNA.930326.0081

40. T. W. Newton, Low Alamos National Laboratory, private communication by telephone (1985).

41. R. J. Silva and H. Nitsche, "Thermodynamic Properties of Chemical Species of Waste Radionuclides," Report NUREG/CP-0052, U.S. Nuclear Regulatory Commission, Washington, D.C. (1983). HQS.880517.2061

42. R. D. Shannon, "Revised Effective Ionic Radii and Systematic Studies of Interatomic Distances in Halogennides and Chalcogenides," Acta Cryst. A **32**, 751–767 (1976). NNA.930326.0080

43. The Polymer Corporation, Product Bulletin BR-10 8/84, Reading, PA (1984). NNA.930406.0029

44. H. Dexpert and P. Caro, "Determination de la Structure Cristalline de le Variete á des Hydroxycarbonates de Terres Rares $LnOHCO_3$ (Ln = Nd)," Mat. Res. Bull, **9**, 1577–1586 (1974). NNA.930406.0030

45. E. M. Standifer and H. Nitsche, "First Evidence for Hexagonal $AmOHCO_3$," Lanthanide and Actinide Research **2**, 383–384 (1988). NNA.880829.0064

APPENDIX A

RESULTS OF NEPTUNIUM SOLUBILITY EXPERIMENTS IN J-13 GROUNDWATER

Appendix AI. Results of neptunium (NpO_2^+) solubility experiments in J-13 groundwater at 25°C.

Sample I.D.	Days	pH	Concentration (M)
1-1A1J2	2	6.01	$(5.21 \pm 0.21) \times 10^{-3}$
1-2A1J2	6	6.02	$(5.12 \pm 0.21) \times 10^{-3}$
1-3A1J2	9	6.01	$(5.05 \pm 0.14) \times 10^{-3}$
1-4A1J2	13	6.02	$(5.06 \pm 0.14) \times 10^{-3}$
1-5A1J2	16	5.93	$(4.89 \pm 0.14) \times 10^{-3}$
1-6A1J2	20	5.99	$(5.26 \pm 0.15) \times 10^{-3}$
1-7A1J2	23	5.96	$(5.61 \pm 0.16) \times 10^{-3}$
1-8A1J2	27	5.91	$(5.71 \pm 0.19) \times 10^{-3}$
1-9A1J2	30	5.88	$(5.08 \pm 0.19) \times 10^{-3}$
1-10A1J2	34	5.93	$(5.67 \pm 0.20) \times 10^{-3}$
1-11A1J2	41	5.97	$(5.17 \pm 0.18) \times 10^{-3}$
1-12A1J2	48	5.90	$(5.62 \pm 0.14) \times 10^{-3}$
1-13A1J2	55	5.82	$(5.61 \pm 0.17) \times 10^{-3}$
1-14A1J2	55	5.87	$(5.18 \pm 0.17) \times 10^{-3}$
average 1-1A1J2 through 1-14A1J2:			$(5.32 \pm 0.28) \times 10^{-3}$

Appendix AII. Results of neptunium (NpO_2^+) solubility experiments in J-13 groundwater at 25°C.

Sample I.D.	Days	pH	Concentration (M)
2-1A1J2	2	6.89	$(6.55 \pm 0.25) \times 10^{-4}$
2-2A1J2	6	6.94	$(5.61 \pm 0.22) \times 10^{-4}$
2-3A1J2	9	6.92	$(5.31 \pm 0.15) \times 10^{-4}$
2-4A1J2	13	6.99	$(3.93 \pm 0.11) \times 10^{-4}$
2-5A1J2	16	6.85	$(4.22 \pm 0.12) \times 10^{-4}$
2-6A1J2	20	6.96	$(2.37 \pm 0.06) \times 10^{-4}$
2-7A1J2	23	6.97	$(2.16 \pm 0.06) \times 10^{-4}$
2-8A1J2	27	6.94	$(2.08 \pm 0.08) \times 10^{-4}$
2-9A1J2	30	6.91	$(1.88 \pm 0.08) \times 10^{-4}$
2-10A1J2	34	6.95	$(1.57 \pm 0.07) \times 10^{-4}$
2-11A1J2	41	6.96	$(1.17 \pm 0.04) \times 10^{-4}$
2-12A1J2	48	7.07	$(1.40 \pm 0.05) \times 10^{-4}$
2-13A1J2	55	7.05	$(1.22 \pm 0.04) \times 10^{-4}$
2-14A1J2	62	7.13	$(1.13 \pm 0.04) \times 10^{-4}$
2-15A1J2	64	6.97	$(1.12 \pm 0.03) \times 10^{-4}$
average 2-10A1J2 through 2-15A1J2:			$(1.27 \pm 0.18) \times 10^{-4}$

Appendix AIII. Results of neptunium (NpO_2^+) solubility experiments in J-13 groundwater at 25°C.

Sample I.D.	Days	pH	Concentration (M)
3P-2A1J2	4	8.30	$(1.33 \pm 0.04) \times 10^{-4}$
3P-3A1J2	7	8.35	$(6.47 \pm 0.18) \times 10^{-5}$
3P-4A1J2	11	8.37	$(5.69 \pm 0.16) \times 10^{-5}$
3P-4A1J2	14	8.47	$(5.38 \pm 0.15) \times 10^{-5}$
3P-5A1J2	18	8.53	$(4.89 \pm 0.17) \times 10^{-5}$
3P-6A1J2	21	8.47	$(3.87 \pm 0.14) \times 10^{-5}$
3P-7A1J2	25	8.35	$(5.03 \pm 0.22) \times 10^{-5}$
3P-8A1J2	28	8.55	$(4.13 \pm 0.14) \times 10^{-5}$
3P-9A1J2	32	8.51	$(4.44 \pm 0.18) \times 10^{-5}$
3P-10A1J2	35	8.49	$(4.20 \pm 0.13) \times 10^{-5}$
3P-11A1J2	39	8.48	$(4.58 \pm 0.12) \times 10^{-5}$
3P-12A1J2	46	8.58	$(5.26 \pm 0.16) \times 10^{-5}$
3P-13A1J2	48	8.40	$(3.28 \pm 0.11) \times 10^{-5}$
3P-14A1J2	58	8.46	$(3.52 \pm 0.13) \times 10^{-5}$
average 3P-4A1J2 through 3P-14A1J2:			$(4.42 \pm 0.69) \times 10^{-5}$

Appendix AIV. Results of neptunium (NpO_2^+) solubility experiments in J-13 groundwater at 60°C.

Sample I.D.	Days	pH	Concentration (M)
1/6F1	0	5.99	$(9.46 \pm 0.38) \times 10^{-3}$
1/7F1	13	5.80	$(8.21 \pm 0.34) \times 10^{-3}$
1/8F1	20	5.84	$(7.81 \pm 0.38) \times 10^{-3}$
1/9F1	28	5.87	$(7.93 \pm 0.40) \times 10^{-3}$
1/10F1	35	5.84	$(7.56 \pm 0.37) \times 10^{-3}$
1/11F1	42	5.92	$(7.85 \pm 0.34) \times 10^{-3}$
1/12F1	54	5.98	$(6.61 \pm 0.28) \times 10^{-3}$
1/13F1	63	6.01	$(6.53 \pm 0.27) \times 10^{-3}$
1/14F1	70	5.82	$(6.59 \pm 0.28) \times 10^{-3}$
1/15F1	80	5.90	$(5.81 \pm 0.24) \times 10^{-3}$
1/16F1	82	5.89	$(6.46 \pm 0.27) \times 10^{-3}$
average 1/12F1 through 1/16F1:			$(6.40 \pm 0.34) \times 10^{-3}$

Appendix AV. Results of neptunium (NpO_2^+) solubility experiments in J-13 groundwater at 60°C.

Sample I.D.	Days	pH	Concentration (M)
2/1F1	3	6.94	$(8.55 \pm 0.35) \times 10^{-4}$
2/2F1	13	7.09	$(7.20 \pm 0.30) \times 10^{-4}$
2/3F1	27	7.07	$(5.38 \pm 0.22) \times 10^{-4}$
2/4F1	44	7.15	$(6.47 \pm 0.30) \times 10^{-4}$
2/5F1	59	6.88	$(7.60 \pm 0.41) \times 10^{-4}$
2/6F1	66	7.07	$(7.02 \pm 0.39) \times 10^{-4}$
2/7F1	73	7.09	$(7.82 \pm 0.33) \times 10^{-4}$
2/8F1	85	7.05	$(1.06 \pm 0.04) \times 10^{-3}$
2/9F1	94	7.02	$(1.11 \pm 0.04) \times 10^{-3}$
2/10F1	101	7.07	$(9.32 \pm 0.38) \times 10^{-4}$
2/11F1	111	7.00	$(8.58 \pm 0.36) \times 10^{-4}$
2/12F1	113	7.03	$(9.42 \pm 0.39) \times 10^{-4}$
average 2/8F1 through 2/12F1:			$(9.80 \pm 1.02) \times 10^{-4}$

Appendix AVI. Results of neptunium (NpO_2^+) solubility experiments in J-13 groundwater at 60°C.

Sample I.D.	Days	pH	Concentration (M)
3/1F1	3	8.44	$(1.84 \pm 0.08) \times 10^{-4}$
3/2F1	13	8.50	$(1.74 \pm 0.08) \times 10^{-4}$
3/3F1	29	8.42	$(1.52 \pm 0.06) \times 10^{-4}$
3/4F1	44	8.58	$(1.37 \pm 0.07) \times 10^{-4}$
3/5F1	59	8.52	$(1.29 \pm 0.07) \times 10^{-4}$
3/6F1	66	8.40	$(1.26 \pm 0.08) \times 10^{-4}$
3/7F1	73	8.54	$(1.18 \pm 0.05) \times 10^{-4}$
3/8F1	85	8.54	$(1.14 \pm 0.05) \times 10^{-4}$
3/9F1	94	8.47	$(1.05 \pm 0.04) \times 10^{-4}$
3/10F1	101	8.45	$(9.05 \pm 0.41) \times 10^{-5}$
3/11F1	111	8.50	$(9.10 \pm 0.57) \times 10^{-5}$
3/12F1	113	8.46	$(8.49 \pm 0.35) \times 10^{-5}$
average 3/7F1 through 3/12F1:			$(1.01 \pm 0.14) \times 10^{-4}$

Appendix AVII. Results of neptunium (NpO_2^+) solubility experiments in J-13 groundwater at 90°C.

Sample I.D.	Days	pH	Concentration (M)
1/1A1	1	6.06	$(5.47 \pm 0.22) \times 10^{-3}$
1/2A1	2	5.93	$(5.41 \pm 0.22) \times 10^{-3}$
1/3A1	7	5.92	$(3.54 \pm 0.14) \times 10^{-3}$
1/4A1	13	6.01	$(1.62 \pm 0.07) \times 10^{-3}$
1/5A1	15	6.10	$(1.49 \pm 0.08) \times 10^{-3}$
1/6A1	20	6.01	$(1.27 \pm 0.07) \times 10^{-3}$
1/7A1	23	5.90	$(1.31 \pm 0.07) \times 10^{-3}$
1/8A1	27	5.90	$(1.32 \pm 0.06) \times 10^{-3}$
1/9A1	31	5.88	$(1.19 \pm 0.06) \times 10^{-3}$
1/10A1	34	5.94	$(1.20 \pm 0.06) \times 10^{-3}$
1/11A1	41	5.98	$(1.13 \pm 0.06) \times 10^{-3}$
average 1/7A1 through 1/11A1:			$(1.23 \pm 0.08) \times 10^{-3}$

Appendix AVIII. Results of neptunium (NpO_2^+) solubility experiments in J-13 groundwater at 90°C.

Sample I.D.	Days	pH	Concentration (M)
2/1A1	1	7.06	$(5.61 \pm 0.24) \times 10^{-4}$
2/2A1	2	7.00	$(3.75 \pm 0.16) \times 10^{-4}$
2/3A1	7	7.07	$(5.18 \pm 0.20) \times 10^{-4}$
2/4A1	13	7.02	$(4.25 \pm 0.19) \times 10^{-4}$
2/5A1	15	7.05	$(5.23 \pm 0.31) \times 10^{-4}$
2/6A1	20	6.96	$(3.56 \pm 0.21) \times 10^{-4}$
2/7A1	23	7.01	$(3.70 \pm 0.19) \times 10^{-4}$
2/8A1	27	7.04	$(1.09 \pm 0.06) \times 10^{-4}$
2/9A1	28	7.02	$(1.58 \pm 0.08) \times 10^{-4}$
2/10A1	31	7.02	$(1.52 \pm 0.08) \times 10^{-4}$
2/11A1	34	6.95	$(2.24 \pm 0.12) \times 10^{-4}$
2/12A1	41	7.05	$(1.27 \pm 0.06) \times 10^{-4}$
average 2/8A1 through 2/12A1:			$(1.54 \pm 0.44) \times 10^{-4}$

Appendix AIX. Results of neptunium (NpO_2^+) solubility experiments in J-13 groundwater at 90°C.

Sample I.D.	Days	pH	Concentration (M)
3/1A1	1	8.23	$(1.13 \pm 0.05) \times 10^{-4}$
3/2A1	2	8.38	$(1.97 \pm 0.04) \times 10^{-4}$
3/3A1	7	8.56	$(9.23 \pm 0.37) \times 10^{-5}$
3/4A1	13	8.44	$(8.99 \pm 0.40) \times 10^{-5}$
3/5A1	15	8.39	$(8.67 \pm 0.53) \times 10^{-5}$
3/6A1	20	8.42	$(8.85 \pm 0.53) \times 10^{-5}$
3/7A1	23	8.39	$(8.45 \pm 0.45) \times 10^{-5}$
3/8A1	27	8.39	$(8.84 \pm 0.42) \times 10^{-5}$
3/9A1	31	8.39	$(9.37 \pm 0.50) \times 10^{-5}$
3/10A1	34	8.38	$(9.29 \pm 0.51) \times 10^{-5}$
3/11A1	41	8.43	$(8.40 \pm 0.44) \times 10^{-5}$
average 3/3A1 through 3/11A1:			$(8.90 \pm 0.35) \times 10^{-5}$

APPENDIX B

RESULTS OF PLUTONIUM SOLUBILITY EXPERIMENTS IN J-13 GROUNDWATER

Appendix BI. Results of plutonium (Pu^{4+}) solubility experiments in J-13 groundwater at 25°C.

Sample I.D.	Days	pH	Concentration (M)
4-1A1J2	4	5.94	$(3.89 \pm 0.29) \times 10^{-7}$
4-2A1J2	7	5.91	$(4.22 \pm 0.26) \times 10^{-7}$
4-3A1J2	11	5.99	$(1.04 \pm 0.78) \times 10^{-6}$
4-4A1J2	14	5.88	$(1.12 \pm 0.09) \times 10^{-6}$
4-5A1J2	18	5.85	$(1.05 \pm 0.08) \times 10^{-6}$
4-6A1J2	21	5.93	$(8.22 \pm 0.60) \times 10^{-7}$
4-7A1J2	25	5.90	$(1.33 \pm 0.09) \times 10^{-6}$
4-8A1J2	28	5.88	$(1.28 \pm 0.08) \times 10^{-6}$
4-9A1J2	32	5.93	$(1.33 \pm 0.08) \times 10^{-6}$
4-10A1J2	35	5.97	$(1.06 \pm 0.07) \times 10^{-6}$
4-11A1J2	39	5.90	$(7.24 \pm 0.53) \times 10^{-7}$
4-12A1J2	46	5.84	$(1.14 \pm 0.09) \times 10^{-6}$
4-13A1J2	53	5.87	$(1.99 \pm 0.13) \times 10^{-6}$
4-14A1J2	60	5.80	$(5.80 \pm 0.36) \times 10^{-7}$
4-15A1J2	73	5.88	$(6.65 \pm 0.42) \times 10^{-7}$
4-16A1J2	88	5.95	$(5.54 \pm 0.36) \times 10^{-7}$
average 4-3A1J2 through 4-16A1J2:			$(1.05 \pm 0.38) \times 10^{-6}$

Appendix BII. Results of plutonium (Pu^{4+}) solubility experiments in J-13 groundwater at 25°C.

Sample I.D.	Days	pH	Concentration (M)
5-1A1J2	4	6.95	$(5.00 \pm 0.41) \times 10^{-8}$
5-2A1J2	7	6.97	$(1.22 \pm 0.08) \times 10^{-7}$
5-3A1J2	11	6.95	$(2.10 \pm 0.16) \times 10^{-8}$
5-4A1J2	14	6.87	$(1.74 \pm 0.15) \times 10^{-7}$
5-5A1J2	18	6.85	$(1.94 \pm 0.12) \times 10^{-7}$
5-6A1J2	21	6.94	$(2.54 \pm 0.20) \times 10^{-7}$
5-7A1J2	25	6.89	$(1.92 \pm 0.12) \times 10^{-7}$
5-8A1J2	28	6.92	$(2.16 \pm 0.13) \times 10^{-7}$
5-9A1J2	32	6.96	$(1.83 \pm 0.12) \times 10^{-7}$
5-10A1J2	35	6.95	$(2.11 \pm 0.14) \times 10^{-7}$
5-11A1J2	39	6.92	$(1.37 \pm 0.11) \times 10^{-7}$
5-12A1J2	46	6.93	$(1.90 \pm 0.15) \times 10^{-7}$
5-13A1J2	53	7.03	$(1.90 \pm 0.12) \times 10^{-7}$
5-14A1J2	60	7.01	$(7.02 \pm 0.44) \times 10^{-7}$
5-15A1J2	73	6.97	$(1.73 \pm 0.12) \times 10^{-7}$
5-16A1J2	88	7.04	$(2.00 \pm 0.13) \times 10^{-7}$
average 5-4A1J2 through 5-16A1J2:			$(2.32 \pm 1.44) \times 10^{-7}$

Appendix BIII. Results of plutonium (Pu^{4+}) solubility experiments in J-13 groundwater at 25°C.

Sample I.D.	Days	pH	Concentration (M)
6-1A1J2	4	8.42	$(4.15 \pm 0.45) \times 10^{-8}$
6-2A1J2	7	8.45	$(1.11 \pm 0.10) \times 10^{-7}$
6-3A1J2	11	8.40	$(2.61 \pm 0.17) \times 10^{-7}$
6-4A1J2	14	8.36	$(1.89 \pm 0.12) \times 10^{-7}$
6-5A1J2	18	8.41	$(2.03 \pm 0.26) \times 10^{-7}$
6-6A1J2	21	8.38	$(3.46 \pm 0.41) \times 10^{-7}$
6-7A1J2	25	8.44	$(2.35 \pm 0.15) \times 10^{-7}$
6-8A1J2	28	8.43	$(2.81 \pm 0.18) \times 10^{-7}$
6-9A1J2	32	8.36	$(3.66 \pm 0.32) \times 10^{-7}$
6-10A1J2	35	8.37	$(3.85 \pm 0.30) \times 10^{-7}$
6-11A1J2	39	8.32	$(3.81 \pm 0.30) \times 10^{-7}$
6-13A1J2	53	8.55	$(2.04 \pm 0.13) \times 10^{-7}$
6-14A1J2	60	8.53	$(4.45 \pm 0.31) \times 10^{-7}$
6-15A1J2	73	8.21	$(2.92 \pm 0.19) \times 10^{-7}$
6-16A1J2	88	8.52	$(2.24 \pm 0.16) \times 10^{-7}$
average 6-3A1J2 through 6-16A1J2:			$(2.93 \pm 0.84) \times 10^{-7}$

Appendix BIV. Results of plutonium (Pu^{4+}) solubility experiments in J-13 groundwater at 60°C.

Sample I.D.	Days	pH	Concentration (M)
4/1F1	3	4.94	$(3.50 \pm 0.60) \times 10^{-8}$
4/2F1	13	5.92	$(3.60 \pm 0.40) \times 10^{-8}$
4/3F1	27	5.67	$(5.16 \pm 0.41) \times 10^{-8}$
4/4F1	44	6.21	$(2.80 \pm 0.50) \times 10^{-8}$
4/5F1	59	5.99	$(2.00 \pm 0.50) \times 10^{-8}$
4/6F1	62	5.99	$(2.70 \pm 0.50) \times 10^{-8}$
4/7F1	73	5.82	$(1.50 \pm 0.30) \times 10^{-8}$
4/8F1	85	5.98	$(1.60 \pm 0.30) \times 10^{-8}$
4/9F1	101	5.94	$(1.80 \pm 0.30) \times 10^{-8}$
4/10F1	120	5.96	$(2.30 \pm 0.30) \times 10^{-8}$
4/11F1	127	5.88	$(2.48 \pm 0.32) \times 10^{-8}$
average 4/1F1 through 4/11F1:			$(2.68 \pm 1.08) \times 10^{-8}$

Appendix BV. Results of plutonium (Pu^{4+}) solubility experiments in J-13 groundwater at 60°C.

Sample I.D.	Days	pH	Concentration (M)
5/1F1	3	6.94	$(5.20 \pm 0.60) \times 10^{-8}$
5/2F1	13	7.02	$(4.47 \pm 0.43) \times 10^{-8}$
5/3F1	27	6.92	$(3.74 \pm 0.46) \times 10^{-8}$
5/4F1	44	7.05	$(3.31 \pm 0.53) \times 10^{-8}$
5/5F1	59	6.93	$(2.74 \pm 0.58) \times 10^{-8}$
5/6F1	73	6.90	$(2.42 \pm 0.30) \times 10^{-8}$
5/7F1	85	7.00	$(2.84 \pm 0.33) \times 10^{-8}$
5/8F1	101	6.89	$(3.69 \pm 0.33) \times 10^{-8}$
5/9F1	120	6.98	$(4.70 \pm 0.40) \times 10^{-8}$
5/10F1	127	6.92	$(4.22 \pm 0.40) \times 10^{-8}$
average 5/1F1 through 5/10F1:			$(3.73 \pm 0.92) \times 10^{-8}$

Appendix BVI. Results of plutonium (Pu^{4+}) solubility experiments in J-13 groundwater at 60°C.

Sample I.D.	Days	pH	Concentration (M)
6‴/1F1	1	8.42	$(1.12 \pm 0.41) \times 10^{-8}$
6‴/2F1	17	8.52	$(9.76 \pm 1.05) \times 10^{-8}$
6‴/3F1	36	8.52	$(7.29 \pm 0.60) \times 10^{-8}$
6‴/4F1	43	8.37	$(6.82 \pm 0.57) \times 10^{-8}$
6‴/5F1	52	8.35	$(1.27 \pm 0.09) \times 10^{-7}$
6‴/6F1	66	8.54	$(1.34 \pm 0.08) \times 10^{-7}$
6‴/7F1	80	8.39	$(1.17 \pm 0.08) \times 10^{-7}$
6‴/8F1	88	8.45	$(1.08 \pm 0.09) \times 10^{-7}$
6‴/9F1	103	8.55	$(1.32 \pm 0.07) \times 10^{-7}$
average 6‴/5F1 through 6‴/9F1:			$(1.24 \pm 0.11) \times 10^{-7}$

Appendix BVII. Results of plutonium (Pu^{4+}) solubility experiments in J-13 groundwater at 90°C.

Sample I.D.	Days	pH	Concentration (M)
4/1A1	1	5.92	$(7.28 \pm 0.62) \times 10^{-10}$
4/2A1	7	6.01	$(4.47 \pm 0.35) \times 10^{-9}$
4/3A1	9	6.04	$(5.68 \pm 0.44) \times 10^{-9}$
4/4A1	14	5.95	$(9.20 \pm 0.72) \times 10^{-9}$
4/5A1	17	5.91	$(8.60 \pm 0.67) \times 10^{-9}$
4/6A1	21	6.00	$(4.37 \pm 0.35) \times 10^{-9}$
4/7A1	25	5.95	$(6.77 \pm 0.52) \times 10^{-9}$
4/8A1	28	5.96	$(5.65 \pm 0.43) \times 10^{-9}$
4/9A1	35	5.91	$(4.50 \pm 0.35) \times 10^{-9}$
average 4/2A1 through 4/9A1:			$(6.16 \pm 1.89) \times 10^{-9}$

Appendix BVIII. Results of plutonium (Pu^{4+}) solubility experiments in J-13 groundwater at 90°C.

Sample I.D.	Days	pH	Concentration (M)
5/1A1	1	7.06	$(6.41 \pm 0.55) \times 10^{-10}$
5/2A1	7	7.06	$(5.83 \pm 0.46) \times 10^{-9}$
5/3A1	9	6.98	$(6.65 \pm 0.51) \times 10^{-9}$
5/4A1	14	7.00	$(8.60 \pm 0.67) \times 10^{-9}$
5/5A1	17	6.98	$(7.66 \pm 0.60) \times 10^{-9}$
5/6A1	21	7.00	$(8.79 \pm 0.68) \times 10^{-9}$
5/7A1	25	7.07	$(8.62 \pm 0.66) \times 10^{-9}$
5/8A1	28	7.02	$(9.10 \pm 0.70) \times 10^{-9}$
5/9A1	35	6.89	$(1.02 \pm 0.08) \times 10^{-8}$
average 5/4A1 through 5/9A1:			$(8.83 \pm 0.83) \times 10^{-9}$

Appendix BIX. Results of plutonium (Pu^{4+}) solubility experiments in J-13 groundwater at 90°C.

Sample I.D.	Days	pH	Concentration (M)
6/1A1	1	8.55	$(1.06 \pm 0.10) \times 10^{-9}$
6/2A1	7	8.54	$(5.93 \pm 0.48) \times 10^{-9}$
6/3A1	9	8.57	$(7.53 \pm 0.59) \times 10^{-9}$
6/4A1	14	8.39	$(7.52 \pm 0.59) \times 10^{-9}$
6/5A1	17	8.40	$(7.23 \pm 0.57) \times 10^{-9}$
6/6A1	21	8.41	$(7.20 \pm 0.56) \times 10^{-9}$
6/7A1	25	8.37	$(6.68 \pm 0.51) \times 10^{-9}$
6/8A1	28	8.51	$(7.20 \pm 0.55) \times 10^{-9}$
6/9A1	35	8.46	$(7.84 \pm 0.60) \times 10^{-9}$
average 6/4A1 through 6/9A1:			$(7.28 \pm 0.37) \times 10^{-9}$

APPENDIX C

RESULTS OF AMERICIUM/NEODYMIUM SOLUBILITY EXPERIMENTS IN J-13 GROUNDWATER

Appendix CI. Results of americium/neodymium ($^{241}Am^{3+}/Nd^{3+}$) solubility experiments in J-13 groundwater at 25°C.

Sample I.D.	Days	pH	Concentration (M)
7-1A1J2	3	6.03	$(6.86 \pm 0.25) \times 10^{-7}$
7-2A1J2	7	5.90	$(6.89 \pm 0.26) \times 10^{-7}$
7-3A1J2	11	5.97	$(5.93 \pm 0.22) \times 10^{-7}$
7-4A1J2	14	5.94	$(5.78 \pm 0.21) \times 10^{-7}$
7-5A1J2	18	5.81	$(5.55 \pm 0.16) \times 10^{-8}$
7-6A1J2	21	5.90	$(1.61 \pm 0.05) \times 10^{-8}$
7-7A1J2	25	5.86	$(5.79 \pm 0.18) \times 10^{-9}$
7-8A1J2	28	5.89	$(3.52 \pm 0.11) \times 10^{-9}$
7-9A1J2	32	6.03	$(3.83 \pm 0.13) \times 10^{-9}$
7-10A1J2	35	5.95	$(1.89 \pm 0.07) \times 10^{-9}$
7-11A1J2	40	5.93	$(1.87 \pm 0.07) \times 10^{-9}$
7-12A1J2	53	5.83	$(1.01 \pm 0.04) \times 10^{-9}$
7-13A1J2	68	5.85	$(2.34 \pm 0.09) \times 10^{-9}$
average 7-10A1J2 through 7-13A1J2:			$(1.77 \pm 0.56) \times 10^{-9}$

Appendix CII. Results of americium/neodymium ($^{241}Am^{3+}/Nd^{3+}$) solubility experiments in J-13 groundwater at 25°C.

Sample I.D.	Days	pH	Concentration (M)
8-1A1J2	3	7.05	$(4.19 \pm 0.16) \times 10^{-8}$
8-2A1J2	7	6.86	$(2.20 \pm 0.08) \times 10^{-8}$
8-3A1J2	11	6.87	$(2.02 \pm 0.08) \times 10^{-8}$
8-4A1J2	14	6.93	$(2.39 \pm 0.09) \times 10^{-8}$
8-5A1J2	18	6.86	$(1.82 \pm 0.05) \times 10^{-8}$
8-6A1J2	21	6.98	$(1.76 \pm 0.05) \times 10^{-8}$
8-7A1J2	25	6.85	$(1.23 \pm 0.04) \times 10^{-8}$
8-8A1J2	28	6.98	$(1.26 \pm 0.04) \times 10^{-8}$
8-9A1J2	32	7.08	$(1.30 \pm 0.04) \times 10^{-8}$
8-10A1J2	35	7.06	$(1.11 \pm 0.04) \times 10^{-8}$
8-11A1J2	40	7.09	$(7.91 \pm 0.24) \times 10^{-9}$
8-12A1J2	53	6.97	$(1.54 \pm 0.05) \times 10^{-9}$
8-13A1J2	68	6.97	$(1.01 \pm 0.03) \times 10^{-9}$
8-14A1J2	81	6.96	$(1.05 \pm 0.04) \times 10^{-9}$
average 8-12A1J2 through 8-14A1J2:			$(1.20 \pm 0.30) \times 10^{-9}$

Appendix CIII. Results of americium/neodymium ($^{241}Am^{3+}/Nd^{3+}$) solubility experiments in J-13 groundwater at 25°C.

Sample I.D.	Days	pH	Concentration (M)
9-1A1J2	3	8.30	$(4.76 \pm 0.19) \times 10^{-9}$
9-2A1J2	7	8.52	$(1.66 \pm 0.07) \times 10^{-9}$
9-3A1J2	11	8.57	$(2.69 \pm 0.09) \times 10^{-9}$
9-4A1J2	14	8.50	$(2.49 \pm 0.09) \times 10^{-9}$
9-5A1J2	18	8.57	$(2.33 \pm 0.08) \times 10^{-9}$
9-6A1J2	21	8.69	$(1.61 \pm 0.05) \times 10^{-9}$
9-7A1J2	25	8.58	$(1.18 \pm 0.04) \times 10^{-9}$
9-8A1J2	28	8.68	$(3.02 \pm 0.11) \times 10^{-9}$
9-9A1J2	32	8.55	$(1.34 \pm 0.05) \times 10^{-9}$
9-10A1J2	35	8.55	$(2.48 \pm 0.09) \times 10^{-9}$
9-11A1J2	40	8.55	$(7.91 \pm 0.24) \times 10^{-9}$
9-12A1J2	53	7.63	$(4.76 \pm 0.16) \times 10^{-9}$
9-13A1J2	68	8.40	$(2.00 \pm 0.07) \times 10^{-9}$
9-14A1J2	81	8.41	$(1.24 \pm 0.05) \times 10^{-9}$
average 9-3A1J2 through 9-14A1J2:			$(2.40 \pm 1.89) \times 10^{-9}$

Appendix CIV. Results of americium/neodymium ($^{241}Am^{3+}/Nd^{3+}$) solubility experiments in J-13 groundwater at 60°C.

Sample I.D.	Days	pH	Concentration (M)
7-1A1J6	1	5.97	$(4.54 \pm 0.21) \times 10^{-5}$
7-2A6J6	5	5.93	$(1.09 \pm 1.09) \times 10^{-4}$
7-3A1J6	13	5.97	$(2.12 \pm 0.10) \times 10^{-6}$
7-4A1J6	20	6.00	$(2.57 \pm 0.12) \times 10^{-6}$
7-5A1J6	27	6.00	$(3.64 \pm 0.17) \times 10^{-6}$
7-6A1J6	44	5.91	$(2.27 \pm 0.11) \times 10^{-6}$
7-7A1J6	60	6.03	$(2.99 \pm 0.15) \times 10^{-6}$
7-8A1J6	74	6.02	$(2.54 \pm 0.12) \times 10^{-6}$
7-9A7J6	81	5.90	$(1.59 \pm 0.08) \times 10^{-6}$
average 7-3A1J6 through 7-9A7J6:			$(2.53 \pm 0.65) \times 10^{-6}$

Appendix CV. Results of americium/neodymium ^{243}Am solubility experiments in J-13 groundwater at 60°C.

Sample I.D.	Days	pH	Concentration (M)
1-1A1J6	1	5.87	$(5.21 \pm 0.18) \times 10^{-5}$
1-2A6J6	5	6.06	$(1.51 \pm 0.05) \times 10^{-5}$
1-3A1J6	13	6.05	$(2.19 \pm 0.11) \times 10^{-8}$
1-4A1J6	20	5.95	$(4.12 \pm 0.18) \times 10^{-7}$
1-5A1J6	27	6.02	$(2.69 \pm 0.10) \times 10^{-6}$
1-6A7J6	44	6.02	$(3.46 \pm 0.12) \times 10^{-6}$
1-7A1J6	60	6.00	$(3.70 \pm 0.13) \times 10^{-6}$
1-8A1J6	74	6.01	$(3.53 \pm 0.13) \times 10^{-6}$
1-9A5J6	81	5.91	$(4.66 \pm 0.17) \times 10^{-6}$
average 1-5A1J6 through 1-9A5J6:			$(3.61 \pm 0.71) \times 10^{-6}$

Appendix CVI. Results of americium/neodymium ($^{241}Am^{3+}/Nd^{3+}$) solubility experiments in J-13 groundwater at 60°C.

Sample I.D.	Days	pH	Concentration (M)
8-1A1J6	1	7.00	$(4.47 \pm 0.21) \times 10^{-5}$
8-2A6J6	5	7.00	$(4.16 \pm 0.29) \times 10^{-7}$
8-3A1J6	13	6.93	$(8.47 \pm 1.13) \times 10^{-9}$
8-4A1J6	20	6.92	$(6.18 \pm 0.90) \times 10^{-9}$
8-5A1J6	27	6.93	$(2.64 \pm 0.77) \times 10^{-9}$
8-6A7J6	44	7.08	$(1.55 \pm 0.45) \times 10^{-9}$
8-7A1J6	60	6.98	$(2.15 \pm 0.65) \times 10^{-9}$
8-8A1J6	74	6.85	$(1.95 \pm 0.11) \times 10^{-8}$
8-9A1J6	81	6.99	$(7.81 \pm 1.08) \times 10^{-9}$
8-10A1J6	108	6.90	$(1.11 \pm 0.07) \times 10^{-8}$
8-11A7J6	138	7.12	$(2.95 \pm 0.20) \times 10^{-8}$
average 8-3A1J6 through 8-11A7J6:			$(9.88 \pm 9.22) \times 10^{-9}$

Appendix CVII. Results of americium/neodymium ^{243}Am solubility experiments in J-13 groundwater at 60°C.

Sample I.D.	Days	pH	Concentration (M)
2-1A1J6	1	7.07	$(2.36 \pm 0.08) \times 10^{-7}$
2-2A6J6	5	7.02	$(3.16 \pm 0.11) \times 10^{-8}$
2-3A1J6	13	6.96	$(1.26 \pm 0.15) \times 10^{-9}$
2-4A1J6	20	6.92	$(9.97 \pm 0.55) \times 10^{-10}$
2-5A1J6	27	6.95	$(1.02 \pm 0.05) \times 10^{-9}$
2-6A6J6	44	7.07	$(8.19 \pm 0.35) \times 10^{-10}$
2-7A1J6	60	7.08	$(7.60 \pm 0.60) \times 10^{-10}$
2-8A1J6	74	6.95	$(1.98 \pm 0.07) \times 10^{-8}$
2-9A7J6	81	6.92	$(2.23 \pm 0.56) \times 10^{-8}$
2-10A1J6	90	7.04	$(3.38 \pm 0.96) \times 10^{-10}$
2-11A1J6	102	7.03	$(2.22 \pm 0.30) \times 10^{-9}$
average 2-3A1J6 through 2-11A1J6:			$(5.50 \pm 8.85) \times 10^{-9}$

Appendix CVIII. Results of americium/neodymium ($^{241}Am^{3+}/Nd^{3+}$) solubility experiments in J-13 groundwater at 60°C.

Sample I.D.	Days	pH	Concentration (M)
9-1A1J6	1	8.44	$(3.40 \pm 0.25) \times 10^{-7}$
9-2A6J6	5	8.41	$(1.69 \pm 0.15) \times 10^{-7}$
9-3A1J6	13	8.41	$(8.08 \pm 1.02) \times 10^{-9}$
9-4A1J6	20	8.35	$(4.27 \pm 0.60) \times 10^{-9}$
9-5A1J6	27	8.39	$(1.56 \pm 0.45) \times 10^{-9}$
9-6A7J6	44	8.43	$(1.55 \pm 0.10) \times 10^{-8}$
9-7A1J6	60	8.38	$(7.09 \pm 0.81) \times 10^{-9}$
9-8A1J6	74	8.40	$(3.62 \pm 0.21) \times 10^{-8}$
9-9A7J6	81	8.41	$(3.04 \pm 0.21) \times 10^{-8}$
9-10A1J6	108	8.55	$(4.23 \pm 0.94) \times 10^{-9}$
9-11A7J6	138	8.49	$(2.18 \pm 0.93) \times 10^{-9}$
average 9-3A1J6 through 9-11A7J6:			$(1.22 \pm 1.28) \times 10^{-8}$

Appendix CIX. Results of americium/neodymium ^{243}Am solubility experiments in J-13 groundwater at 60°C.

Sample I.D.	Days	pH	Concentration (M)
3-1A1J6	1	8.44	$(2.63 \pm 0.09) \times 10^{-7}$
3-2A6J6	5	8.52	$(8.16 \pm 0.28) \times 10^{-8}$
3-3A1J6	13	8.44	$(2.07 \pm 0.09) \times 10^{-8}$
3-4A1J6	20	8.44	$(5.81 \pm 0.35) \times 10^{-10}$
3-5A1J6	27	8.42	$(8.21 \pm 0.02) \times 10^{-11}$
3-6A7J6	44	8.50	$(4.96 \pm 0.41) \times 10^{-9}$
3-7A1J6	60	8.36	$(4.64 \pm 0.24) \times 10^{-9}$
3-8A1J6	74	8.41	$(1.28 \pm 0.04) \times 10^{-8}$
3-9A7J6	81	8.49	$(1.95 \pm 0.09) \times 10^{-8}$
3-10A1J6	103	8.55	$(3.54 \pm 0.17) \times 10^{-8}$
3-11A7J6	136	8.48	$(1.73 \pm 0.11) \times 10^{-8}$
average 3-6A7J6 through 3-11A7J6:			$(1.58 \pm 1.14) \times 10^{-8}$

Appendix CX. Results of americium/neodymium ($^{241}Am^{3+}/Nd^{3+}$) solubility experiments in J-13 groundwater at 90°C.

Sample I.D.	Days	pH	Concentration (M)
7-1A1J9	1	5.96	$(7.93 \pm 0.84) \times 10^{-9}$
7-2A1J9	5	5.89	$(5.16 \pm 0.69) \times 10^{-9}$
7-3A1J9	8	6.05	$(2.28 \pm 0.33) \times 10^{-9}$
7-4A1J9	12	6.03	$(1.85 \pm 0.27) \times 10^{-9}$
7-5A1J9	15	6.38	$(7.62 \pm 2.73) \times 10^{-10}$
7-7A1J9	26	6.20	$(1.93 \pm 0.15) \times 10^{-9}$
7-8A1J9	30	5.92	$(2.07 \pm 0.36) \times 10^{-9}$
7-9A1J9	35	5.80	$(1.63 \pm 0.44) \times 10^{-9}$
7-10A1J9	40	6.06	$(1.02 \pm 0.25) \times 10^{-9}$
7-11A1J9	44	5.99	$(9.79 \pm 3.56) \times 10^{-10}$
7-12A1J9	47	5.78	$(8.22 \pm 3.32) \times 10^{-10}$
7-13A1J9	57	6.18	$(1.12 \pm 0.47) \times 10^{-9}$
7-14A1J9	64	5.92	$(4.19 \pm 0.66) \times 10^{-9}$
7-15A1J9	98	6.28	$(1.49 \pm 0.36) \times 10^{-9}$
average 7-3A1J9 through 7-15A1J9:			$(1.68 \pm 0.94) \times 10^{-9}$

Appendix CXI. Results of americium/neodymium ($^{241}Am^{3+}/Nd^{3+}$) solubility experiments in J-13 groundwater at 90°C.

Sample I.D.	Days	pH	Concentration (M)
8-1A1J9	1	7.09	$(3.53 \pm 0.37) \times 10^{-9}$
8-2A1J9	5	7.03	$(3.77 \pm 2.37) \times 10^{-10}$
8-3A1J9	8	7.00	$(2.32 \pm 1.87) \times 10^{-10}$
8-5A1J9	15	7.14	$(3.06 \pm 1.81) \times 10^{-10}$
8-6A1J9	19	7.00	$(0.82 \pm 1.57) \times 10^{-10}$
8-7A1J9	26	7.05	$(4.03 \pm 2.63) \times 10^{-10}$
8-8A1J9	30	7.03	$(5.81 \pm 1.92) \times 10^{-10}$
8-9A1J9	35	7.07	$(1.12 \pm 2.24) \times 10^{-10}$
8-10A1J9	40	6.83	$(4.16 \pm 2.13) \times 10^{-10}$
8-11A1J9	44	6.89	$(4.78 \pm 2.78) \times 10^{-10}$
8-12A1J9	47	7.13	$(1.57 \pm 1.73) \times 10^{-10}$
8-13A1J9	57	6.97	$(4.48 \pm 1.89) \times 10^{-10}$
8-14A1J9	64	7.07	$(4.40 \pm 1.82) \times 10^{-10}$
8-15A1J9	98	7.17	$(0.52 \pm 1.42) \times 10^{-10}$
average 8-2A1J9 through 8-15A1J9:			$(3.14 \pm 1.71) \times 10^{-10}$

Appendix CXII. Results of americium/neodymium ($^{241}Am^{3+}/Nd^{3+}$) solubility experiments in J-13 groundwater at 90°C.

Sample I.D.	Days	pH	Concentration (M)
9-1A1J9	1	8.41	$(3.44 \pm 0.57) \times 10^{-9}$
9-2A1J9	5	8.43	$(3.29 \pm 0.48) \times 10^{-9}$
9-3A1J9	8	8.38	$(4.60 \pm 0.66) \times 10^{-9}$
9-4A1J9	12	8.34	$(6.52 \pm 1.62) \times 10^{-10}$
9-5A1J9	15	8.47	$(6.57 \pm 2.79) \times 10^{-10}$
9-6A1J9	19	8.39	$(1.34 \pm 1.94) \times 10^{-10}$
9-8A1J9	30	8.34	$(1.27 \pm 0.20) \times 10^{-10}$
9-9A1J9	35	8.30	$(3.14 \pm 2.05) \times 10^{-10}$
9-10A1J9	40	8.23	$(4.00 \pm 1.98) \times 10^{-10}$
9-11A1J9	44	8.57	$(5.00 \pm 2.71) \times 10^{-10}$
9-12A1J9	47	8.50	$(4.33 \pm 2.48) \times 10^{-10}$
9-13A1J9	57	8.67	$(1.34 \pm 1.72) \times 10^{-10}$
9-14A1J9	64	8.47	$(1.41 \pm 1.57) \times 10^{-10}$
9-15A1J9	98	8.51	$(2.12 \pm 1.58) \times 10^{-10}$
average 9-4A1J9 through 9-15A1J9:			$(3.37 \pm 2.06) \times 10^{-10}$

APPENDIX D

YMP LABORATORY RECORD BOOK REFERENCE

The data used to write this report are recorded in the following YMP Laboratory Record Books:

TWS-LBL-10-85-01, pp. 1–95;

TWS-LBL-06-86-01, pp. 1–305;

TWS-LBL-06-86-02, pp. 1–300;

TWS-LBL-06-86-01, pp. 1–302;

TWS-LBL-01-87-01, pp. 1–304;

TWS-LBL-01-88-01, pp. 1–95;

TWS-LBL-05-88-01, pp. 1–299;

TWS-LBL-05-88-02, pp. 1–299;

TWS-LBL-10-88-01, pp. 1–297;

TWS-LBL-01-89-02, pp. 1–301;

TWS-LBL-02-90-03, pp. 1–69;

TWS-LBL-02-90-04, pp. 55–229;

TWS-LBL-04-90-07, pp. 1–170;